

**PREDICTION OF TEXTURE
CHARACTERISTICS IN APPLE DRYING
USING COMPUTER VISION**

By

Dandan Wang

Submitted in partial fulfilment of the requirements

for the degree of Master of Science

At

Dalhousie University

Halifax, Nova Scotia

July 2016

© Copyright by Dandan Wang, 2016

Table of Contents

List of Tables	v
List of Figures	vi
Abstract	ix
List of Abbreviations Used	x
Acknowledgements	xiii
Chapter 1. Introduction	1
Chapter 2. Literature Review	3
2.1 Effects of Drying Technologies on Microstructure and Texture	3
2.1.1 Convective Drying	4
2.1.2 Freeze Drying	6
2.1.3 Microwave Drying	8
2.1.4 Osmotic Dehydration	10
2.1.5 Hybrid Technologies	12
2.2 Relationship of Food Microstructure to Texture	16
2.3 Food Texture	17
2.4 Food Plant Microstructure	24
2.4.1 Initial Structure of Plant Tissue	24
2.4.2 Food Microstructural Properties	27
2.5 Relevance for the Industry	35
Chapter 3. Hypothesis and Objectives	36
3.1 Problem Statement	36
3.2 Hypotheses	36
3.3 Objectives and Scope	37
Chapter 4. Estimation of Total, Open- and Close-Pore Porosity of Apple Slices During Drying	38
Abstract	38
4.1 Introduction	39
4.2 Materials and Methods	41
4.2.1 Materials and Sample Preparation	41
4.2.2 Instrumentation	42
4.2.3 Experimental Procedure	43

4.2.4 Porosity Estimation	43
4.2.5 Statistical Analysis	44
4.3 Results	44
4.4 Discussion	48
4.5 Conclusions	51
Connecting Statement	52
Chapter 5. Computer Vision for Bulk Volume Estimation of Apple Slices During Drying	53
Abstract	53
5.1 Introduction	54
5.2 Materials and Methods	55
5.2.1 Materials and Sample Preparation	55
5.2.2 Instrumentation	55
5.2.3 Experimental Procedure	56
5.2.4 Bulk Volume Measurements	56
5.2.5. Statistical Analysis	59
5.3 Results and Discussion	60
5.3.1 Image Analysis	60
5.3.2 Correlation Between Imaging and Physical Caliper Measurements of Diameter	66
5.3.3 Verification	67
5.3.4 Correlation Between Diameter and Volume	68
5.4 Conclusions	70
Connecting Statement	71
Chapter 6. Texture Changes of Apple Slices Under Convective Drying	72
Abstract	72
6.1 Introduction	72
6.2 Materials and Methods	78
6.2.1 Materials and Sample Preparation	78
6.2.2 Instrumentation	78
6.2.3 Experimental Procedure	80
6.3 Results and Discussion	80
6.3.1 Effects of Drying Temperature and Moisture Content on Porosity	80

6.3.2 Effects of Moisture Content on Texture	81
6.3.3 Effects of Drying Temperature, Porosity and Glass Transition on Texture	87
6.4 Conclusions	94
Chapter 7 General Conclusions and Recommendations	97
7.1 Achievements and General Discussion of the Results	97
7.2 Recommendations for Future Research	98
References	100
Appendices	120
Copyright Permission (A)	120
Copyright Permission (B)	122
Copyright Permission (C)	123
Copyright Permission (D)	126
Copyright Permission (E)	130
Copyright Permission (F)	131
Copyright Permission (G)	132

List of Tables

Table 2-1 Physical definitions of texture parameters (Szczesniak, 2002)	21
Table 2-2 TPA parameters and calculations from force-time curve.....	23
Table 4-1 Effect of grinding on particle density measured with a pycnometer.....	45

List of Figures

Figure 2-1. Force and deformation curve under loading and unloading for texture measurement.....	20
Figure 2-2. Texture machines with sample simple geometries. T: the machine part representing the human tissue; F: the tested food specimen (Campanella and Peleg, 1988, copyright permission has been obtained).....	21
Figure 2-3. TA-XT plus texture analyzer (Stable Micro System, Surrey, UK)....	22
Figure 2-4. Force-Time curve of texture measurement from TA-XT plus texture analyzer.....	23
Figure 2-5. A schematic representation of the parenchyma tissue of apple. (is): intercellular space; (cw): cell wall; (pl): plasmalemma; (vac): vacuole; (cyt): cytoplasm. (Prothon et al., 2003, copyright permission has been obtained).....	24
Figure 4-1 Schematic drawing of experimental drying apparatus.....	42
Figure 4-2 Kinetics of moisture content (trend line is based on three replications)	45
Figure 4-3 Kinetics of porosity estimated from three approaches (trend lines connect average values)	47
Figure 4-4 Porosity estimated from three approaches as a function of moisture content...	47
Figure 4-5 Total (circles), open-pore (triangles) and closed-pore (squares) porosity as a function of moisture content.....	50
Figure 5-1. Schematic drawing of imaging and region of interest (ROI) from the cameras.....	57
Figure 5-2. The IMAQ clamp measurements of diameter and thickness of fresh samples: (a) Maximum clamp for diameter measurement (b) Maximum clamp for thickness measurement	60
Figure 5-3. Diameter and thickness measured from imaging (Im) and physical caliper (Cp).....	61

Figure 5-4 (a) Semi-dried samples from side camera (b) Maximum clamp for thickness measurements of semi-dried samples.....	61
Figure 5-5. (a) Dried samples from side camera; (b) Imaging thickness of dried samples...	62
Figure 5-6. Imaging thickness with multiple calipers subroutine	62
Figure 5-7. Comparison of thickness changes measured from imaging (single and multiple calipers) and physical caliper (Cp).....	63
Figure 5-8. Diameter shrinkage measured under different threshold (45, 50 and 55) in time (a) and moisture content (b) domains.....	64
Figure 5-9. Diameter changes measured under different modes in time (a) and moisture (b) domains.....	65
Figure 5-10. Correlation of diameter estimated from imaging and physical caliper at 80 °C.....	66
Figure 5-11. Diameter estimated from imaging and physical caliper in the range 40- 80 °C.....	67
Figure 5-12. Correlation of volume and imaging diameter at 80 °C, 60 °C and 40 °C.....	69
Figure 6-1 Characteristics of transition from liquid to glass. (a) Volume, (b) Viscosity. (White and Cakebread, 1966, copyright permission has been obtained).....	73
Figure 6-2 Relationship of food deterioration rate as a function of water activity (Barbosa-Cánovas et al., 2003, copyright permission has been obtained).....	76
Figure 6-3 Water desorption isotherm of apple flesh at 20-22 °C. X is on moisture content on dry basis. (Bourne, 1986, copyright permission has been obtained).....	76
Figure 6-4 Relationship between glass transition temperature (T _g) and moisture content (X) on dry basis for air dried apple tissue.....	78
Figure 6-5 Porosity development respect to moisture content under different drying temperatures	81
Figure 6-6 Hardness changes during drying of apple slices in moisture content domain....	83

Figure 6-7 Adhesiveness changes during drying of apple slices in moisture content domain.....	84
Figure 6-8 Springiness changes during drying of apple slices in moisture content domain.....	85
Figure 6-9 Cohesion changes during drying of apple slices in moisture content domain	86
Figure 6-10 Chewiness changes during drying of apple slices in moisture content domain.....	86
Figure 6-11 Hardness changes in moisture domain at different drying temperatures.....	88
Figure 6-12 Adhesiveness changes in moisture domain at different drying temperatures...	89
Figure 6-13 Cohesion changes in moisture domain at different drying temperatures.....	90
Figure 6-14 Springiness changes in moisture domain at different drying temperatures...	90
Figure 6-15 Chewiness changes in moisture domain at different drying temperatures.....	91
Figure 6-16 Moisture distribution of apple slices under convective drying.....	93
Figure 6-17 Effects of drying regimes on texture development.....	95

Abstract

It was proved that computer vision is applicable for continuous estimation of bulk volume from diameter imaging of apple slices and an empirical model with an average relative percent error of approximately 6.45 % was established, which allowed continuous estimation of total porosity as a function of volume shrinkage and moisture content. Texture parameters were dependent on porosity evolution and glass transition, which was a function of drying temperature and moisture content. Glass transition occurred within moisture content range of 1.0 g/g to 0.26 g/g when open-pores converted into closed-pores. To create crispy texture, the drying process should be carried out at 80 °C to moisture content of less than 0.5 g/g with a total porosity of more than 0.7 when materials undergo glass transition and case hardening. This knowledge makes it possible to develop an optimal industrially-scaled drying process, using computer vision for continuous monitoring and prediction of texture.

List of Abbreviations Used

Nomenclature

θ	Contact angle (°)
A	Area (m ²)
BP	Ball probe
Cph	Heat capacity
CP	Compression plate
cw	Cell wall
cyt	Cytoplasm
d	Diameter (cm)
d.b.	Dry basis
De	Elastic deformation
DELTY	Degree of elasticity
Dp	Plastic deformation
DSC	Differential scanning calorimeter
DTA	Differential thermal analysis
E	The modulus of elasticity
ESR	Electron spin resonance
F	Force (N)
h	Thickness (cm)
is	Intercellular space
K,k	Constant
L	Length (m)
m	Mass (g)
n	Number of replications
P	Pressure (psi)
pl	Plasmalemma
r	Radius of pores (cm)
ROI	Region of interest
S.D./s	Standard deviation
T	Temperature
TMA	Thermal mechanical analysis
TPA	Textural profile analysis
V	Volume (cm ³)
vac	Vacuole
w	Weight fraction
w.b.	Wet basis
X	Moisture content on dry basis (g/g)
y	Measurement

α, β	Density ratio coefficients
α_0	Geometric value corresponding to the full turgor situation
γ	Surface tension (N/cm)
ε	Bulk porosity
λ	Ratio cube side/sphere diameter (cm)
ξ	Bulk volumetric shrinkage/ shrinkage coefficient
ρ	Density (g/cm ³)
\bar{y}	The average of measurements

Subscript	
1	Reading after pressurizing just the reference volume
2	Reading after expanding gas into the sample cell holder
a	Air
b	Bulk
c	Cellular
C	Carbohydrates
CE	Cell holder
cp	Closed
cr	Critical point
expt	Experimental
g	Glass transition
gs	Glass transition of solids
gw	Glass transition of water
i	i th measurement
L	Lipids
o	Initial
op	Open
p	Particle
Pr	Protein
pycn	Pycnometer
R	Reference
s	Solid
t	Instantaneous
theo	Theoretical
w	Water

Abbreviation	
AD	Convective drying
CV	Computer vision
EHD	Electrohydrodynamic
FD	Freeze drying
MWD	Microwave drying
MWVD	Microwave vacuum drying
PME	Pectin methyl esterase
RF	Radiofrequency
VD	Vacuum drying

Terminology	Definition	Synonyms
Bulk volume change	Dimensional changes of material in drying, depends on drying technology. Usually shrinkage in air drying, puff in microwave vacuum drying or constant in freeze drying and final stage of air drying	
Computer vision (CV)	Computer system for process control	Machine vision
Imaging	A component/process of CV	
Real-time	The actual time during which a process or event occurs	On-line, continuous
Shrinkage	Reduction in sample's bulk volume in convective drying	

Acknowledgements

I would like to express my special thanks of gratitude to my supervisor Dr. Alex Martynenko for encouraging me to pursue a graduate study and giving me an opportunity to do this project as well as his endless guidance and support throughout my graduate years at Dalhousie University. It is my great pleasure to work with him. His contributions are sincerely appreciated and gratefully acknowledged.

I wish to express my thanks to Dr. Kenneth Corscadden, Dr. Sophia (Quan) He for being my advisory committee members and for their patience, knowledge and willingness to help me with all problems I faced during my program. I am also grateful to Dr. Kenneth Corscadden and Dr. Sophia (Quan) He for their strong encouragement and contributions to this manuscript.

In addition, I thank Dr. Bruce Rathgeber for providing technical equipment. I would like to extend my thanks to those who offered collegial guidance and support over the years: Dr. Peter Havard, Dr. Ashutosh Singh, and technicians: Scott Read and Chris Nelson and administrative coordinator: Mandi Wilson. Their contributions are greatly appreciated.

I would also like to acknowledge Ms. Marg Rovers, Dr. Vilis Nams, Yougui Chen, Alissa Spinney and Patrick Wells for their help in proofreading of some of the chapters in this thesis. Thanks to the Natural Sciences and Engineering Research Council of Canada (NSERC) for funding this research.

To all relatives, friends and others who, in one way or another, shared their support, thank you. This thesis is dedicated to all of you.

Chapter 1. Introduction

Drying is a commonly used food processing operation, which extends food shelf life by reducing water activity. Dehydration techniques, including convective air (AD), microwave (MWD), and freeze (FD) drying have influences on quality indicators of dried and semi-dried food including porosity, density and texture. For example, FD preserves the food structure with high porosity and low shrinkage, but the capital investment is high (Krokida et al., 2000b). Microwave vacuum drying (MWVD) leads to uniform dried products with high operation costs (Hu et al., 2006). AD products are characterized by low porosity and high shrinkage with significant color changes (Lewicki and Pawlak, 2003). AD is commonly used in food industries due to its low investment and operation costs.

Removing extra water from fresh food affects the appearance and the market value. On the other hand, food properties, microstructure and texture, are influenced by both external (different drying conditions and methods) and internal (shape and size of samples) factors during drying. Due to the variety of food shapes and states, such as powdered, sliced, wet solid, liquid, etc., and a series of physiochemical changes during drying (such as shrinkage, case hardening and porosity), as well as flavor change, the drying methods are largely dependent on food properties. In other words, the initial food properties determine which drying methods are preferred. Inversely, the drying techniques affect the final properties of the food, which directly influence consumer preferences.

Consumers' perception of quality usually includes visual and textural characteristics, so it is important for industry to preserve food structure which is closely related to food texture. Texture parameters are difficult to be measured directly during drying. However, they could be related to structural changes (porosity), which are measurable in real-time

(Kawas and Moreira, 2001). Understanding the relationship between texture and microstructure is of great importance for industries to determine the end point of the drying process and to produce food with desirable qualities. Knowledge has been expounded on food microstructure and texture independently, but very little information is available as to the relationship between them. A few researchers had focused on the effects of microstructure as they relate to texture parameters and strong relationships have been reported for fried tortilla chips (Kawas and Moreira, 2001) and apple discs (Acevedo et al., 2008, Do Trong et al., 2014). Hence, further investigation is needed to determine how texture is affected by microstructure during the drying process.

Computer Vision (CV), a novel technology, has been considered as an efficient tool for real-time food quality assessment but also in other fields, such as medical diagnostics, autonomous vehicles and robot guidance (Brosnan and Sun, 2004). Imaging is the core process of CV and has been applied in fields of quality inspection, classification and evaluation of images (Sun, 2004). This newly developed method is a fast, automatic, and non-destructive technique for monitoring food quality by acquiring non-contact surface imaging, with objective information for evaluation. CV could be used as an element of a robust real-time control system for on-line monitoring of area shrinkage, according to image morphological attributes (Martynenko, 2006).

The relationship between food microstructure and texture is still unknown. It is important for the food industry to understand texture changes during drying and create products with desirable textural properties. Due to a lack of instruments, texture cannot be directly measured in real-time during drying. Thus, the aim of this research was to use a CV to monitor structural changes (bulk volume) of apple slices for texture prediction.

Chapter 2. Literature Review

Changes in food texture and microstructure under different drying technologies has been receiving considerable attention. Most researchers and scientists have worked on the effect of drying methods on food texture and microstructure separately, however little work has been done on investigating their relationship or the effect of microstructure on food texture. Moreover, the importance and application of the relationship have not been taken into consideration in the food processing industry. This chapter reviews the effects of processing methods on microstructure, texture and their relationship. In addition, the examination of texture and microstructure has also been reviewed to imply the possibility of designing a computer vision system for continuously predicting food texture by controlling microstructure during drying in the food processing industry.

2.1 Effects of Drying Technologies on Microstructure and Texture

Dehydration not only removes water from food materials, but also preserves food quality. The dehydrated materials are more stable at room temperature when compared to fresh fruits and vegetables (Aguilera et al., 2003). There are a variety of drying methods applied all over the world, used either as a sole technology or in hybrid with other technologies. This study only reviews drying technologies that apply to solid foods, which include solar, convective air, microwave, freeze and osmotic drying as well as hybrid of these drying technologies, such as microwave vacuum drying, microwave hot air drying, microwave vacuum and freeze drying. More advanced drying technologies, such as airless drying, sonic drying, electrohydrodynamic drying (EHD) and radio-frequency drying (Kudra and Mujumdar, 2009), are under development in order to satisfy the producers' and consumers' requirements. For instance, the food processing industry has expectations of

low manufacturing costs, while the consumer demand for high quality products is increasing (Saravacos, 1993, Saravacos, 1967, Krokida et al., 2000b). It was found that drying technology significantly affects microstructure and texture of dried and semi-dried foods (Krokida et al., 1998). Since then, a number of studies have been carried out to determine the impacts of different drying methods on food microstructure and texture, such as shrinkage, porosity, pore size, pore size distribution, crispiness and hardness (Aguilera et al., 2003, Acevedo et al., 2008). It is important to choose an appropriate drying approach to reach the desired microstructure and texture. There are four common drying technologies used in the food industry and research: convective drying, freeze drying, microwave drying and osmotic dehydration.

2.1.1 Convective Drying

Convective drying technology is the most frequently used method in the food processing industry due to its simple operation and low cost (Krokida et al., 2000b, Xu et al., 2004). Food microstructure and texture are mainly affected by the air temperature, drying time and material shrinkability. Convective drying mainly takes place at a constant rate and falling rate periods (Mujumdar, 1995). When the surface is wet and contains free water at the beginning of drying, the dehydration rate is constant. The inside moisture is transported out, as a result of the concentration gradient. When a dry spot appears on the surface, insufficient water transport to the surface causes falling dehydration rate. In a fresh apple, the concentration gradient is not large, solid skeleton is firm and water is distributed uniformly on the surface and the interior of the material, which makes the material viscoelastic and can be easily deformed. During the early stage of drying, as surface water is removed, the material starts to shrink, which prevents the space where water was

removed from being replaced by air. At this stage, the shrinkage is proportional to the amount of water evaporated. As the drying progresses, loss of water gives additional strength and rigidity to the cell wall. The cell wall is not able to shrink, as the material reaches glass transition temperature (Lewicki, 1998). This process occurs at the end of convective drying, where volume shrinkage is not able to compensate for evaporated water volume.

Shrinkage under convective drying can be explained as a result of heat and mass transfers in the solid phase, which leads to moisture and thermal gradients and generates mechanical stress. Moisture gradient occurs through the entire drying process. Stress, which is generated from the thermal gradient, only affects shrinkage at the early drying stage (Musielak, 2000). Accordingly, material shrinkage and deformation are mainly caused by stress generated by the moisture gradient (Lewicki and Pawlak, 2003). Ptasznik et al. (1990) stated that tensile stress generated by the moisture gradient caused internal cracks and fissures. Musielak (2000) illustrated that tensional state occurs in the region close to the surface and it is caused by water removal. The compression state occurs at the center of the sample. Tension force is stronger than compression force; thus, brittle damage occurs at the region near the surface. A negative pressure (-90kPa), formed in the center of the material undergoing convective drying, was observed and considered as a contribution to deformation (Pakowski and Adamski, 2012). Pakowski and Adamski (2012) also stated that shrinkage released pressure at the center of the sample and reduced the number of pores and pore size in the materials. From their observations, pressure increased slightly at the initial drying stage, and then negative pressure formed quickly, reaching a minimum. Then

it increased, but still remained negative explaining the concave surface on the samples under convective drying.

Lewicki and Pawlak (2003) reported that the cell wall was disrupted as water was removed and Lewicki and Drzewucka-Bujak (1998) stated that the extent of this disruption depended on moisture content especially before moisture content reached 2 g/g (d.b.). In convective drying apples shrank isotropically compared to raw flesh, their cell volume and area were reduced; likely due to their cavities being doubly elongated and irregular. Small pores formed in the layers close to the surface and big pores spread all over the cut surface. The formation of big pores may be the result of the joining of adjacent cells (Lewicki and Pawlak, 2003). Consequently, convective air dried products are characterized by low porosity (30-60 %) with most porosity formed at the end of drying when material stops shrinking (Zogzas et al., 1994, Karathanos et al., 1996). Most food materials shrink, even undergo irreversible structure changes with long exposure time under high temperature, which leads to quality degradation, including taste, appearance and texture. To preserve the material bulk volume and quality, freeze drying was introduced.

2.1.2 Freeze Drying

Freeze dried products have the most desirable properties with preserved texture of fresh foods without negatively impacting their structure. A freeze dryer consists of three parts: the refrigeration system, vacuum pump and heating system. In the freeze drying process, materials are first kept at low temperature until they are frozen and the vapor is condensed to ice, which will be easily removed in the next step. A vacuum environment is maintained when ice is removed by sublimation. To convert ice into vapor, a heating system is required to increase the product temperature. Heat can be supplied either by contact or

microwave; however, the amount of energy supplied is critical. It should be able to obtain a high rate of sublimation, but avoid melting the food. A variety of food materials (apple, banana, carrot and potato) under freeze drying have been investigated (Krokida et al., 1998). Ice crystals are created within the material during freezing and voids are formed when water is removed by ice sublimation. When material exceeds collapse temperature, cells lose their structure and shrinkage occurs (Prothon et al., 2003). Structural collapse and porosity reduction are due to viscosity reduction, caused by the increased “plasticity” of the solid matrix that is surrounded by the ice crystals (Krokida et al., 1998).

According to Prothon et al. (2003), there is no structural collapse but the samples are texturally fragile under collapse temperature. It has been proven that rehydrated freeze dried products have loose and soft material texture (Prothon et al., 2003). Textural collapse was explained as a result of ice crystal formation during freezing. This was also proposed by Hills and Remigereau (1997) who found that during freezing the formation of ice crystals destroyed membrane integrity and caused cell wall collapse. There are two phase mixtures in the frozen products including ice crystals and a concentrated amorphous solution, in which the solvent is the unfrozen water and it is dependent on temperature (Krokida et al., 1998). Krokida et al. (1998) raised an assumption stating that it is the surface tension of the capillaries that causes collapse. The high complex viscosity of the matrix prevents the material from collapsing. They found that collapse occurs in a short time at relative high temperatures. At relative low temperatures, it takes a longer time because of the higher complex viscosity. Witrowa-Rajchert et al. (1995) stated that, drying rate decreased at the final stage of drying because of the surface rigidity. Little or no shrinkage under freeze drying provides a porous structure, which results in higher

absorption and apparent diffusivity of water. After freeze drying, doubly large and irregular pores were observed (Lewicki and Pawlak, 2003). Compared with convective air dried products, samples under freeze drying have lower bulk density and specific volume (Saravacos, 1967, Krokida and Maroulis, 1997). Well-defined intercellular voids created within materials increase the rehydration rate (Karathanos, 1993), which could be desirable for some applications, e.g. vegetable drying. Freeze drying is not executable in the food industry, due to the slow sublimation process, which requires high energy consumption as well as a high installation and maintenance costs. Besides that, freeze drying took the longest time (72 hours) to dry blanched carrot from 91.4 % to 10 % moisture content, followed by air drying with 8 hours; while it only took 33 minutes for microwave vacuum drying (Lin et al., 1998). Hence, microwave drying was introduced not only to increase the drying rate, but also to produce foods with crispy texture due to the puffing phenomena.

2.1.3 Microwave Drying

Compared to convective air and freeze drying, microwave drying is rapid, more uniform and energy efficient significantly shortening the drying process. Microwave drying applies an electromagnetic field to the product causing dielectric oscillation of water molecules. The oscillation of the water molecules produces heat and increases the temperature of the material and moisture is removed by evaporation (Liu et al., 2012). Microwave drying consists of three basic drying periods: heating-up, rapid drying (constant drying rate) and falling drying rate periods (Soysal, 2004, Yan et al., 2010). Soysal (2004) dried parsley under microwave conditions and found that 40.5 % of water was removed during the constant rate period. As drying continued, the decreased moisture in the material led to a reduction of microwave power absorption, which caused falling dehydration rate.

In this period, by increasing the microwave power (360W-900W), drying time decreased to some extent. It was also reported for wild cabbage (Xu et al., 2004), mint leaves (Therdthai and Zhou, 2009), apple slices (Han et al., 2010, Cui et al., 2008) and carrot pieces (Cui et al., 2008, Yan et al., 2010) that high microwave power shortened the drying time significantly. However, air bubbles were found in the wild cabbage when the microwave power ranged between 1400W and 1900W negatively affecting the quality of the final product (Xu et al., 2004). The reason for the bubble formation was not reported, but it is possibly due to the hot spots caused by the caramelization of sugar in the wild cabbage (Xu et al., 2004), or the non-uniformity of the electromagnetic field (Therdthai and Zhou, 2009). Zhang et al. (2010) summarized the following advantages of microwave drying: (1) increased drying speed; (2) uniform heating throughout the material, which avoids the large temperature gradient; (3) high energy efficiency; (4) better process control (e.g. selective heating); (5) improved product quality due to desirable chemical and physical effects occurs during drying. However, in reality, microwave drying still has some disadvantages. It is clear that poor quality products may be produced if excessive microwave power, such as 600W, is applied (Han et al., 2010, Drouzas and Schubert, 1996). Rapid mass transfer, caused by high microwave power led to burning of dried whole strawberries (Venkatachalapathy and Raghavan, 2000, Therdthai and Zhou, 2009). In addition, due to the uneven temperature distribution on the material that was caused by inherent non-uniform electric field intensity inside the drying cavity, some parts of the material may be overheated (Dolan, 1994, Zhang et al., 2010). Hence a moderate mass transport rate by microwave power is essential to prevent undesirable changes caused by puffing and produce high quality products (Nijhuis et al., 1998, Yan et al., 2010).

2.1.4 Osmotic Dehydration

Osmotic dehydration relies on immersing materials in aqueous solutions of high concentration; a 50 % w/w sucrose solution with a water activity value of 0.936 is commonly used (Mavroudis et al., 1998). The osmotic process includes water diffusion from material to solution (water loss) and sugar diffusion from solution to material (solid gain). At the early stage of osmotic dehydration, solid and water flux are large due to high concentration gradients between the solution and the material (Lewicki and Porzecka-Pawlak, 2005). The initial structure and temperature control the mass transfer phenomena under osmotic dehydration (Mavroudis et al., 1998). Mavroudis et al. (1998) found that for apple osmotic drying, at the same process temperature, lower water loss and higher solute uptake occurred in the inner parenchyma, which is close to the core, compared to outer parts near the skin. This can be explained by the effects of the mass transfer phenomena on cell structure and solution penetration. Different solid gains and water losses can be explained by the mass transfer pathways for sucrose through three phases in tissue: cell, cell wall and intercellular space phases (Gekas and Mavroudis, 1998, Mavroudis et al., 1998). Mavroudis et al. (1998) stated that the inner cells with high volume are more susceptible to a loss of cell vitality than the outer cells with low volume due to the morphology of the intercellular space, as well as the viscosity of the solution. Plasmolysis of the outer cells develops a gradient of turgor pressure, which deforms structure and hinders water flow (Maguer, 1997). Water and solid diffusions are more dependent on temperature than material structures: as the temperature rises, water losses and solid gains increase (Mavroudis et al., 1998). Mavroudis et al. (1998) found that solution penetration can be increased by reducing viscosity and increasing temperature. The drying rate is

dependent on surface phenomena and partial pressure differentials (Farkas and Lazar, 1969).

Depending on the materials and solutions, the results for dehydration behavior and structural collapse are different. Sadiq Nargal and Ooraikul (1996) noticed that immersion in water with glycerol also prevented collapse. They proposed that partial water replacement by glycerol decreased shrinkage. Neumann (1972) stated that the hydroxyl groups of polyhydroxy compounds minimized hydrogen bonding of the cell wall, which keeps tissue soft, moist and pliable. Monsalve-Gonzalez et al. (1993) and Bolin and Huxsoll (1993) observed that apple and pear samples shrank under 40 % sucrose, with breaking cells, detachment of one cell from the other and softening of the surface layer. It was followed by increasing firmness of apple samples, which caused new intercellular spaces (Lewicki and Porzecka-Pawlak, 2005).

Bulk and particle density changes are dependent on the initial structure of materials (Krokida and Maroulis, 1997, Mavroudis et al., 1998). An increasing porosity was found from the inner to outer layers of apples (Mavroudis et al., 1998). Lozano et al. (1983) reported that collapse can be reduced in osmotic dehydration by increasing initial solids content. At the same temperature, a high initial solids content increased molecule weight and viscosity; moreover, the collapse temperature increased (Tsourouflis et al., 1976). The higher the initial solids content, the less sample tissue collapse occurred. Processing temperature may have positive or negative effects on tissue collapse, as reported by Witrowa-Rajchert et al. (1995) and Mavroudis et al. (1998). This can be explained by the activity of pectin methyl esterase (PME), which helps to solidify plant tissue (Mavroudis et al., 1998). Osmotic dehydration can be used for shrinkage and collapse prevention,

especially in pre-treatment. It was proven by Witrowa-Rajchert et al. (1995) that apple slices undergoing convective drying after osmotic pre-treatment shrank less. The longer exposure to osmotic solution, the less sample shrinkage occurs in convective drying. Other than osmotic pretreatment, application of different technologies simultaneously or continuously also helps to improve food quality.

2.1.5 Hybrid Technologies

Hybrid drying employs a variety of methods at the same stages of the drying cycle (Xu et al., 2004). Hybrid drying is now attracting more and more attention in the food processing industry due to better thermal performance and quality control. The proper hybrid drying methods is also economic and ecological, it avoids the disadvantages from a specific technique as well (Hu et al., 2006, Duan et al., 2007).

2.1.5.1 Microwave Vacuum Drying

According to Duan et al. (2007), microwave vacuum drying had the highest drying rate as compared to other drying techniques. Microwave drying heats the water in an instantaneous and homogenous way, which is efficient for removing internal free water. Vacuum drying increases the moisture gradients between inner and outer parts of the products at low temperature, which is an advantage for drying products with heat sensitive nutritional content. Hu et al. (2006) found that as the vacuum increased, boiling temperature decreased and the driving force for mass transfer increased accelerating moisture evaporation and reducing drying time. However, if the pressure is too high, the samples will be overheated, causing irreversible damage to the products. In microwave vacuum drying, heat and mass transfers are in the same direction from inside to outside of the material facilitating the drying rate and making the drying process more efficient (Hu et al.,

2006). However, microwave vacuum drying is not commonly applied in industries due to its high capital investment and high operating cost. The size of installed microwave vacuum equipment depends on the initial moisture content. Higher moisture contents require higher investment, so it is rarely used in industries (Hu et al., 2006). Also, due to the enclosed system, vapor is formed on the inner wall of the material under drying and influences the quality of the final products. In the microwave drying, the whole material is heated from the inside and water is transported to the surface in a fast and unified manner causing a puffing phenomenon which prevented shrinkage and resulted in a crispy and delicate texture (Sham et al., 2001, Zheng et al., 2013). Lin et al. (1998) and Nahimana and Zhang (2011) found that, compared to convective drying, carrot slices dried under microwave vacuum had less color deterioration, higher rehydration potential, higher nutritional content (α -carotene, vitamin C), lower density and softer texture. They also indicated that the quality of carrot slices under microwave vacuum drying is equal or even better than the freeze dried materials as presented by a sensory panel for color, texture, flavor and overall texture preference (Nahimana and Zhang, 2011).

2.1.5.2 Convective Air and Microwave Drying

Convective air removes water from the outer to inner flesh with an opposite direction of mass transfer. The dried surface acts as a poor heat conductor and reduces the drying rate, especially at the last drying stage. Xu et al. (2004) found that two-thirds of the time was spent on removing one-third of moisture at the last drying stage. Hence, microwave drying hybrid with forced convective drying to accelerate the drying rate. They stated increasing microwave power from 1400W to 1900W the less time was consumed and better quality was achieved for drying wild cabbage. The convective air and microwave vacuum

drying not only reduced drying time significantly, but also changed the macro- and micro-structures, providing more porous products and improving food quality (Andres et al., 2004, Xu et al., 2004). Khraisheh et al. (1997) stated that the shrinkage of apple samples, convective air and microwave vacuum drying was dependent on the air velocity and microwave power, instead of the samples' geometry and air temperature. Funebo and Ohlsson (1998) explained that this was due to the minimization of thermal gradients within samples, which maintained the microstructure. Several factors, including quality of raw material, physical changes during drying (such as shrinkage of cell, loss of rehydration ability, wettability and case hardening) and storage conditions could affect the quality of the final products (Villota et al., 1980, Karel, 1991). Khraisheh et al. (1997) reported that the shrinkage of potato samples during convective drying was homogenous at the initial stage. However, as more water was removed, severe particle deformation was observed and the shape of the samples became irregular. Shrinkage and volume changes were much smaller under microwave vacuum drying, compared to convective drying. The introduction of microwave drying with proper power is advantageous in reducing case hardening, which greatly improved the products' final quality and appearance. Figiel (2007) found that the drying time of microwave drying had no significant effect on sample shrinkage. However, as the microwave power increased, sample shrinkage decreased due to the puffing phenomena, which increased the sample volume.

2.1.5.3 Convective Air and Freeze Drying

Another commonly employed hybrid drying method is convective air and freeze drying, in which convective air is used for pre-drying and freeze drying is applied to complete the drying procedure. A linear mode of structural collapse was reported by

Karathanos et al. (1996). No matter when the freeze drying was applied, either after or before air drying, the volume change was negligible and thus effectively kept constant, which reduced sample shrinkage. It was found that the reduction of sample volume in air drying was only related to the moisture content changes and weakly related to other drying conditions such as air temperature. The volume of the sample remained stable throughout the whole drying process with respect to its initial volume, with a linear decrease of bulk density (Donsi et al., 1998). With the hybrid of convective air and freeze drying, satisfactory quality could be achieved. However, sample shrinkage was still observed at the first stage under air drying. When freeze drying was applied to remove 70 % of the moisture, followed by convective drying, the collapse was reduced significantly because of the increasing resistance under freeze drying in the outer layer of the samples (Anglea, 1994).

Karathanos et al. (1996) reported that the properties of products under hybrid of convective air and freeze drying were between those dried with convective air and freeze drying alone. For instance, the porosity was lower than that in freeze drying and higher than it in convective dried products. Compared to samples under convective drying a higher drying rate and more desirable texture properties were obtained under hybrid drying due to better control under freeze drying.

Besides the conventional technologies, novel technologies are under development through technology-push (technologies developed for other applications and applied to drying) and market-pull (to meet current or future market demand). Other newly developed thermal and non-thermal processing technologies include radiofrequency (RF) or high-frequency microwave, infrared, refractance window, electrohydrodynamic drying, and

acoustic drying which avoid the damages caused by high temperature and they can be applied independently or hybridized with others (Rawson et al., 2011, Kudra and Mujumdar, 2009, Ramaswamy and Marcotte, 2005). For instance, under RF drying, food materials are placed in between two electrode plates that generate electromagnetic energy. This method achieves a more uniform heat compared to microwave drying (Ramaswamy and Marcotte, 2005). In the food processing industry, RF and infrared drying can be applied for the whole drying process or at the end stage of drying.

These research projects demonstrated that drying technologies, either as it is or hybrid, have a significant impact on microstructure and texture of the dried material. Knowledge of the influences of microstructure on texture formation with different drying methods is necessary and helpful in designing food with ideal properties.

2.2 Relationship of Food Microstructure to Texture

Attempts have been made to investigate the relationship between microstructure and texture. Aguilera (2005) mentioned that the way food is structured was directly related to food quality, including texture, in which food microstructure was affected by the method that food was processed. This was confirmed by Kawas and Moreira (2001) who correlated porosity with crunchiness in fried tortilla chips. The more the chips shrank, the higher degree of puffiness and the lower degree of crunchiness was observed, due to the hard texture. Furthermore, water sorption properties, which cause different diffusions and reactions, also change food texture. This was also verified by Acevedo et al. (2008) who found that apple discs obtained by vacuum drying were harder than those under freeze drying due to a denser structure provoked by shrinkage. It was explained that the dehydrated cell wall provided structural integrity and mechanical resistance for the dried

apple slices therefore increasing the hardness of the dried apple slices. Do Trong et al. (2014) put forward the idea that apple rings with osmotic dehydration prior to air drying had larger pore sizes and higher porosity, compared to those without pre-treatment. Besides that, samples without pre-treatment had thicker tissue which contributed to its crispier attribute. These researches showed that food texture is closely and directly related to its microstructure. A more in-depth understanding of texture is necessary for continuous prediction of texture from microstructural changes during drying.

2.3 Food Texture

Texture involves synthetic sensory properties and is considered to be an indicator of quality attributes. Understanding texture properties makes it possible to control the texture changes during processing so that desirable quality can be achieved. Part of texture perception takes place in the mouth during the dynamic process of food breakdown, which is affected by oral processes, such as motility, saliva production and temperature (Wilkinson et al., 2000). Food texture measurement can be quantified by subjective (sensory) and objective (instrument) methods. Although sensory evaluation gives subjective information about the texture, multiple randomized responses allow texture perception to be quantified. However, the defects such as the high-cost, training and organization of panelists (labor-intensive) and time constraints make it rarely used in the food industry. Usually, sensory evaluation could be hybridized with instrumental methods as a reference in research (Baiano et al., 2012, Chauvin et al., 2010, Ismail et al., 2001), which is important for simulating consumers' preferences. Instrumental methods are objective tools for texture determinations, and apply a controlled force on the surface or into materials, in response to the deformation curve. Based on the general nature of the test,

instrumental methods of texture measurement can be classified into three categories: fundamental, empirical and imitative (Blair, 1958). The fundamental method measures rheological properties of material, such as viscosity and elastic moduli, in which information obtained is independent of sample size and dimension (Wilkinson et al., 2000). The fundamental test was initially developed by engineers for material texture measurement, but it is destructive. Destructive methods for texture measurements include three-points bending test, single-edge notched bend test, compression and puncture test, stress relaxation test, Warner-Bratzler shear force test, etc., and non-destructive methods include mechanical techniques, ultrasound techniques and optical techniques (Chen and Opara, 2013).

Compression and puncture tests are the most common fundamental methods for food texture measurement. The simulated force used to bite the intact product copies the consumer's primary evaluation of food quality. In this case, the force applied is proportional to the biting area and perimeter of the product. A plate with a constant speed is applied to compress the sample into 20 % (typically) deformation or a needle is inserted into samples, the depth of the compression is depending on the size and properties of the samples. The force used to simulate the bite of the intact product indicates sample hardness and elastic parameters (Chen and Opara, 2013). The stress-strain (or force-deformation) behavior is usually investigated for elasticity and plasticity by generating a deformation curve. Depending on moisture content, the hardness and elasticity varies. Treitel (1944) found that at low moisture content, plant tissue showed low modulus elasticity, which was calculated based on the slope of the curve. Also, for the patterns of stress-strain curves, softer materials show flatter curves. A sample is placed between two parallel rigid plates

for uniaxial compression for the modulus of elasticity measurement. The literature gives examples for grains and apples (Mohsenin et al., 1963, Zoerb and Hall, 1960).

The modulus of elasticity (E) for uniaxial compression was found by taking the ratio of conventional stress to conventional strain, calculated as follow (Mohsenin, 1970):

$$E = \frac{F/A}{\Delta L/L} \quad (2-1)$$

Where, F is force applied (N), A is original cross-sectional area of the sample (m²), ΔL is deformation corresponding to force F and L is initial length of the sample.

In order to get the accurate modulus of elasticity, a series of loading and unloading is applied until there is no residual deformation observed (Mohsenin et al., 1963); usually two cycles are sufficient. A force-deformation graph with one cycle is presented in Figure 2-1. It follows that deformation includes plastic and elastic components. The Y-axis indicates loading and unloading force applied for 20 % sample deformation. The X-axis indicates the deformation length under loading and unloading. The distance from the end of loading to the end of unloading indicates the elastic deformation, while the difference between total deformation and elastic deformation is the plastic deformation. From Figure 2-1, the degree of elasticity (DELTY) can be calculated as (Kaletunc et al., 1991):

$$DELTY = \frac{D_e}{D_e + D_p} \quad (2-2)$$

Where, D_e and D_p are elastic and plastic deformations, respectively.

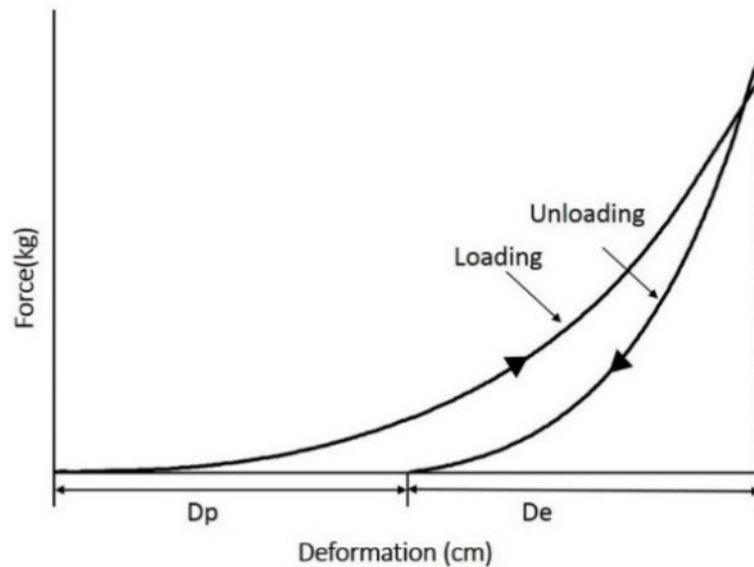


Figure 2-1. Force and deformation curve under loading and unloading for texture measurement

The fundamental test is not sufficient for texture analysis of foodstuffs, due to their complex rheological properties. Empirical measurement is based on practical experience on the resistance of the sample to force deformation. Most instrumental measurements are empirical, including penetrometers, compressors, consistometers, shear measures and other devices, reported by Szczesniak (1963b). Although empirical methods have the advantage of simplicity, the measurements are not well correlated with sensory texture measurement and are poorly defined (Wilkinson et al., 2000, Szczesniak, 1963a).

The imitative test combines the advantages of fundamental and empirical tests. A typical example is the GF texturometer. The GF texturometer provides seven textural parameters on one curve in every bite: hardness, adhesiveness, fracturability, cohesion, springiness, chewiness and gumminess. The physical definitions of texture parameters are listed in Table 2-1 given by Szczesniak (2002). However, due to different opinions of individuals and their traditions, in some cases, the same terminology is given by different

definitions and the same definition is given to different terminologies as discussed by Jowitt (1974) and Breene (1975).

Table 2-1. Physical definitions of texture parameters (Szczesniak, 2002)

Texture Parameters	Definitions
Hardness	Force necessary to attain a given deformation
Adhesiveness	Work necessary to overcome the attractive forces between the surface of the food and the surface of the other materials with which the food comes in contact
Fracturability	Force with which a material fractures: a product with high degree of hardness and low degree of cohesion
Cohesion	Extent to which a material can be deformed before it ruptures
Springiness	Rate at which a deformed material goes back to its original condition after the deforming force is removed
Chewiness	Energy required to masticate a solid food to a state ready for swallowing: a product of hardness, cohesion and springiness
Gumminess	Energy required to disintegrate a semi-solid food to a state ready for swallowing: a product of a low degree of hardness and a high degree of cohesion

The deformation measurements on cylindrically shaped food material with commonly applied texture probes (plate and ball) are shown in Figure 2-2. In this case, the geometry of probes should be taken into consideration to evaluate the deformation of food tissues and will be discussed later in this thesis.

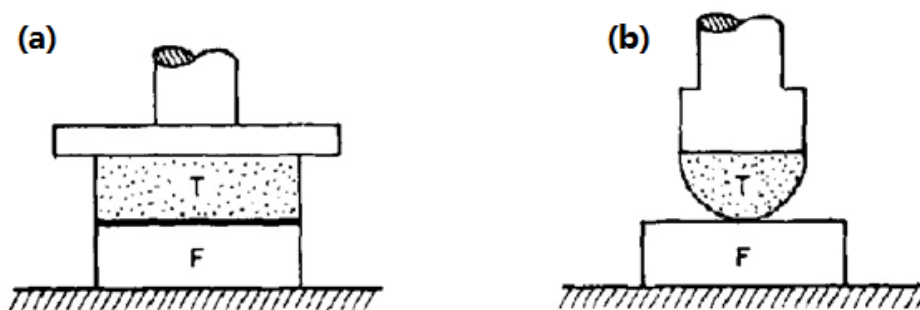


Figure 2-2. Texture machines with sample simple geometries. T: the machine part representing the human tissue; F: the tested food specimen (Campanella and Peleg, 1988, copyright permission has been obtained)

Textural Profile Analysis (TPA) is used as the foundation for the texture measurement of apples and to determine their strong correlation with sensory attributes. By using the TPA approach, Anantheswaran et al. (1985) found that the changes of texture during thermal processing was complex. Hardness decreased dramatically during the first few minutes of processing and the other texture attributes reacted differently depending on the different variety of apples.

Texture is largely dependent on the treatment. Askari et al. (2006) studied the effects of different processing methods on the texture of apple slices. It was reported that samples under air drying had higher firmness than other methods (freeze drying and microwave drying) due to the shrunken structure. Compared to air dried, the freeze dried and microwave samples were more porous but less firm. Osmotic pretreatment decreased hardness of tomato samples during drying. Specifically, convective air microwave drying decreased hardness by 60 % (Askari et al., 2009).

Chauvin et al. (2010) measured sensory attributes of apple and pear samples by using a Guss Fruit Texture analyzer for compressive forces. They employed both tensile and compression elastic modulus for tensile determination, compared to results from a sensory panel. Strong relationships were found between instrumental determinations and sensory attributes, using both the Sinclair iQ™ and the Guss pressure sensor.

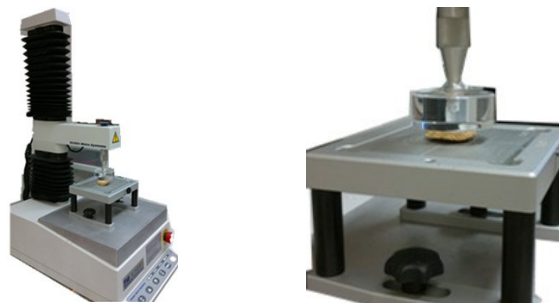


Figure 2-3. TA-XT plus texture analyzer (Stable Micro System, Surrey, UK)

A recent texture measurement machine - TA-XT plus texture analyzer (Stable Micro System, Surrey, UK) (Figure 2-3), automatically simulates specific or real-life situations of oral processing with variable speed and a stress-strain curve performed by the software during measurement. An example of a TPA plot of a force-time curve is given in Figure 2-4. It represents hardness-time as automatically plotted by the computer.

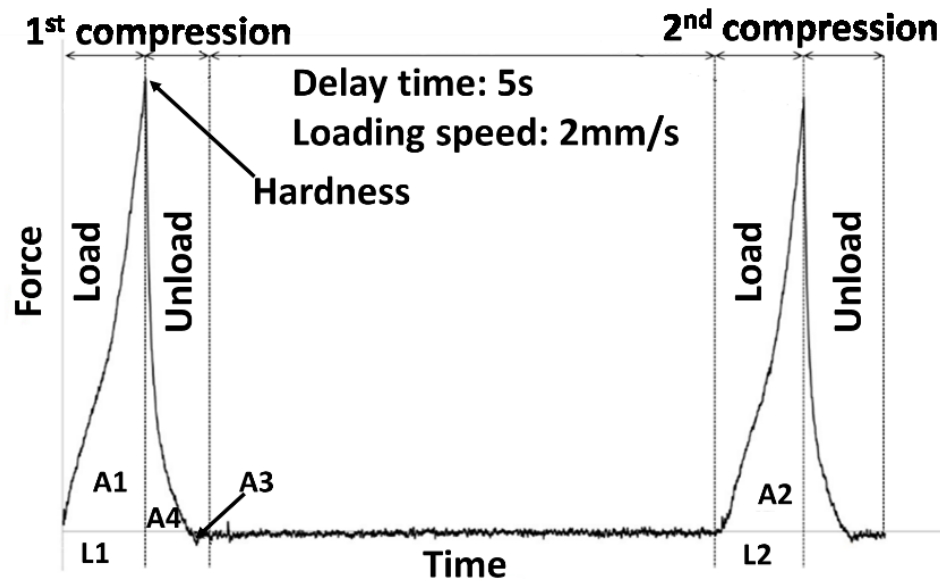


Figure 2-4. Force-Time curve of texture measurement from TA-XT plus texture analyzer

Table 2-2. TPA parameters and calculations from the force-time curve (Bourne, 2002)

Parameters	Calculations
Hardness	The peak force at the first loading cycle
Cohesion	The ratio of load area of second compression (A2) to the load area of first compression (A1): $A2/A1$
Adhesiveness	The negative unload area in the first compression: A3
Springiness	The ratio of height after second load (L2) to the height after first load (L1): $L2/L1$
Resilience	The ratio of unload (A4) area to load area (A1) in the first compression: $A4/A1$

The other texture parameters calculated from the force-time curve are presented in Table 2-2 (Bourne, 2002). Strong relationships were found between instrumental determinations with TPA and sensory attributes (Szczeniak, 1963b).

To date, despite the long time commercial availability of TA-XT, real-time prediction is not accessible from texture measurement. Hence, food plant microstructure should be investigated to give the possibility of continuous estimation.

2.4 Food Plant Microstructure

2.4.1 Initial Structure of Plant Tissue

The living plant tissue has a well-organized structure. Crapiste et al. (1988) defined plant tissue as a four-component system: vacuole, cytoplasm, cell wall and intercellular spaces (Figure 2-5). The shapes of mature parenchyma cells are isodiametric polyhedrals with an average flesh cell being 14-hedral (Lewicki and Porzecka-Pawlak, 2005, Lewicki and Pawlak, 2003, Sterling, 1963). The cell's size depends on its location in the plant tissue. Cells in the outer flesh are slightly smaller than those in the inner flesh near the core (Lewicki and Pawlak, 2003).

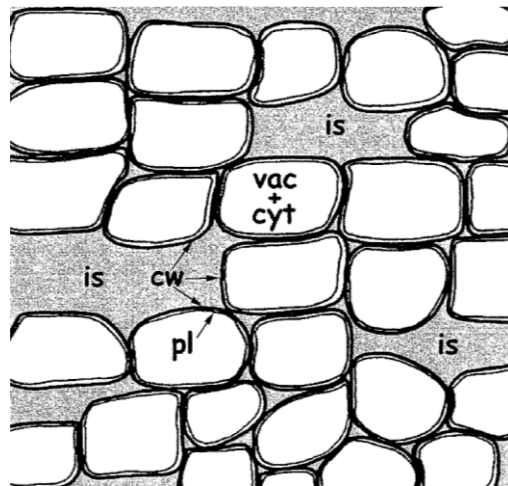


Figure 2-5. A schematic representation of the parenchyma tissue of apple. (is): intercellular space; (cw): cell wall; (pl): plasmalemma; (vac): vacuole; (cyt): cytoplasm. (Prothon et al., 2003, copyright permission has been obtained)

Ninety percent of plant water has low molecular-weight constituents (sugars, organic acids and salts) and they are located in the vacuole. Aqueous solutions with high osmotic

pressure (0.3-1.0 MPa) maintain a turgor on the cell interface (Lewicki and Pawlak, 2003), which is responsible for the firmness and crispness of fresh plant tissue (Ilker and Szczesniak, 1990).

Cytoplasm consists of colloidal solution enclosed within the plasmalemma. The cytoplasm is composed of proteins and lipoproteins in water, salts and organic molecules, which maintain high viscosity. The adjacent plant cells are interconnected with thin strands known as plasmadesmata regulating the transport of water, small molecules and ions between cells (Aguilera and Stanley, 1999).

The cell wall consists of complex organic polyphenols (fiber, cellulose). Carpita and Gibeaut (1993) interpreted cell wall structure as three interacting, but structurally independent domains. The semi-elastic cell wall structure is primarily built with cellulose. Depending on the maturity of plant tissue, the contents of the cellulose-hemicellulose domain varies from 50 % to 65 % of the dry weight of the cell wall. Around 50 % to 60 % of cellulose in the plant cell wall is in a crystalline state, interconnected with amorphous regions. Under high moisture content, the rubbery state gives high matrix mobility and low mechanical strength of amorphous solids. The rapid removal of water leads to the formation of an amorphous solid. At low moisture, the amorphous solid becomes glassy, with low mobility and high mechanical strength. The glass transition occurs when moisture content under a critical range and temperature of dried material becomes equal to the glass transition temperature. This temperature is calculated from the Gordon-Taylor equation (Gordon and Taylor, 1952):

$$T_g = \frac{T_{gs}w_s + kT_{gw}w_w}{w_s + kw_w} \quad (2-3)$$

Where, T_g and T_{gs} are the glass transition temperatures of the binary mixture and dry matter (solids). T_{gw} is the glass transition temperature of water taken at $-135\text{ }^\circ\text{C}$ (Johari et al., 1987). w_s and w_w are the weight fractions of solids and water, respectively. k is a constant parameter of the model.

After glass transition, the material becomes rigid and volume reduction is restricted (Katekawa and Silva, 2007, Roos, 1995).

The structural skeleton of the cell wall consists of fine, unbranched threads called cellulose microfibrils, which are interlocked by hemicellulose; the interstices are filled with pectin substances. Lewicki and Pawlak (2003) stated that cellulose gives rigidity and strength to the cell wall, along with the divalent cations such as magnesium and calcium (Feinberg et al., 1973). The presence of hemicellulose and pectin substances are the most important factors in providing plasticity and resistance to cell wall collapse during drying. The function of cell wall carbohydrates to bond and hold water affects the textural attributes of plant tissue.

The middle lamella (mainly formed by pectin) is a thin membrane, which glues the adjacent cells together. Aguilera (2005) found that the state of the middle lamellae has significant impact on hardness of plant tissues. It was reported that in soft beans the middle lamellae between cells were dissolved, while in hard beans it adhered cells to another. The intercellular spaces (air) occupy 25 % to 40 % of the tissue volume. Mature apple tissue is not fully saturated contributing to pore formation during drying (Prothon et al., 2003, Khan and Vincent, 1993). As cells got matured, intercellular spaces were formed and distributed anisotropically (Lewicki and Pawlak, 2003). The distribution of intercellular free space in plant tissue affects porosity development. The air volume in fresh fruits is quite small at

less than 10 percent in pears (Ho et al., 2009, Schotsmans et al., 2002). During storage, intercellular spaces and porosity increase (Alvarez et al., 2000). The food microstructure properties depend on the evolution of the initial structure of plant tissue.

2.4.2 Food Microstructural Properties

2.4.2.1 Density

Carbohydrates, proteins and lipids are the three main components of plant tissue (Ilker and Szczesniak, 1990). Carbohydrates maintain the hardness of fruits, while proteins and lipids maintain the membrane integrity. Solid density (ρ_s) of plant tissue depends on the density of each component, carbohydrates, lipids and protein, and their proportion, which is expressed as:

$$1/\rho_s = w_C/\rho_C + w_L/\rho_L + w_{Pr}/\rho_{Pr} \quad (2-4)$$

Where, w is the specific weight of each component. ρ_C , ρ_L and ρ_{Pr} are the densities of carbohydrates, lipids and proteins, respectively. The proportion of each component varies from species and maturity. Typically, in a ripe apple, the proportion of carbohydrate in weight is 96.55 %, 2.07 % and 1.38 % for protein and lipids, respectively (USDA, 2014).

$$1/\rho_s = 96.55 \%/ \rho_C + 1.38 \%/ \rho_L + 2.07 \%/ \rho_{Pr} \quad (2-5)$$

Bulk (ρ_b) and particle (ρ_p) densities are determined by the volumetric ratio of moisture and air content in the plant tissue. They can be measured (see 2.4.2.3) or calculated from theoretical relationships (Guine, 2006):

$$\rho_b = \frac{1+X}{\left(\frac{1}{\rho_{bo}}\right) + \xi\left(\frac{X}{\rho_{bo}}\right)} \quad (2-6)$$

$$\rho_p = \frac{1+X}{\left(\frac{1}{\rho_s}\right) + \left(\frac{X}{\rho_w}\right)} \quad (2-7)$$

Where, X is moisture content on the dry basis, ξ is the volumetric shrinkage coefficient, ρ_{bo} is the bulk density of dry solids, ρ_s is the solid density and ρ_w is the water density.

2.4.2.2 Porosity

As fruits ripen, cell size is enlarged and more intercellular spaces are filled with air directly affecting porosity (ε). At early drying stages, as water content decreases causing the cells to shrink, which compensates with tissue shrinkage. As drying continues, a disproportion between water removal and shrinkage results in different degrees of porosity development. Porosity is calculated from bulk and particle density, which is expressed as (Guine, 2006):

$$\varepsilon = 1 - \frac{\rho_b}{\rho_p} \quad (2-8)$$

Assuming theoretical relationships (equations 2-6, 2-7 and 2-8), porosity can be also determined as a function of moisture content (X) and bulk volume shrinkage (ξ_V) (Martynenko, 2008):

$$\varepsilon = 1 - \alpha \frac{1+\beta X}{1+X_0} * \frac{1}{\xi_V} \quad (2-9)$$

$$\xi_V = \frac{V(t)}{V_0} \quad (2-10)$$

Where, X_0 is original moisture content, α and β are density ratio, $\alpha = \rho_o/\rho_s$, $\beta = \rho_s/\rho_w$, ρ_o is initial density, ρ_s is solid density and ρ_w is water density.

2.4.2.3 Volume

2.4.2.3.1 Bulk Volume

Bulk volume includes the volume of solids, liquid and pores (both open and closed). It can be calculated from either dimensional measurements or by volume displacement (Webb, 2001). The most direct instrument for dimensional measurements is using a digital

caliper. The best accuracy is achieved by using the caliper measurements, if a sample has a regular shape (cube, rectangle or cylinder). However, non-homogenous shrinkage of food materials during drying distorts regular shape (Katekawa and Silva, 2004). In this case, an individual's skill and applied force may have a significant effect on the accuracy of measurements.

Bulk volume can be also measured by solid or liquid displacement (Levine et al., 1990, Rodríguez-Ramírez et al., 2012). For example, Joardder et al. (2015) used glass beads of 57 μm diameter to measure volume of coated apple slices with a high accuracy. The other method is based on Archimedes principle, where bulk volume is determined by buoyant force. Accuracy of measurements depends on the liquid used. If it is mercury, coating is not required due to the high surface tension at the air interface. However, coating is necessary when samples are immersed in water or organic solvent (toluene, heptane and hexane) with low surface tension. Katekawa and Silva (2004) found that compared to water, measuring bulk volume in N-hexane is faster and the accuracy are similar. However, mercury and organic solvents are toxic, which brings environmental and safety concerns. Besides that, the thickness of coating could affect the accuracy of volume measurements.

Imaging is a promising computer-aided technique for bulk volume measurements with the advantages of continuous volume change observation (Sabliov et al., 2002, Deltel et al., 2001, Hahn and Sanchez, 2000, Levine et al., 1990). However, the accuracy of imaging depends on multiple factors, such as illumination, pixel distortion, sample morphology, etc. (Martyntenko, 2006). Imaging of axi-symmetrical samples requires specialized algorithms (Wang and Nguang, 2007, Sabliov et al., 2002).

2.4.2.3.2 Particle Volume

Particle volume includes solid, water and closed-pore volumes (Webb, 2001). Particle volume is measured using displacement method with some modifications, such as application of vacuum or additional pressure. In a vacuum pycnometer, samples are immersed in water or other liquid, which brings the risk of liquid absorption and possible error of volume measurement. When using the positive pressure pycnometer, the samples are exposed to external pressure. The advantage of the positive pressure pycnometer is that it measures pore size distribution from the pressure applied (Webb, 2001). In the case of mercury, calculations are based on the Washburn equation in the assumption of cylindrical pores (Vennat et al., 2009, Karathanos et al., 1996):

$$P \cdot r = 2 \cdot \gamma \cdot \cos\theta \quad (2-11)$$

where, P is pressure, r is radius of pores (cm), γ is surface tension (N/cm) and θ is contact angle ($^{\circ}$).

Mercury displacement provides accurate readings as high as $\pm 3\%$ using known volume of nonporous solids as references (Lozano et al., 1980). Helium is a safer alternative to mercury (Marousis and Saravacos, 1990). It is widely applicable for volume measurements of different biomaterials due to the best penetration ability (Guine et al., 2006, Rahman et al., 2005). However, it should be noted that some isolated pores inside of certain biomaterials are not accessible to helium (Chang, 1988). Volume is calculated from pressure difference (Instruments, 2012):

$$V = V_{CE} - V_R \left(\frac{P_1}{P_2} - 1 \right) \quad (2-12)$$

where coefficients V_{CE} and V_R are specific for the particular measuring chamber. P_1 is pressure reading of the reference volume and P_2 is pressure reading of the sample holder.

2.4.2.3.3 Solid Volume

For solid (true) volume measurements, all other phases (liquid, gas) should be excluded. To exclude the liquid phase, samples must be bone-dried. To exclude closed pores, samples must be fine-grinded (Sereno et al., 2007, Chang, 1988).

2.4.2.4 Examining of Food Microstructure

There is a variety of techniques for volume, density and porosity determination, objective of measurements help to choose an appropriate technique. Measurement accuracy largely depends on the methods applied due to the degree of void spaces included in the sample materials. Open pores are on sample surface, which are connected to the ambient environment and closed pores are located inside the sample, inaccessible from the surface. Based on the pores included in the samples, density is divided into three common categories. Density of sample including open and closed pores is defined as bulk density. Apparent density (also called particle density) including only open pores but not closed pores. The term true density reflects density of solid matrix (skeleton). In other words, it excludes open and closed pores. Porosity, as showed above, is calculated from bulk and particle density. Hence, the determination of volume is important for both density and porosity identification. There is a variety of methods (pycnometer, buoyancy, density gradient column, etc.) for density and porosity determination for regular and irregular shapes of samples through volume measurement.

2.4.2.4.1 Dimensional Measurement

The most direct measurement of bulk volume is to use a vernier or physical caliper (Karathanos et al., 1996, Marousis and Saravacos, 1990, Guine et al., 2006, Moreira et al., 2000, Ochoa et al., 2002). The advantage of direct dimensional measurement is its

simplicity and the results obtained were found to be sufficiently accurate for the dehydration of apple slices (Moreira et al., 2000) and other fruits and vegetables. For instance, Ochoa et al. (2002) reported percentage error of area estimation of the whole sour cherry fruit, ranging from -6.86 % to 6.92 %. This method works well when the samples have regular shapes but it is not always accurate at the last stages of convective drying. In addition, the error could increase for semi-dried samples, which are particularly sensitive to the force applied by the operator. Hence, the physical properties of materials and subjective judgement of an operator could affect the results of direct dimensional measurements.

2.4.2.4.2 Buoyancy Force

The buoyancy force method requires weighing samples in the air and liquid with a known density (water, mercury, toluene etc.) (Rahman et al., 2005, Khraisheh et al., 2004, Lozano et al., 1983). Volume can be calculated from the density and mass measurements. Coating is necessary when samples are immersed in specific liquid (e.g. water), as the liquid might be absorbed by the samples and resulting in an overestimation of weight. For mercury, coating is not required because of high surface tension and negligible absorption (Lozano et al., 1980). Ochoa et al. (2002) have investigated volumetric shrinkage measured using buoyancy force and dimensional methods and reported that the percentage error between two methods ranged from -11.9 % to 8.1 %. This method is recommended for separation of materials according to the density (Webb, 2001). The density of material is determined when materials either begin to sink or float or suspended at the neutral density in the liquid (Webb, 2001). Hence, this method is not able to measure the exact density of

the material, instead it only gives an estimate of density with reference to the density of liquid medium, and is not employable for continuous estimation during drying.

2.4.2.4.3 Liquid Displacement

Samples are placed in a container of known liquid volume and the resultant volume displacement measured (Wu et al., 2007, Venir et al., 2007, Madiouli et al., 2007, Lewicki and Jakubczyk, 2004, Azzouz et al., 2002, Tsami and Katsioti, 2000). Similar as the buoyancy force method, coating is necessary, due to possible absorption of the material immersed in the liquid. A comparison of results for the bulk volume of pears estimated from both dimensional measurements and liquid displacement was performed by Guine et al. (2006). Liquid displacement was considered as more accurate, due to a more consistent replication when compared with dimensional measurements (Guine et al., 2006). Compared with water and toluene displacement, the differences were less than 2 % (Guine et al., 2006). The application of n-heptane yielded the lowest coefficient of variance and was recommended for bulk volume measurements of both fresh and dried fruit samples (Yan et al., 2008). This liquid displacement enables the measurements of irregular samples but not appropriate for real-time measurement. Also, most of the displacement media are toxic, such as mercury and toluene. Besides that, the effect of the volume of the coating material should be taken into consideration.

2.4.2.4.4 Solid Displacement

The use of solids-air pycnometer (glass beads) was reported as a reliable and reproducible volume measurement for materials within a wide range of moisture contents from 6.5-0.5 g/g (Joardder et al., 2015, Yan et al., 2008, Cui et al., 2008, Oppenheimer et al., 1997, Levi and Karel, 1995). The size of glass beads should correspond to the size of

open pores. Pore sizes were found to range from 50 nm to 200 μm on the surface of apple slices when dried in an oven at 70 $^{\circ}\text{C}$ under natural convection (Joardder et al., 2015). Coating of material is necessary, if the diameters of the glass beads are smaller than the pore sizes, glass beads may enter the open pores. However, when glass beads have larger diameters than the pore size, the low compactness increases the uncertainty of the spare spaces between beads during measurements, which increase the error of measurements. Thus, selecting an appropriate size of glass beads is important. It was found that the difference between direct dimensional measurements and bulk volume measured with solid displacement with glass beads' with a diameter of 57 μm was between 0.1-2 % (Joardder et al., 2015). Hence, knowing the pore size and the size of glass beads is of great importance for volume measurements of porous materials. Moreover, due to the fluidity of the glass beads, it might be difficult to maintain the constant density and the volume of the glass beads during measuring possibly strongly influencing volume measurements. Solid displacement is also not adequate for continuous bulk volume estimation.

2.4.2.4.5 Imaging Method

Non-destructive methods include laser micrometers (May and Perré, 2002), X-Ray microtomography (Léonard et al., 2003) and imaging (Madiouli et al., 2011). High-speed laser scan micrometers have also been used to monitor the shrinkage of potatoes, carrots, apples and avocados, which allows evaluation of the exchange surface area at any time during drying (May and Perré, 2002). X-Ray microtomography with Skyscan at 1 mA and a spatial resolution of 41 μm was also used to monitor the evolution of the volume of sludge samples. In addition, a 3D Digital Image Correlation method (3D-DIC) has also been used to determine the volume of banana during drying by reconstruction of its 3D shape

(Madiouli et al., 2011). Chen and Martynenko (2013) used imaging to determine the volume of blueberries by capturing images from the top (diameter) and side (diameter) cameras during convective drying. They stated that the accuracy depends on the pixel resolution of cameras. When samples twist or bend, the void spaces are invisible to a vision system, which is a limitation of imaging methods. It has been reported that these methods are accurate for volume measurements of symmetric and uniform samples (Martynenko, 2006). Recently, measurement of the volume of irregular non-symmetric materials (the salmon fillet) was achieved using stereoscopic computer vision (Quevedo and Aguilera, 2010). Compared to other methods, the biggest advantage of imaging is that it allows continuous estimation of bulk volume, which makes possible for texture prediction in food processing industry.

2.5 Relevance for the Industry

The final target of this research is to equip the food processing industry with a versatile and scalable CV technique to optimize drying operations. Once the objectives of the proposed research have been achieved, a scalable CV system could be designed for the food industry, which will allow to process foods with desired texture for different groups of consumers by controlling the microstructure in real-time. Later, the application of developed CV technique for apples could also be used to optimize drying of other fruits and vegetables.

Chapter 3. Hypothesis and Objectives

3.1 Problem Statement

The effect of drying conditions on microstructure and texture have been separately and extensively studied, however, the gap in the relationship between microstructure and texture has not been filled. Although it was found from the literature that texture of final food products is affected by the microstructure formed during drying; the detailed information on their relationships are scarce. The evolution of microstructure, texture and their relationship need to be investigated, and results would be used to optimize the drying process and improving quality of dried food materials.

Dimensional changes of materials can be monitored by a computer vision system in real-time, however, texture cannot be assessed during drying. We assumed that the estimation of texture changes from a computer vision system in real-time will be achievable, once the relationship between texture parameter and porosity are defined.

The overall goal of this research is to develop a computer vision system that is able to predict and control texture changes of apple slices during convective drying and produce dried apple slices with desired qualities.

3.2 Hypotheses

In this thesis, we assumed that texture is affected by porosity changes during drying. The relationship between texture and porosity could be represented by taking the moisture content and dimensional changes of apple slices into consideration. It is possible to predict and control texture changes of apple slices during drying by using a computer vision system with subsequent image processing and extraction of information on area shrinkage, and continuous moisture content identification from real-time mass monitoring.

3.3 Objectives and Scope

The following objectives must be implemented in order to prove/reject the initial hypothesis:

Objective 1: Determine if CV is applicable for bulk volume measurements:

- Off-line: Off-line bulk volume measured with digital caliper will be used as a reference volume, assuming cylindrically shaped apple slices throughout the entire drying process. Conduct dimensional measurements of bulk volume at different drying time with different moisture contents.
- Real-time: Use different algorithms of CV to estimate bulk volume of apple slices during process of drying with regular shape assumption.
- Evaluate applicability of CV by correlating results with off-line measurements.
- Verify of the relationship at drying different temperatures (40°C and 60°C).

Objective 2: Study the effect of porosity on texture parameter at different stages during the process:

- Porosity determination: Calculate and measure porosity at different moisture contents from a theoretical model and helium pycnometer, respectively.
- Texture measurement: Measure texture of apple slices at different stages with different moisture contents using TA-XT texture analyzer.
- Correlate texture parameters with porosity changes.
- Evaluation performance of various drying scenarios (40°C and 60°C).

Chapter 4. Estimation of Total, Open- and Close-Pore Porosity of Apple Slices During Drying

Copyright permission:

A version of this chapter has been published in the Drying Technology: An International Journal 34 (2016) 892-899. The co-authors' permission is in Appendix under requirement.

Contribution statement:

I was responsible for preparing samples, designing and performing all the experiments, samples and data analysis, as well as manuscript preparation.

Abstract

The purpose of this research was to develop an approach for porosity estimation in the process of convective drying. Fresh apple slices were exposed to 80 °C convective drying to equilibrium moisture content 0.2 g/g. Porosity at different stages of drying was estimated using three approaches: (1) direct volume and mass measurements, (2) pycnometer measurements and (3) theoretical model. All three approaches were in good agreement in the range of moisture contents above 1.0 g/g. However, at moisture contents below 0.26 g/g, significant deviation of pycnometer measurements from both experimental estimates and theoretical model was observed. This difference could be explained by transformation of open pores into closed pores due to glass transition phenomena. This study presents an example of separate quantitative estimation of total, open- and closed-pore porosity.

4.1 Introduction

Porosity is one of the most important indicators of food microstructure and texture. It is defined as the ratio of total volume of air voids of a given porous material to its total bulk volume of the material (Webb, 2001).

$$\varepsilon = \frac{V_a}{V_s + V_w + V_a} \quad (4-1)$$

Where, ε is porosity, V_a is air volume, V_w is water volume and V_s is solid volume.

Experimental measurements of volumetric changes and mathematical calculation of porosity are commonly used approaches (Zogzas et al., 1994, Sereno et al., 2007, Martynenko, 2011, Lozano et al., 1980, Chang, 1988). Usually, porosity is calculated from the ratio of bulk (ρ_b) and particle (ρ_p) densities, equation 2-8 (Zogzas et al., 1994).

Since density and porosity are calculated from volume measurements, accurate estimation of volume is of great importance. Accuracy of measurements depends largely on the microstructure and moisture content. Since a biological sample is usually a multi-phase system containing air, water and solids, it is important to make the distinction between bulk, particle and solid (true) volumes (Refers to 2.4.2.3).

Measurements of bulk, particle and solid volumes allow calculation of porosity (ε) on the different stages of drying from the equations 4-1 and 2-8. Since periodic measurements of particle volume in the process of drying is technically difficult, some researchers use mathematical models for estimation.

Mathematical models create opportunities to real time porosity estimation. Accurate prediction of porosity changes during drying has a great importance for the optimization of the drying process and control of food quality. Most mathematical models use moisture

content as a predictor. For example, Lozano et al. (1980) gave an empirical correlation for the prediction of open-pore porosity of apples as a function of moisture content (X):

$$\varepsilon = 1 - \frac{\rho_b}{\rho_p} = \frac{0.852 - 0.462 \exp(-0.66X)}{1.54 \exp(-0.051X) - 1.15 \exp(-2.4X)} \quad (4-2)$$

For total porosity of apples, they proposed the equation based on the ratio of cellular (ξ_c) and bulk (ξ_b) shrinkages and cellular dimensions:

$$\varepsilon = 1 - \frac{\xi_c}{\xi_b} \cdot \frac{\pi \alpha_o}{6 \lambda_o^3} \quad (4-3)$$

where, α_o is the geometric value corresponding to the full turgor situation and λ_o is the initial ratio cube side/sphere diameter (cm).

Theoretical models have definite advantages over empirical models, because they are applicable to a range of products and experimental conditions, as well as physical meanings of the parameters (Martynenko, 2008, Rahman, 2003, Chang, 1988). For example, Zogzas et al. (1994) proposed the theoretical model for particle density (ρ_p) as a function of solid (ρ_s), water (ρ_w) densities and moisture content (X), equation 2-7.

It should be noted that this model of particle density takes into account only water and solid volumes. Hence, this approach allows calculation of total porosity without distinction between open and closed pores.

This approach was verified for a variety of fruits and vegetables by Krokida and Maroulis (1997). The same model was also used by Moreira et al. (2000) in convective drying of Golden Delicious apples at 70 °C. They also modified the equation for bulk density (ρ_b) estimation, as a simple function of initial density (ρ_o), shrinkage (ξ) and moisture content (X), as shown in equation 2-6.

The theoretical approach was further developed in the form of a mathematical model for porosity, equation 2-9 (Martynenko, 2008). The accuracy of this model depends on the

accuracy of shrinkage and moisture measurements, as well as the error in parametrical estimation of initial (ρ_o) and solid (ρ_s) densities.

Lozano et al. (1980) indicated that in the process of drying, all pores remain open until moisture content reaches 1.5 g/g (d.b.). They concluded that transformation of open pores into closed pores occurs due to the cellular collapse at the critical moisture content. The empirical equations 4-2 and 4-3 were used for estimation of open-pore and total porosity. However, it has never been verified whether or not the theoretical models (2-6, 2-7 and 2-9) are applicable for separate estimation of open- and total porosity.

The objective of this paper was to verify the accuracy of theoretical model (equation 2-9) for porosity estimation in the range of moisture contents. For this purpose, porosity at different stages of drying was estimated using three approaches: (1) direct volume and mass measurements, (2) pycnometer measurements and (3) theoretical model. Apple slices were used as an experimental object.

4.2 Materials and Methods

4.2.1 Materials and Sample Preparation

Golden Delicious apples harvested in 2014, were purchased locally and stored in a refrigerator at 4 ± 1 °C. Before each experiment, the apples were taken out of the refrigerator and exposed to room temperature (20 °C) for one hour. They were then cut into cylindrical slices with a diameter of 40 ± 1 mm and a thickness of 10 ± 1 mm, from the outer cortex on the plane parallel to the stem-calyx axis. To minimize the fruit-related components of variability, an average of three samples was taken from each apple. Samples were placed randomly and evenly in a single layer on a perforated two-level tray $34 \times 18 \times 10$ cm. Each batch contained 27 samples and the experiments were performed in triplicate.

4.2.2 Instrumentation

Air drying of apple slices was performed in a pilot-scale tray convective dryer UOP8 (Armfield Ltd., Ringwood, UK) (Figure 4-1).

Air temperature was controlled and maintained with precision thermistors YSI 44033 (YSI, Inc., Yellow Springs, OH, USA) with 0.1°C accuracy. Air velocity was constant at 0.9 m/s and periodically measured using Thermo-Anemometer HD300 (Extech Instruments, NI, USA) with 3 % accuracy. The mass of each individual sample was measured with a digital scale HCB1002 (Adam Equipment, Danbury, CT, USA) with 0.01g accuracy. Instantaneous moisture content on dry basis X was calculated on the basis of mass measurements, equation 4-4.

$$X_t = \frac{m_t - m_s}{m_s} \quad (4-4)$$

Bulk volume (V_b) was calculated from dimensional measurements with the assumption of cylindrical shape of the sample. Dimensions (diameter and thickness) of each sample were measured with digital caliper (Mastercraft, TN, USA) with ± 0.02 mm accuracy.

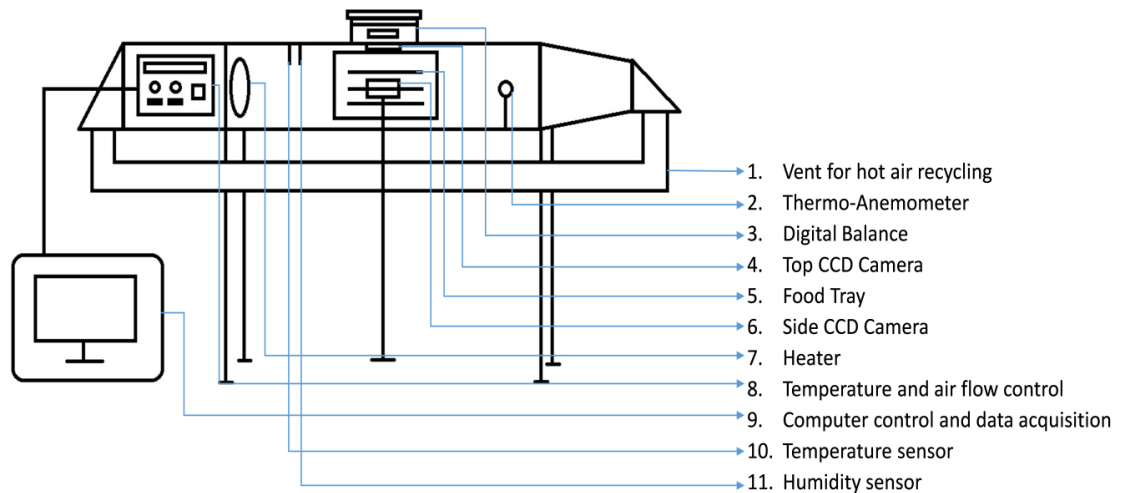


Figure 4-1 Schematic drawing of experimental drying apparatus

Particle volume of intact and semi-dried samples was measured with pycnometer MVP-6DC (Quantachrome, FL, USA) and estimated from equation 2-12, using pycnometer constants $V_{CE} = 11.573 \text{ cm}^3$ and $V_R = 6.089 \text{ cm}^3$ (Instruments, 2012). True volume was measured similarly, but with preliminary bone-drying and grinding of each sample. Calculated values of densities were used to calculate porosity from equation 2-8.

Bulk, particle and true densities were calculated as a ratio of mass and volume:

$$\rho = \frac{m}{V} \quad (4-5)$$

4.2.3 Experimental Procedure

Dryer was preheated to the target temperature (80 °C) before experiment. This temperature was chosen to make sure that samples undergo glass transition at the end of drying. Every hour three samples were randomly taken out of dryer and cooled to room temperature (20 °C) for mass, bulk and particle volume measurements. All samples were dried at 105 °C for 24 hours in the oven 255G (Fisher, ON, Canada) for remove residual moisture. Fine grinding of bone-dried samples was carried out in a coffee grinder CBG100S (Black & Decker, NB, USA). Particle and true volumes were measured with the helium pycnometer before and after grinding to verify initial hypothesis about effect of microstructure on true volume measurements.

4.2.4 Porosity Estimation

Three approaches were used for porosity estimation: direct volume and mass measurements (*expt*), pycnometer measurements (*pycn*) and theoretical model (*theo*).

Direct volume and mass measurements: porosity was calculated from bulk volume (V_b) and mass measurements according to the porosity definition (equation 4-1) by subtraction of volume of solids V_s and volume of water V_w :

$$\varepsilon = \frac{V_a}{V_b} = \frac{V_b - V_w - V_s}{V_b} = \frac{V_b - m_s X - \frac{m_s}{\rho_s}}{V_b} \quad (4-6)$$

Pycnometer measurements: porosity was calculated from bulk volume (V_b) and pycnometer measurements in the assumption that pycnometer measures combined volume of water and solids ($V_w + V_s$):

$$\varepsilon = \frac{V_a}{V_b} = \frac{V_b - (V_w + V_s)}{V_b} \quad (4-7)$$

Theoretical model: equation 2-9.

4.2.5 Statistical Analysis

Each experiment was repeated in triplicate. Porosity estimated from three approaches in nine separate experiments was analyzed from one-way analysis of variance (ANOVA) using Minitab 17 with 95 % significance level of the acceptance limit. Boxplot was used to check the outliers. Tukey's comparison was used to compare the means, variability in the data was expressed as the standard deviation and a $p < 0.05$ was considered as statistically significant (Montgomery, 2013).

4.3 Results

Direct mass measurements show that in the process drying at 80 °C moisture content decreased exponentially, following first-order behavior (Figure 4-2). After six hours, the moisture content reached equilibrium around 0.20 g/g. Volumetric shrinkage followed the decrease of moisture content during 4 hours of drying, until moisture content reached 0.26 g/g. After this point, shrinkage was not observed, which indicated case hardening. This leads to the conclusion that this moisture content should be interpreted as critical, where glass transition occurred.

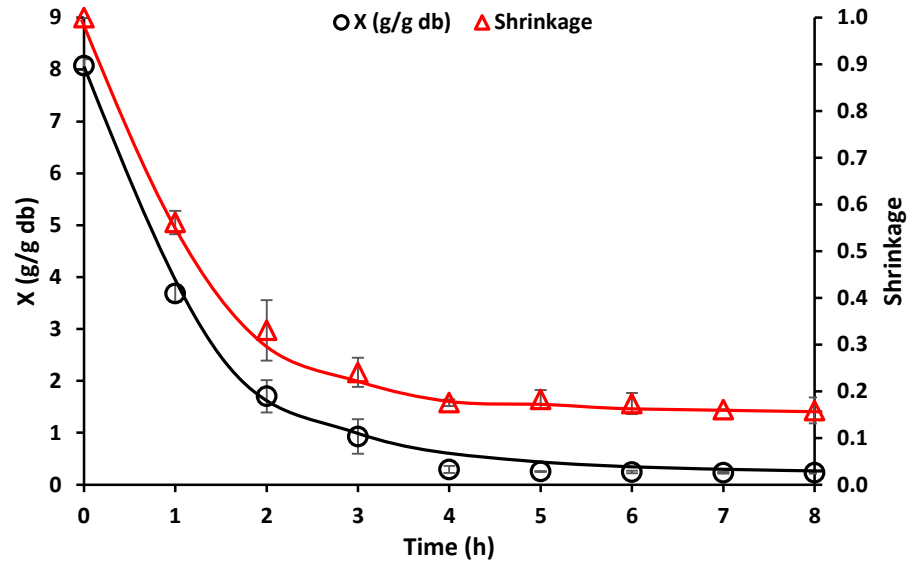


Figure 4-2 Kinetics of moisture content (trend line is based on three replications)

In previous research significant effect of glass transition on sample shrinkage was reported (Katekawa and Silva, 2007). Effect of glass transition on the hardening of apple slices in the range of temperatures from 40 to 80 °C was studied by Martynenko and Janaszek (2014). However, to our knowledge, the effect of glass transition on particle density has never been investigated. In order to investigate if sample microstructure had any significant effect on particle density, the density of bone-dried samples was measured with the pycnometer twice: before and after grinding (Table 4-1).

Table 4-1 Effect of grinding on particle density measured with a pycnometer

Grinding	Density	Number	Mean ± S.D.	P-value
Before	ρ_p	26	0.28±0.02	0.000
After	ρ_s	26	1.50±0.04	

It follows that the density of the samples before grinding was significantly smaller than that after grinding. It could be explained only by the fact of significant effect of close-pore volume. It is logical to assume that before grinding, samples consisted of volume of solids and air trapped in closed pores. From our experiment, it became obvious that closed

pores are not accessible to helium, which is in agreement with Chang (1988). Therefore, it was concluded that density measured by pycnometer before grinding could be considered as particle density, whereas density measured after grinding is solid or true density. From Table 4-1 it follows that solid density was $1.50 \pm 0.04 \text{ g/cm}^3$, which is in the range of 1.025 to 1.620 g/cm^3 for apples (Rodríguez-Ramírez et al., 2012). Hence, fine grinding of samples should be considered as a mandatory step in solid density determination with pycnometer.

Porosity estimated at different stages of drying is presented in Figure 4-3 in time domain and in Figure 4-4 in moisture domain. It follows that all three estimates were in good agreement during the first three hours of drying or in the range of moistures above 1.0 g/g. It is important to mention that the pycnometer was able to accurately measure particle volume at high moisture content, which is in agreement with Sereno et al. (2007). However, after four hours of drying or 0.26 g/g of moisture content, significant difference of pycnometer measurements became obvious. Below this moisture, the pycnometer showed a dramatic decrease in porosity to 0.15. Similar behavior of porosity was observed earlier by Lozano et al. for apples (Lozano et al., 1980) and carrots (Lozano et al., 1983). Since our experiments showed negligible shrinkage at low moisture content, this phenomenon could only be attributed to partial transformation of open pores into closed pores. Table 4-1 proves that closed pores volume is not measurable with the pycnometer, so pycnometer estimation should be considered as open-pore porosity.

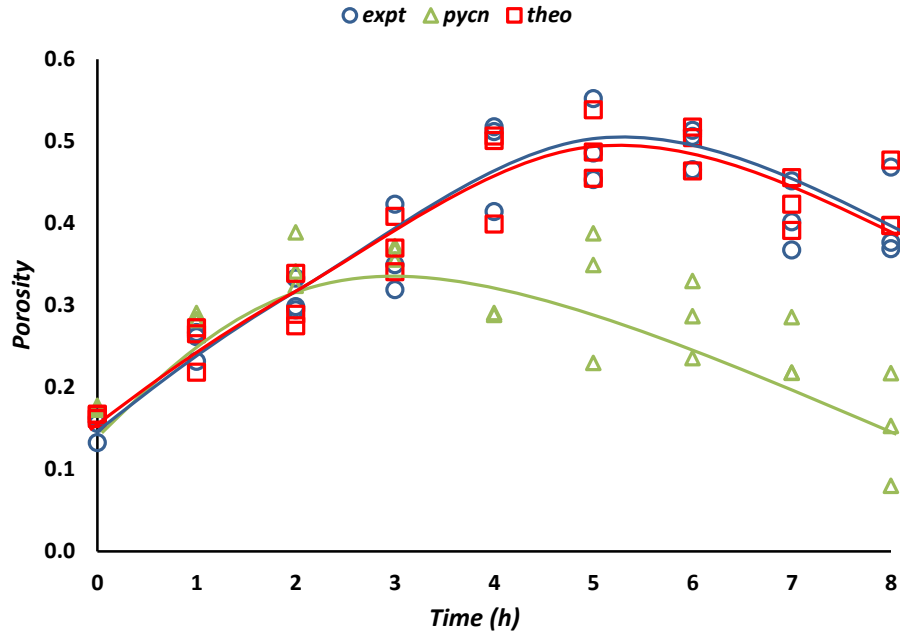


Figure 4-3 Kinetics of porosity estimated from three approaches (trend lines connect average values)

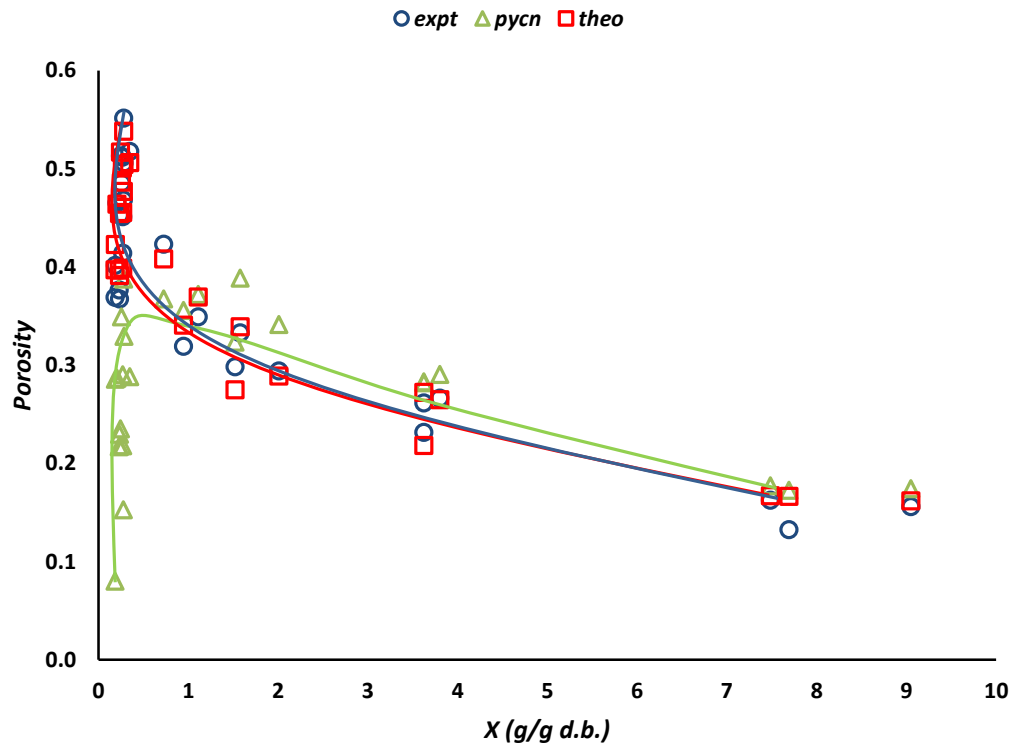


Figure 4-4 Porosity estimated from three approaches as a function of moisture content

In contrast, porosity estimated from experiment and theoretical model increase to 0.5 until samples moisture reached 0.26 g/g and then slightly decreased to 0.45 at the end of drying. It follows that in the whole range of moisture contents the theoretical model was in a good agreement with the experimental measurements. It is important to note, that both theoretical model and experimental measurements give similar estimates of total porosity.

Total porosity progressively increased with the decreasing moisture content, reaching 0.5 ± 0.05 at the end of drying. Open-pore porosity coincided with total porosity in the range of high moisture contents. It means that above 1.0 g/g closed-pore porosity could be neglected. However, below critical moisture content (0.26 g/g in our experiment), open-pore porosity rapidly dropped to 0.15 ± 0.07 , while closed-pore porosity increased to 0.28 ± 0.06 .

Because of the hourly intervals between sampling, it was difficult to identify the exact value of critical moisture content. However, it definitely occurs between 1.0 and 0.26 g/g, which is in the region of glass transition for apple tissue (Peleg, 1994).

4.4 Discussion

Mechanical changes in biomaterials at glass transition point were carefully investigated by Peleg, who developed a relationship between temperature, moisture content and hardness corresponding to glass transition (Peleg, 1994). Implications of glass transition on viscoelastic properties of biomaterials in hot air drying were also discussed by Bhandari and Howes, who identified water activity and temperature as major determinants (Bhandari and Howes, 1999).

Structural changes of apple slices in convective drying were reported by Bourne (1986), Krokida et al. (2000b), Lewicki and Lukaszuk (2000) and Martynenko and

Janaszek (2014). Critical moisture content, where hardness dramatically increased, was identified as 1.8 g/g at 70 °C drying (Lewicki and Lukaszuk, 2000, Krokida et al., 2000b) or 0.04 g/g at room temperature (Bourne, 1986). These findings are in agreement with Martynenko and Janaszek (2014), who found hardening of apple slices occurred on surface layer and core tissue when moisture content below 2.0 g/g and 0.5 g/g, respectively.

In our experiments, absence of shrinkage below 0.26 g/g of moisture content indicated glass transition of the core tissue. It significantly affected the sample microstructure by case hardening and formation of closed pores inside of the sample. A significant difference between particle density before and after grinding, measured with helium pycnometer, suggests fine grinding as a mandatory step in solid density determination.

By comparing experimental data with the theoretical model, it can be concluded about validity of theoretical model for total porosity estimation on all stages of drying. Initial porosity of fresh samples, calculated from pycnometer measurements, was 0.15 ± 0.01 , coinciding with both experimental values and the theoretical model. All three approaches showed initial increasing of porosity with the next decreasing at the end of drying, which is in agreement with other publications (Rodríguez-Ramírez et al., 2012, Lozano et al., 1980). However, moisture content had a significant effect on pore formation. Above critical moisture content (in our experiments 1.0 g/g), open-pore porosity, measured with pycnometer, coincided with experimental values and the theoretical model of total porosity.

$$\varepsilon_{total} = \varepsilon_{op}, (X > X_{cr}) \quad (4-8)$$

where ε_{total} is total porosity, ε_{op} is open-pore porosity and X_{cr} is moisture content at critical point.

Below critical moisture (in our experiments 0.26 g/g), open-pore porosity was much smaller than total porosity, which could be attributed to significant effect of close-pore porosity.

$$\varepsilon_{total} = \varepsilon_{op} + \varepsilon_{cp}, (X < X_{cr}) \quad (4-9)$$

where, ε_{cp} is closed-pore porosity.

Total porosity can be either measured experimentally or calculated from the theoretical model. Considering open- and closed-pore porosity as additive components of total porosity, combined instrumental and theoretical approaches allow calculation of the closed pore porosity by simple subtraction. As an example, data obtained in this research were used to present all components of porosity in Figure 4-5.

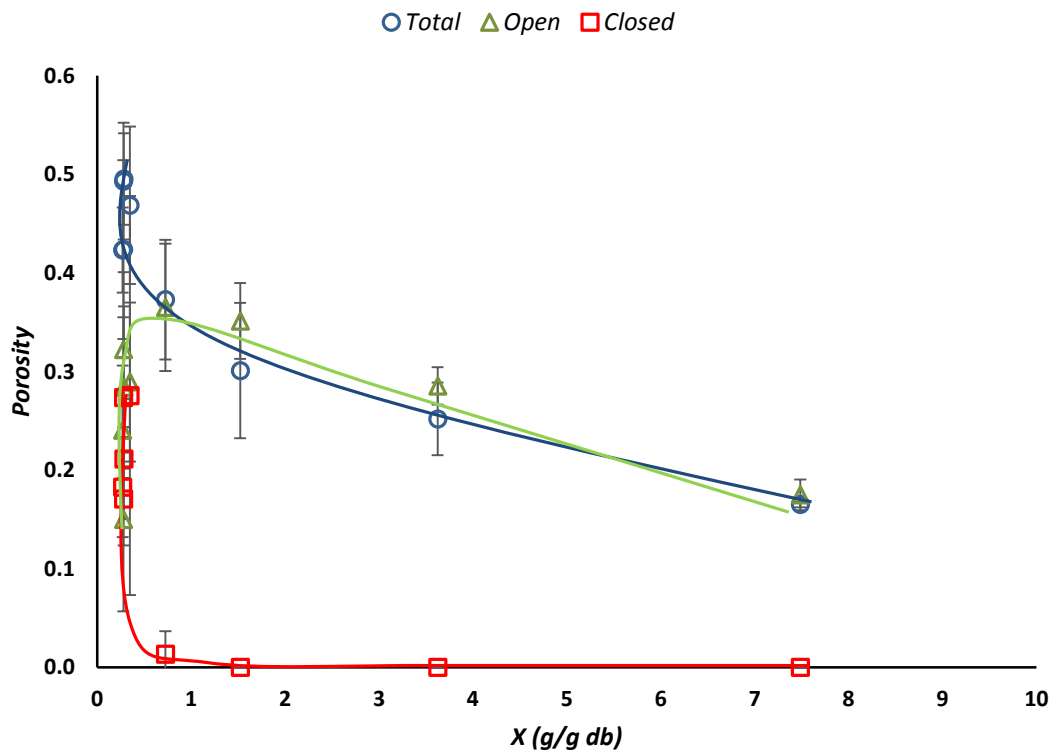


Figure 4-5 Total (circles), open-pore (triangles) and closed-pore (squares) porosity as a function of moisture content

Figure 4-5 shows no significant difference between total and open-pore porosity at high moisture content (above 1.0 g/g). Dramatic decrease of open-pore porosity and subsequent increase of close-pore porosity at the end of drying was observed because of glass transition and case hardening, which made internal pores inaccessible for measurements.

4.5 Conclusions

1. The theoretical model of total porosity (equation 2-9) is valid for the entire period of drying. It is a reliable tool for the estimation of total porosity from volumetric shrinkage and mass measurements in all ranges of moisture content. However, equation 2-8 should be used with appropriate care, taking into account the methodology of particle density measurements. If particle density is measured with the pycnometer, it gives an estimate of open-pore porosity. If particle density is calculated from moisture content (equation 2-7), it gives an estimate of total porosity.
2. Helium pycnometer measures open-pore porosity. In this research it was proved that high moisture content did not affect volume measurements by pycnometer. Therefore, it could be used for measurements of multiphase particle volume.
3. Moisture content had a significant effect on pore formation. Below critical moisture content, the pycnometer showed a dramatic decrease of open-pore porosity, which could be attributed to glass transition and transformation of open pores into closed pores. Open- and close-pore porosities are additive components of total porosity and could be estimated separately on the different stages of drying. By simultaneous measurements of total and open pore-porosity it is possible to calculate closed-pore porosity, which becomes significant below critical moisture content.

Connecting Statement

In the previous chapter, the total porosity was estimated as a function of moisture content and bulk volume shrinkage. The bulk volume shrinkage was calculated from periodic dimensional measurements using a physical caliper. In the next chapter, computer vision was introduced for continuous measurement of diameter and thickness, which could help to estimate bulk volume shrinkage in real-time.

Chapter 5. Computer Vision for Bulk Volume Estimation of Apple Slices During Drying

Copyright permission:

A version of this chapter has been accepted for publication in *Drying Technology: An International Journal*, 2016. The co-authors' permission is in Appendix under requirement.

Contribution statement:

I was responsible for preparing samples, designing and performing all the experiments, samples and data analysis, as well as manuscript preparation.

Abstract

The accuracy of imaging for bulk volume estimation of apple slices in the process of drying at temperatures from 40 °C to 80 °C was investigated and compared with physical caliper measurements. The initial hypothesis was that bulk volume of cylindrically-shaped apple slices could be estimated from diameter and thickness imaging. Imaging of diameter showed strong agreement with caliper measurements throughout the entire drying process, however imaging of thickness was not accurate due to the irregular shrinkage and bending phenomena. A linear model reflecting the relationship between diameter and bulk volume was developed and validated at temperatures of 40 °C, 60 °C and 80 °C. It showed good correlation between imaging diameter and bulk volume changes in the range of moisture contents from 9.1 g/g to 0.25 g/g. The relative percentage error of the prediction model was approximately 6.45 %, which suggests that imaging can be used as a robust tool for bulk volume estimation of apple slices during convective drying.

5.1 Introduction

Bulk volume estimation is critically important for calculation of density and porosity of food materials. Bulk volume changes in drying are caused by changes in the original plant cellular microstructure with water removal. Different foods have different shrinkability, which depends on the drying technology (Martynenko and Janaszek, 2014). For example, freeze drying usually results in non-significant changes to bulk volume (Prothon et al., 2003). Microwave vacuum drying has a faster dehydration rate compared to conventional drying, which results in a rapid increase in bulk volume referred to as explosion puffing (Zhang et al., 2006). In contrast, convective drying leads to a reduction of bulk volume, often called shrinkage (bulk shrinkage). Shrinkage is defined as an instantaneous variable, reflecting relative changes of volume, refers to equation 2-10 (Lozano et al., 1980). Hence, special attention should be given to the bulk volume changes of materials during the dehydration process in order to develop desirable food texture, (Madamba, 2003).

Many methods have been used for bulk volume measurement, namely, dimensional measurement, buoyancy force, liquid displacement, solid displacement and imaging (refers to section 2.4.2.4). However, the challenge of this research was continuous measurement of bulk volume through the entire process of drying.

The objective of this study was to evaluate the accuracy of imaging for continuous bulk volume estimation in the wide range of moisture contents from 9.5 to 0.025 g/g (d.b.). In order to develop a reliable, accurate and robust technique, in-depth understanding of relationship between imaging and physical caliper measurements was needed. The hypothesis was that two-dimensional imaging of diameter and thickness would allow

continuous estimation of bulk volume changes during drying. To prove/reject this hypothesis, an experimental study of apple slices drying under different temperatures using continuous (imaging) and discrete (caliper) measurements of bulk volume at different moisture contents was designed.

5.2 Materials and Methods

5.2.1 Materials and Sample Preparation

Golden Delicious apples harvested in 2014, were purchased locally and stored in a refrigerator at 4 ± 1 °C. Before each experiment, the apples were taken out of the refrigerator and exposed to room temperature (20 °C) for one hour. They were then cut into cylindrical slices with a diameter of 40 ± 1 mm and a thickness of 10 ± 1 mm, from the outer cortex on the plane parallel to the stem-calyx axis. To minimize the fruit-related components of variability, an average of three samples was taken from each apple. Samples were placed randomly and evenly in a single layer on a perforated two-level tray $34 \times 18 \times 10$ cm. Each batch contained 27 samples and the experiments were performed in triplicate.

5.2.2 Instrumentation

Air drying of apple slices was performed in a pilot-scale tray convective dryer UOP8 (Armfield Ltd., Ringwood, UK). Air temperature was controlled and maintained with precision thermistors YSI 44033 (YSI, Inc., Yellow Springs, OH, USA) with 0.1 °C resolution. Air velocity was constant at 0.9 m/s and periodically measured using Thermo-Anemometer HD300 (Extech Instruments, NI, USA) with 3% accuracy. The mass of each individual sample was measured with a digital scale HCB1002 (Adam Equipment, Danbury, CT, USA) with 0.01 g resolution. Another digital scale (WSB-8015, Omega Engineering, Laval, QB, Canada) with 0.1 g resolution was mounted on the top of the dryer for continuous

mass measurement (m_t) of samples during drying. Instantaneous moisture content on a dry basis (X_t) was calculated from instantaneous mass (m_t) reduction from equation (4-4).

5.2.3 Experimental Procedure

Before each experiment, the dryer was preheated to the target temperature. A high temperature of 80 °C was chosen to ensure that samples would develop a crispy texture. According to the Gordon-Taylor equation, moisture content of apple slices below 0.0383 g/g (d.b.) is sufficient for glass transition at room temperature 20 °C (Bai et al., 2001).

Throughout the entire process, every 30 minutes, three samples were randomly taken out of the dryer and cooled to room temperature (20 °C) for mass and bulk volume (V_b) measurements. The other two temperatures, 60 °C and 40 °C, were chosen for verification. Materials were dried until there was no significant mass changes, 480 minutes, 675 minutes and 1860 minutes for 80 °C, 60 °C and 40 °C, respectively. The sampling interval was 45 minutes for 60 °C and 60 minutes for 40 °C, since lower temperature requires more time for water removal.

5.2.4 Bulk Volume Measurements

Bulk volume at different stages of drying was estimated using two methods: (i) direct dimensional measurement with physical digital caliper (Cp) and (ii) imaging (Im) with computer vision.

5.2.4.1 Dimensional Measurements Using Caliper

Dimensions (diameter and thickness) of each sample were measured using a digital caliper (Mastercraft, TN, USA) with ± 0.02 mm resolution, were considered as true values. Bulk volume was calculated from dimensional measurements, assuming cylindrical geometry of the samples. The thickness and diameter measurements with physical caliper

were repeated at least three times at different positions to avoid errors from non-uniform shrinkage and bending. The bended part of the apple slices was visually distinguished and avoided in manual measurements. To reduce the systematic and random error during the experiment with physical caliper, dimensions were measured at different locations of the material. To minimize human factor, only one operator was involved in dimensional measurements with physical caliper. Thickness and diameter values were averaged, based on the physical caliper measurements. The effect of operator and force applied were not considered in the physical caliper measurement.

5.2.4.2 Imaging

Bulk volume was also estimated, using imaging with LabVIEW 8.5 (National Instruments, Austin, TX, USA) imaging acquisition software. It was used to acquire images of apple slices from the top and side and record the data every 2 minutes (Figure 5-1).

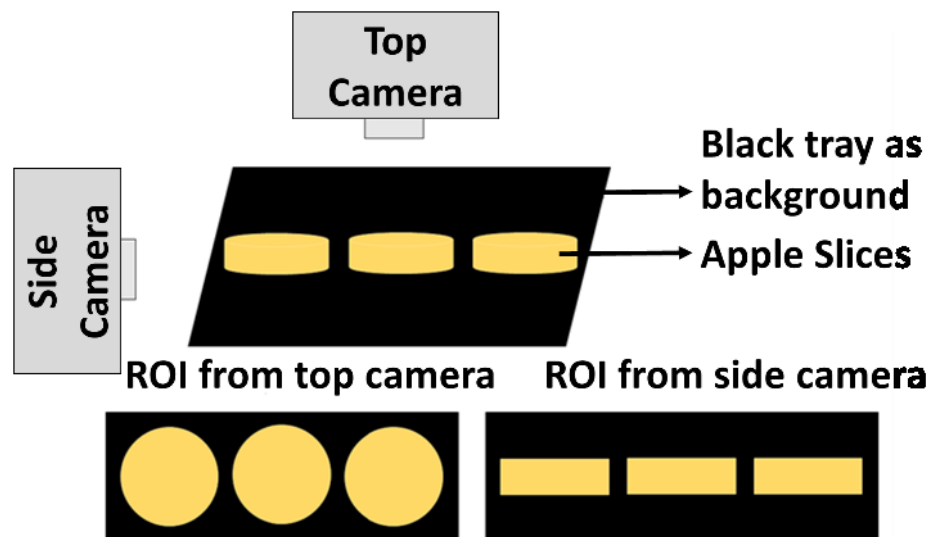


Figure 5-1. Schematic drawing of imaging and region of interest (ROI) from the cameras

The diameter and thickness of apple slices were measured by image processing using different algorithms. The first step for image processing was to set the region of interest

(ROI) and extract the masked region. Hue color plane was used to convert original images to grey images. An appropriate threshold was chosen to convert the grey images to binary images resulting in clear separation of object from the background. Diameter and thickness were estimated, using conversion factors 0.33 mm/pix and 0.14 mm/pix, respectively. Volume was calculated from estimated diameter and thickness, as described in section 5.2.4.1.

5.2.4.2.1 IMAQ Clamp subroutine (single soft caliper)

The diameter and thickness of samples were determined using the IMAQ Clamp subroutine (IMAQ 6.5). The single caliper algorithm was based on edge detection of binary images, measuring the maximum distance between edges along two parallel lines. The IMAQ Horizontal and Vertical Max Clamps' subroutines were applied for diameter and thickness measurements. The Horizontal Clamp measured the maximum distance between two horizontal sides of sample in the vertical direction. The Vertical Clamp measured maximum distance between two vertical sides of sample in the horizontal direction. Diameter was calculated as an average from two orthogonal measurements for each sample. Thickness was measured with only Horizontal Clamp. Three samples were measured simultaneously. Averages, calculated for three samples, were used as representative values for diameter and thickness of apple slices.

5.2.4.2.2 IMAQ Clamp subroutine (multiple calipers)

The multiple caliper algorithm was based on multiple (five) edge detections for thickness measurement of the same sample. This procedure minimized the risk of inaccurate measurements caused by non-uniform shrinkage and sample bending. Unexpectedly

increased thickness and brighter color caused by the reflection were found suitable to be used as indicators of bending. In this case, outliers were removed manually.

5.2.4.2.3 Effect of threshold on segmentation

From previous research it was known that threshold could be easily affected by changes in illumination (Martynenko, 2006). To increase robustness of estimation, the effect of different threshold values at 45, 50 and 55 of grey intensity on the accuracy of diameter estimation were studied. In this experiment, 9 samples were used with 3 samples for each threshold. Average values were calculated from 3 replicates.

5.2.4.2.4 Effect of caliper position adjustments and manual sampling on diameter measurement

Two modes of adjustment of the caliper position were investigated for the single caliper algorithm. In automatic mode (*Auto*) the software detected the sample edges and adjusted the imaging calipers automatically. In the manual mode (*Manu*) caliper position was adjusted manually every 30 minutes. Manual mode was tested in two situations: with (*ManuWi*) and without (*ManuWo*) physical moving of samples required for manual sampling. The effects of caliper position adjustment and manual sampling on the accuracy of diameter measurements were estimated using 9 samples were placed on the top level of the tray, with 3 samples for *Auto*, 3 samples for *ManuWo* and 3 samples for *ManuWi*.

5.2.5. Statistical Analysis

Each of experiment and measurement was carried out in triplicate. The results represented were mean value with standard deviation (s), which was calculated as:

$$s = \sqrt{\frac{\sum(x-\bar{x})^2}{n-1}} \quad (5-1)$$

where, x is the value of each single measurement, \bar{x} is the average of measurements and n is the number of replications.

Relative percent error was calculated to determine the agreement between caliper (Cp) and imaging (Im) values:

$$E(\%) = \sum \frac{|x_{Cp} - x_{Im}|}{x_{Cp}} \times 100\% \quad (5-2)$$

The results obtained by two different measurements were analyzed using two sample t-test at significance level $\alpha=0.05$ in Minitab 17 software (Minitab, State College, PA, USA).

5.3 Results and Discussion

5.3.1 Image Analysis

5.3.1.1 Diameter and thickness estimation with IMAQ clamp subroutine (single caliper)

The IMAQ clamp subroutine was used to determine diameter and thickness from binary images, as shown in Figure 5-2a and 5-2b.

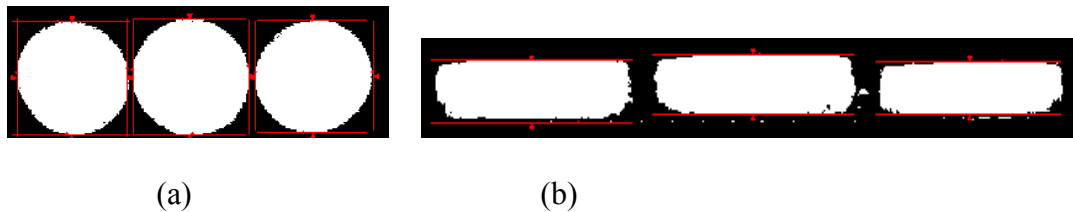


Figure 5-2. The IMAQ clamp measurements of diameter and thickness of fresh samples:
(a) Maximum clamp for diameter measurement (b) Maximum clamp for thickness measurement

For each of 3 samples, diameter was determined twice with a Vertical and a Horizontal Clamp. The average value was used as an estimate of diameter. Graphical representation of diameter and thickness changes, measured with both imaging and physical calipers are shown in Figure 5-3.

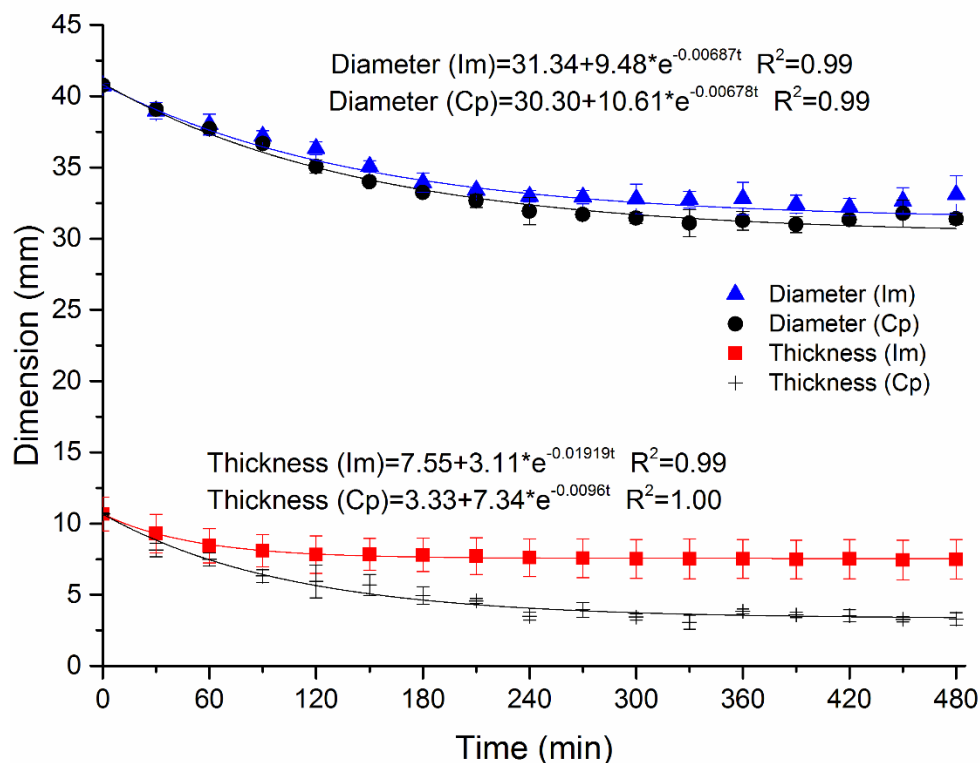


Figure 5-3. Diameter and thickness measured from imaging (Im) and physical caliper (Cp)

At the beginning of the drying process (within 60 minutes), samples shrank uniformly. Imaging diameter was found in a good agreement with the physical caliper measurements through the entire drying process with p-value of 0.098. However, imaging determinations of thickness were found to be statistically deviated from the physical caliper measurements (p-value < 0.05), especially after sample bending (after 60 minutes of drying) (Figure 5-4).

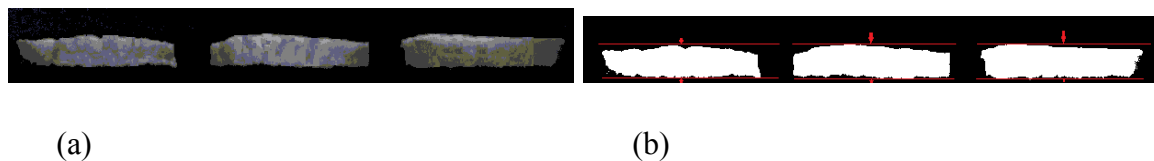


Figure 5-4 (a) Semi-dried samples from side camera; (b) Maximum clamp for thickness measurements of semi-dried samples

The error of estimation became unacceptable towards the end of drying with 127.40% of relative percent error, when samples are bended and hard. Figure 5-5a shows the image

of the dried sample captured from the side camera. Figure 5-5b shows the distorted imaging of thickness, based on the IMAQ clamp procedure.

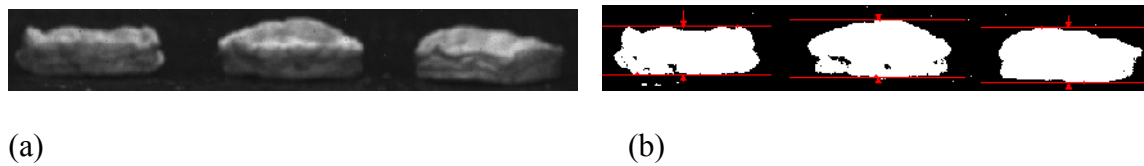


Figure 5-5. (a) Dried samples from side camera; (b) Imaging thickness of dried samples

Since the IMAQ clamp determines the maximum distance between two horizontal lines, when samples started bending, the projection of the distance between the two lines became larger and no longer represented the sample thickness, as shown in Figure 5-5b. Because of the poor fit between single caliper imaging and the physical caliper measurements of thickness, a multiple caliper procedure was tested.

5.3.1.2 IMAQ clamp subroutine (multiple caliper) on thickness measurement

In this case, thickness was measured using multiple calipers. (Figure 5-6).

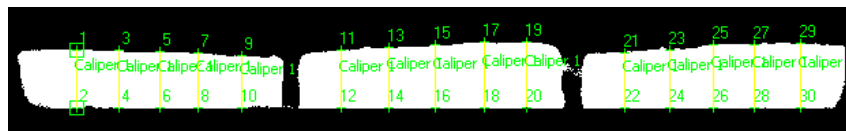


Figure 5-6. Imaging thickness with multiple calipers subroutine

The results of thickness estimation with single and multiple calipers are presented in Figure 5-7. Single- and multiple-caliper imaging corresponded physical caliper measurements for only the first 60 minutes of drying with 8.87% and 4.00% of relative error, respectively.

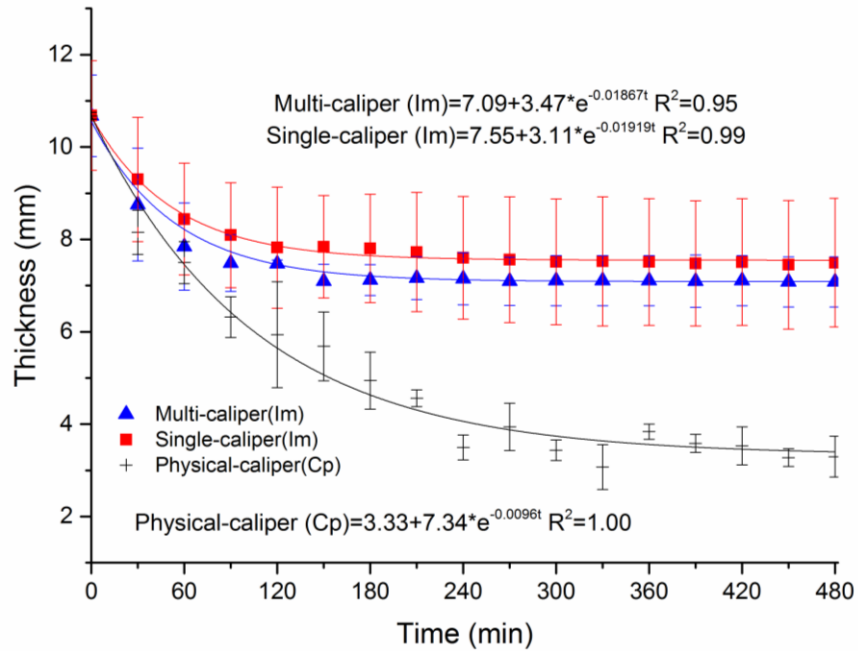


Figure 5-7. Comparison of thickness changes measured from imaging (single and multiple calipers) and physical caliper (C_p)

As the drying continued and the sample started bending, the outliers measured from the points of bending were removed from multiple caliper measurements to avoid systematic error. However, at the end of drying the multiple-caliper estimation resulted in 114.81% error, as compared to 127.40% error by the single-caliper. It could be explained that after 60 minutes of drying, the non-uniform shrinkage led to concave surfaces on the samples, which were not measurable by imaging.

It could be concluded that imaging thickness is not reliable due to the effects of irregular shrinkage and bending. In contrast, imaging of diameter was consistent with physical caliper measurement through the entire drying process.

5.3.1.3 Effect of threshold on diameter measurement

Figure 5-8 compares the imaging of diameter with thresholds 45, 50 and 55 in both time and moisture content domains.

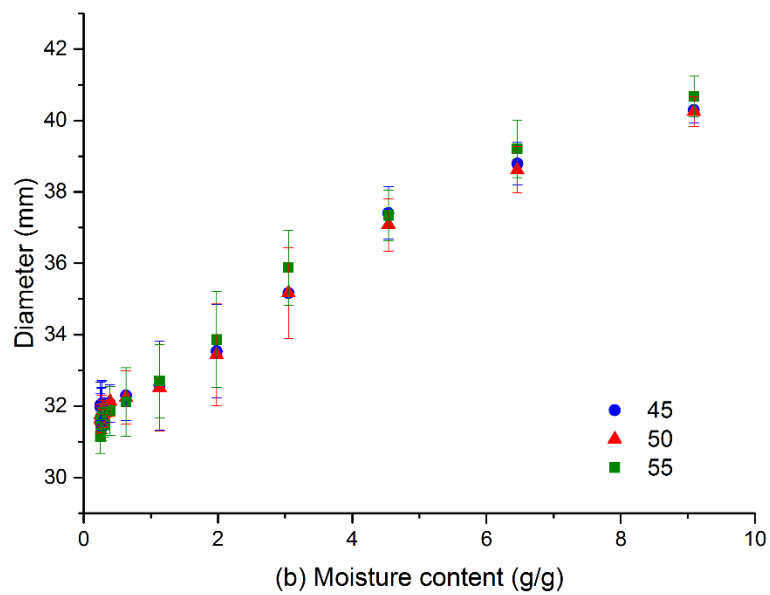
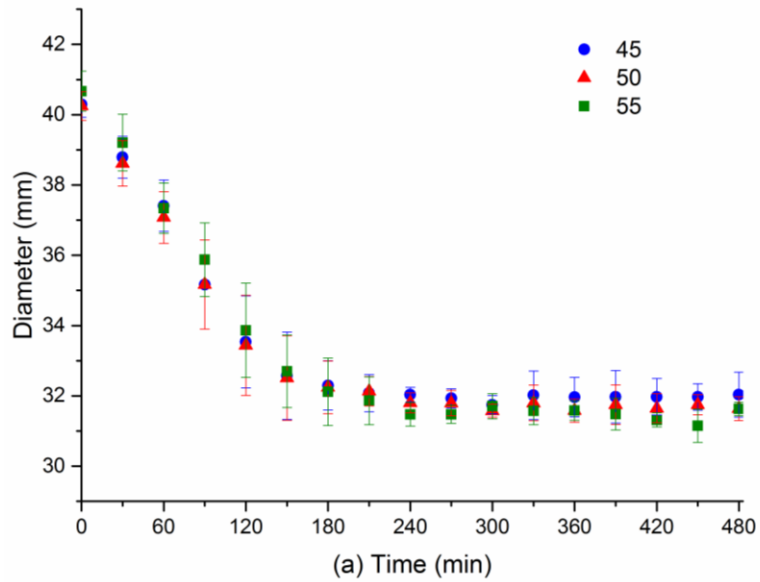


Figure 5-8. Diameter shrinkage measured under different threshold (45, 50 and 55) in time (a) and moisture content (b) domains

In the range from 45 to 55, there was no statistically significant effect of threshold on diameter imaging, which means that samples were well represented in this interval. To improve stability of imaging, the middle value of threshold at 50 was used in further experimental study.

5.3.1.4 Effect of caliper position adjustments and manual sampling on diameter measurement

Effect of caliper position adjustment on the accuracy of diameter estimation is shown in Figure 5-9.

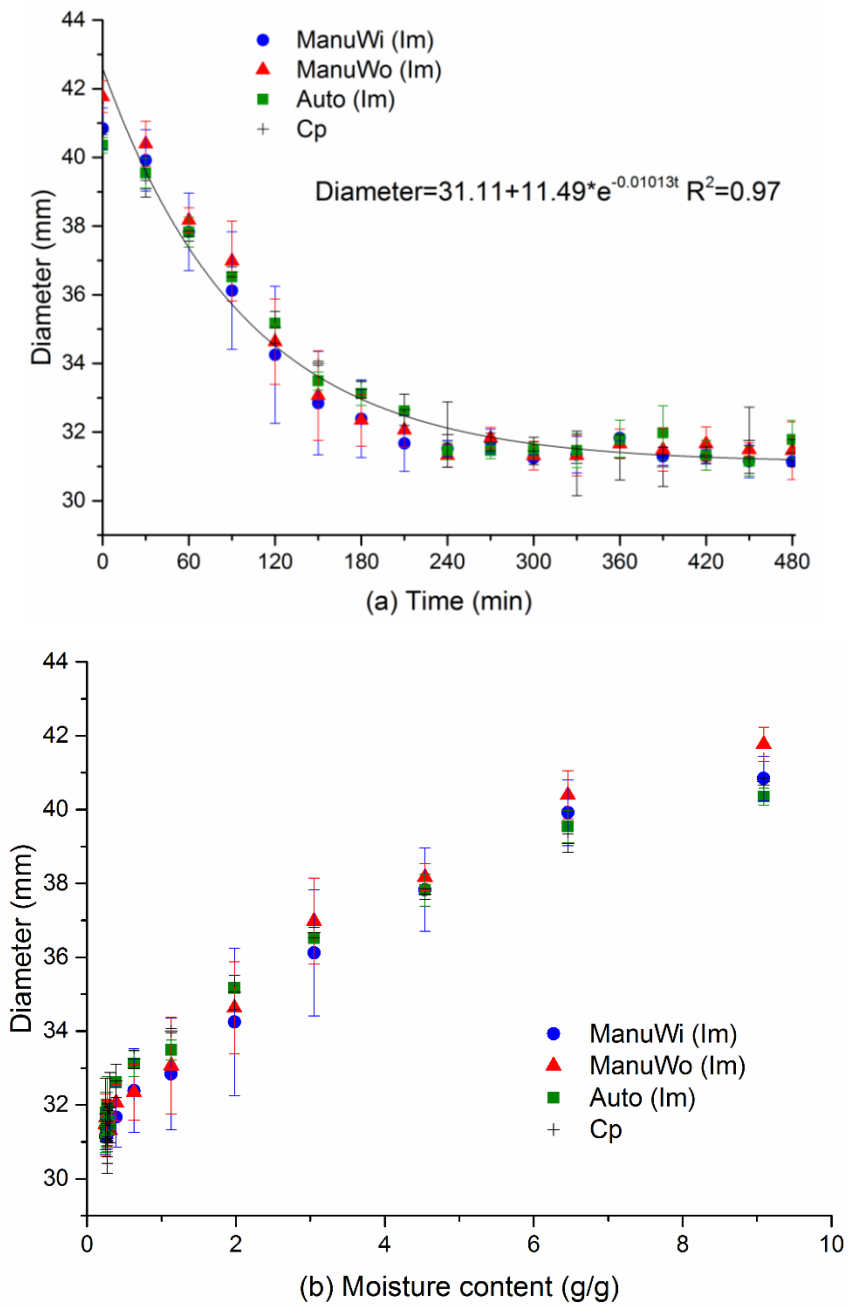


Figure 5-9. Diameter changes measured under different modes in time (a) and moisture content (b) domains

It follows that there was no significant difference of diameter imaging under different situations compared to physical caliper measurement of diameter. Therefore, the automatic mode of imaging was used in further experimental study.

5.3.2 Correlation Between Imaging and Physical Caliper Measurements of Diameter

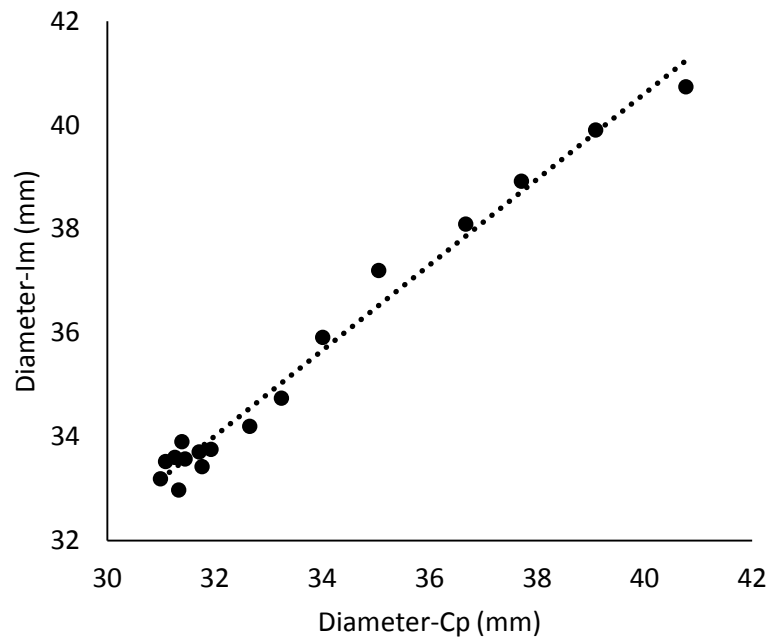


Figure 5-10. Correlation of diameter estimated from imaging and physical caliper at 80 °C

The relationship was approximated by linear equation:

$$D_{Im} = 0.8244 * D_{Cp} + 7.6298 \quad (R^2 = 0.9833) \quad (5-3)$$

Equation 5-3 establishes a relationship between imaging diameter and physical caliper measurements as presented in Figure 5-10. Imaging of diameter gave higher values than those measured using physical caliper. This overestimation of imaging could be due to the illumination effect (light reflection) on the tray near the sample edge, which was captured by imaging as diameter measurement. The other reason could be the underestimation of physical caliper because the materials under drying are soft and sensitive to force applied.

5.3.3 Verification

The relationship between imaging and physical caliper measurements was further verified under different drying conditions, 60 °C and 40 °C (Figure 11).

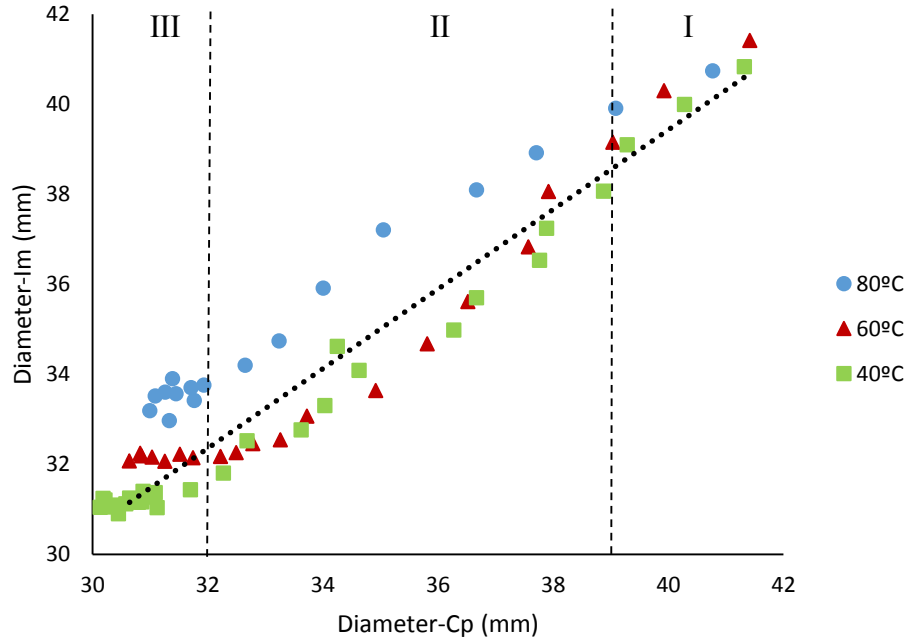


Figure 5-11. Diameter estimated from imaging and physical caliper in the range 40- 80 °C

In this verification experiment, imaging diameter was correlated with real diameter measured with physical caliper (equation 5-4). Trend line represents the correlations between physical caliper and imaging diameter at 80 °C, 60 °C and 40 °C.

$$D_{Im} = 0.8597 * D_{Cp} + 5.186 \quad (R^2 = 0.9098) \quad (5-4)$$

According to the sample diameter kinetics, the drying cycle can be divided into three periods (Figure 5-11). In the first period (I), samples were rigid with high moisture content ($X > 4.5$ g/g) in the first hour of drying. The difference of diameter changes measured by physical caliper and imaging at different drying temperatures were not significantly different until diameter shrank to approximately 39 mm. As drying continued, moisture

content decreased dramatically to 1.1 g/g with diameter reduced to approximately 32 mm (Period II), data points at 60 °C and 40 °C are below the trend line, while data at 80 °C fall above the trend line. In other words, physical caliper measurements of diameter are higher than the imaging of diameter at 60 °C and 40 °C, while smaller than imaging diameter at 80 °C. This could be explained that under the lower drying temperature, the moisture removal rate went slower, providing more time for samples to shrink. In this period, material dried under higher temperature (80 °C) are softer and more sensitive to the force applied on the physical caliper, which affected the texture measurements. When the moisture content reached around 1.1 g/g where diameter was less than 32 mm (Period III), samples started getting harder due to low moisture content, and were not sensitive to the force applied. The higher temperature the materials dried, the higher diameter obtained. As mentioned before, lower temperatures gave enough time for materials to shrink, which led to smaller diameter. Another reason might be that at higher temperature, materials underwent glass transition, which prevented the sample structure from further shrink. Assumptions about possible reasons of discrepancy between physical caliper measurement and imaging of diameter should be experimentally verified.

This verification experiment gives the possibility for further study of relationship between diameter and bulk volume.

5.3.4 Correlation Between Diameter and Volume

Bulk volume was determined from physical caliper measurements of diameter and thickness of apple slices. Since thickness was not measurable with imaging, only diameter was used for volume prediction. To correlate diameter to bulk volume with respect to the

physical relationship between diameter and volume, a non-linear cubic power approximation was applied:

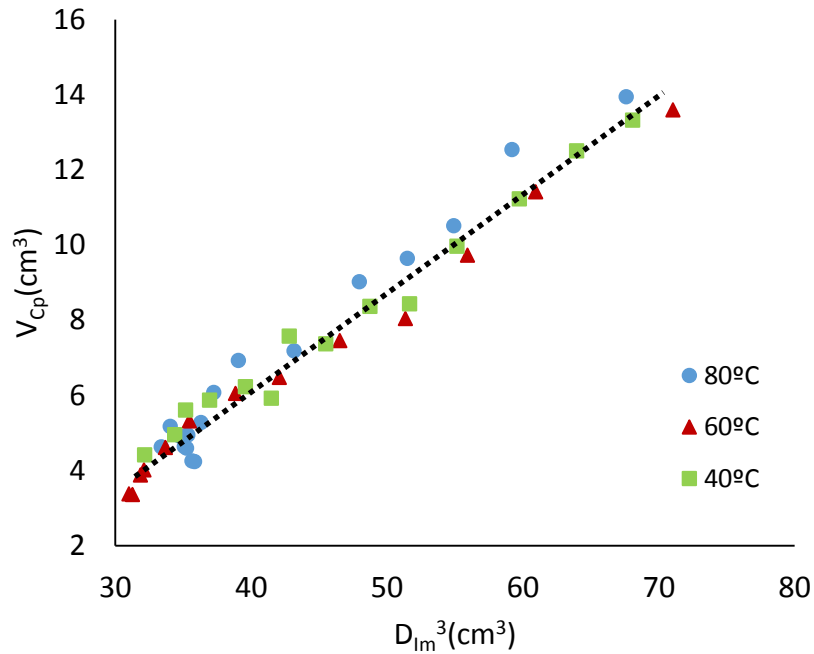


Figure 5-12. Correlation of volume and imaging diameter at 80 °C, 60 °C and 40 °C

It was found that the cube of diameter corresponds well to measured bulk volume.

Hence, a linear model between D^3 and V was developed:

$$V_{Cp} = 0.2593 * D_{Im}^3 - 4.1754 \quad (R^2 = 0.9696) \quad (5-5)$$

Predicted volume (Equation 5-5) at 80 °C corresponded well with the physical caliper measurement through the entire drying process with 7.56 % of relative error. Figure 12 shows that temperature did not significantly affect the relationship between volume and diameter. For apples dried at 60 °C, prediction error did not exceed 6.63 %. For apples dried at 40 °C prediction error at the end of drying reached 4.92 %. In general, volume predicted from imaging was not statistically different (p-value=0.986) from the volume measured with a physical caliper with a relative error of 6.45 %.

The error of predicted model increased as moisture content decreased, especially at the end of drying where shrinkage stopped. The higher relative error at low moisture content is possibly due to the intrinsic properties of materials, as well as the systematic errors in physical caliper measurements and imaging, which need to be further experimentally investigated. In general, the error throughout the entire drying process was consistent. Therefore, the developed model was considered as a robust tool for bulk volume estimation at different drying temperatures and moisture contents.

5.4 Conclusions

Bulk volume, predicted from diameter imaging, was in good agreement with physical caliper measurements, which proved the initial hypothesis that imaging is reliable tool for continuous estimation of bulk volume during drying. Diameter of apple slice was estimated from real-time imaging in the range of temperatures from 40 °C to 80 °C and moisture contents from 9.1 g/g to 0.25 g/g. Digital caliper adjustment or threshold variation in the range from 45 to 55 of grey intensity did not significantly affect the accuracy of imaging. In our study a linear relationship between diameter and bulk volume was established as $V = 0.2593 \times D_{Imaging}^3 - 4.1754$. The coefficients of this equation are specific for our study, however general linear model is applicable for convective apple slice drying.

Connecting Statement

It was possible to estimate continuously microstructure and porosity of the material during drying. Next in Chapter 6, texture changes of apple slices during drying and its relationship with porosity are presented. The effect of glass transition on the texture measured with ball and compression plates was also discovered.

Chapter 6. Texture Changes of Apple Slices Under Convective Drying

Abstract

Apple slices under convective drying showed three periods under 20 % compression of texture measurement: softening, uniform hardness and hardening. The objectives of this chapter was to investigate the effect of glass transition on texture of apple slices during drying. Our research revealed that when moisture content reached a critical point of 0.5 g/g (we considered this as the glass transition point), texture parameters had significant changes. Hardness increased sharply when moisture content was less than 0.5 g/g. Due to low moisture content and the shrinkage phenomenon, material became rigid and solid, which made dried apples harder than the fresh apple. Adhesiveness decreased as moisture was removed and reaches 0 at the glass transition point. Springiness and cohesion reduced, while chewiness increased below the critical moisture content. This could be explained by the water removal during drying, as well as the structural changes caused by shrinkage. Samples shrank to compensate for the volume that was occupied by water until it reached critical point where shrinkage remained constant.

6.1 Introduction

A great number of dried food products remain in the amorphous state under most drying conditions, which is mainly due to the insufficient time for crystallization to occur (Bhandari and Howes, 1999). The amorphous matrix exists either as a glassy state with high viscosity, or as a liquid-like rubbery structure (Chirife and Buera, 1995). In the rubbery state, shrinkage occurs throughout the entire process to compensate for moisture loss, where the decrease in material volume is equal to the amount of moisture removed. As drying

continues, food products become glassy and rigid, which restricts further volume reduction (Bhandari and Howes, 1999, Mayor and Sereno, 2004). The glassy state is metastable and eventually tends to be converted to crystal if critical temperature and moisture content are reached (Flink, 1983, Bhandari and Howes, 1999). Typically, glassy material has high viscosity; for example, the viscosity of glass is greater than 10^{13} Poises (Sperling, 2015). Food products with high viscosity are able to support their own weight against the force of gravity. White and Cakebread (1966) stated that the discontinuities of certain physical parameters (such as coefficient of expansion, free volume, dielectric constant and viscosity) indicate the transition of amorphous state from liquid to glassy. Figure 6-1 shows the changes of free volume and viscosity. As mentioned earlier, volume decreases until materials become glassy and then it remains constant. During the vitrification process, viscosity increases due to the immobilization of the disordered structure, which supports its own structure.

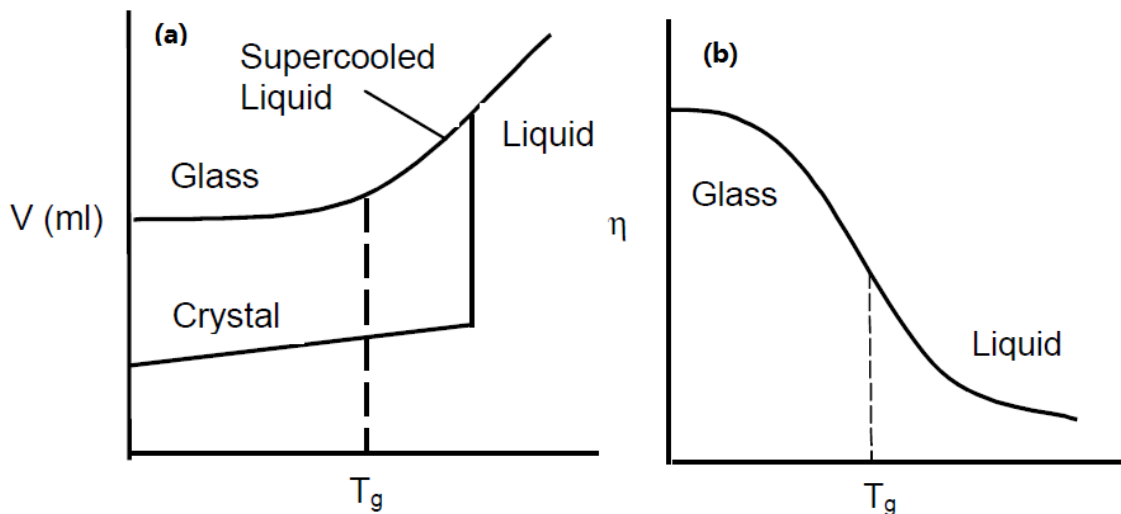


Figure 6-1 Characteristics of transition from liquid to glass. (a) Volume, (b) Viscosity. (White and Cakebread, 1966, copyright permission has been obtained)

As indicated in Figure 6-1, glass transition point is where the amorphous state and physical properties change during processing. The transition of amorphous material from

a liquid-like rubbery state ($T > T_g$) to a glassy ($T < T_g$), highly viscous solid, is defined as glass transition. The temperature at this point is called the glass transition temperature (T_g) (Lievonon and Roos, 2002) and largely depends on water content (Levine and Slade, 1986). Glass transition temperature is an important parameter for predicting and controlling the behavior of food material during processing in order to optimize the drying process and achieve the desired food quality. Karathanos (1993) mentioned that T_g may be related to the shrinkage and hardening of solid products. Foods at the glassy state are very stable because glass transition results in immobilization of water, and thus decreases the molecular mobility, slows down chemical reactions and diminishes free volume while increasing viscosity (Rahman, 1999). The indicators of glass transition include discontinuity in physical, mechanical, electrical and thermal properties of a material and these indicators has been used for development of analytical measurements for glass transition temperature, such as differential scanning calorimetry (DSC), differential thermal analysis (DTA), thermal mechanical analysis (TMA) and electron spin resonance (ESR). DSC and DTA detect changes in heat capacity (C_{ph}) between the glassy and rubbery states, while TMA measures changes in the elastic modulus (Bhandari and Howes, 1999). Due to the increased free volume in rubbery state compared to the glassy state, ESR detects glass transition temperature by measuring the mobility of a free radical probe (Labuza et al., 1992). The Gordon-Taylor equation 2-3 (referred to Chapter 2) has been developed for glass transition temperature calculation as well. Glass transition is second-order time-temperature-moisture dependent (Rahman, 1999), and thus, either changes of intrinsic conditions (such as moisture content, pH and oxygen tension) or extrinsic conditions (such as temperature) help glass transition to occur (Rahman, 1999). For instance, when a product

with a high sugar content is dried at a temperature that is higher than T_g , the product becomes soft as water is removed. However, hardening occurs when the product is cooled below T_g , with a glass transition moisture content (Bhandari and Howes, 1999). During drying, a state change of the amorphous matrix from rubbery to glassy may occur because of decreasing moisture content, since glass transition temperature is dependent on moisture content. As previously mentioned, materials under glassy state are more stable than those under rubbery state due to low moisture content. It is well known that chemical reactions and microorganism activities are restricted below a critical water activity as illustrated in Figure 6-2 (Barbosa-Cánovas et al., 2003). Most bacteria cannot grow at water activity less than 0.85, while molds and yeast are more tolerant as they cannot grow when water activity is below 0.60. Xerophilic molds and osmophilic yeasts are the most common microorganisms which spoil foods with water activity higher than 0.6 and thus fruits are usually dried with water activity below 0.6. Hence, it is important to obtain food within the safe water activity range. Water activity is majorly related to the moisture content of foods. A relationship between moisture content and water activity of apple flesh at 20-22 °C is illustrated in Figure 6-3. Under the dehydration process, a decrease in moisture content results in a reduction of water activity.

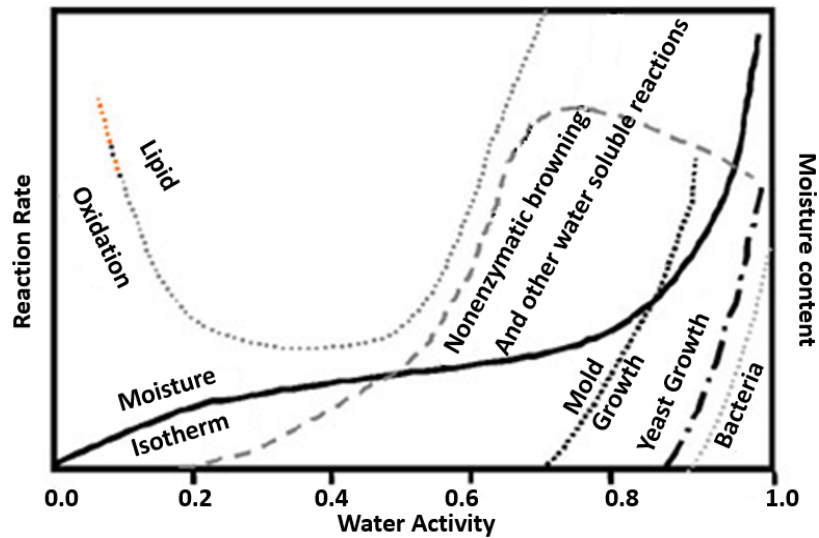


Figure 6-2 Relationship of food deterioration rate as a function of water activity (Barbosa-Cánovas et al., 2003, copyright permission has been obtained)

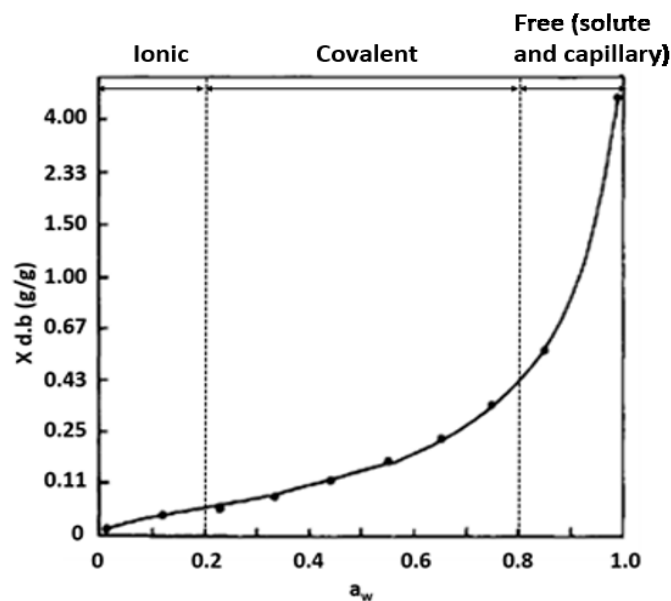


Figure 6-3 Water desorption isotherm of apple flesh at 20-22 °C. X is on moisture content on dry basis. (Bourne, 1986, copyright permission has been obtained)

Glass transition occurs when moisture content reaches the critical point. The relationship between glass transition temperature and moisture content (dry basis) has been found for wheat starch (Zeleznaek and Hosenev, 1987), rice starch (Biliaderis et al., 1986), maltodextrins (Roos and Karel, 1991), sugars and sugar mixes (Roos and Karel, 1991, Chan

et al., 1986, Finegold et al., 1989, Hatakeyama et al., 1989, Soesanto and Williams, 1981), horseradish root (Paakkonen and Roos, 1990), soybean seeds (Bruni and Leopold, 1991), cabbage, carrots and potatoes (Karmas et al., 1992) and apple slices (Bai et al., 2001). In their researches, certain levels of material moisture contents were achieved by placing materials in a controlled humidity environment. Glass transition temperatures can be either measured by methods aforementioned, or calculated from the Gordon-Taylor equation, with determined T_g and K values for a specific substance.

A glass transition moisture content equation has been derived from the Gordon-Taylor equation 2-3:

$$X_g = \frac{T_{gs} - T_g}{(T_g - T_{gw}) * K} \quad (6-1)$$

The constant K value is different from one material to another; hence, determination of K value is of great importance in estimating glass transition moisture content. The estimation of moisture content at glass transition point can be used to formulate materials with desired physical properties during drying by terminating the dehydration process at an appropriate point. It has been reported that as moisture content (d.b.) decreased, glass transition temperature increased for both vegetables and fruits such as horseradish, soybean, cabbage, carrots, potatoes, corn embryo, strawberries and apple slices (Paakkonen and Roos, 1990, Karmas et al., 1992, Bruni and Leopold, 1991, Bai et al., 2001). Taking apple slices for example, the T_{gs} , T_{gw} and K value were estimated as 41.3 °C, -135 °C and 3.59, respectively (Bai et al., 2001). Hence, in order to prevent apple from reabsorbing water at room temperature (20 °C), samples should be dried below 3.69 % (w.b.) or 0.0383 g/g (d.b.) of moisture content. A relationship between moisture content and glass transition

temperature of apple slices undergoing hot air drying based on Gordon-Taylor equation (with the parameters mentioned above) is shown in Figure 6-4.

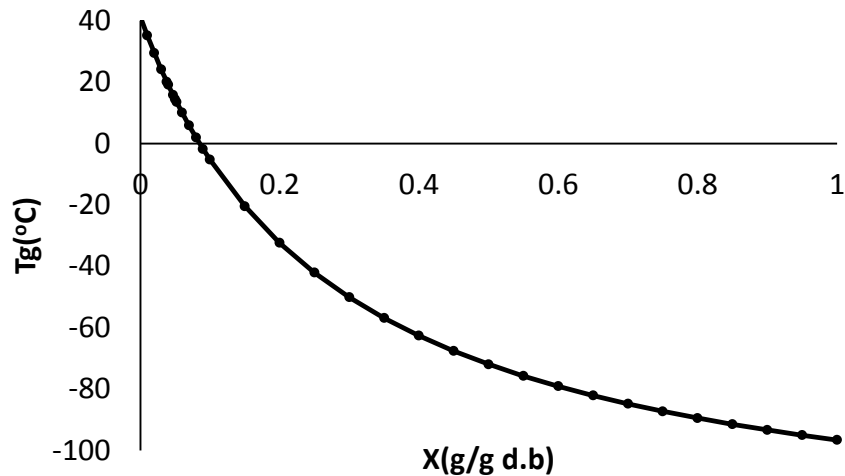


Figure 6-4 Relationship between glass transition temperature (T_g) and moisture content (X) on dry basis for air dried apple tissue (Adopted from Bai, et al., 2001)

The study of glass transition helps explain and control the physical changes that occur during food drying and storage, as well as the textural properties of food systems, such as softening and hardening (Abbas et al., 2010). Ribeiro et al. (2003) reported that material undergoing a flowable melt becomes soft once temperature increases above glass transition temperature and materials become like clear glass with brittle texture when they are cooled. Hence, glass transition affects material texture significantly. This chapter aims at studying the textural changes of apple slices during drying, specifically beyond glass transition point.

6.2 Materials and Methods

6.2.1 Materials and Sample Preparation

Refers to Section 4.2.1.

6.2.2 Instrumentation

Drying instrumentation refers to section 4.2.2 and 5.2.2.

The TA-XT plus texture analyzer (Stable Micro System, Surrey, UK) (Figure 2-3) was applied for texture parameter measurements, including hardness, adhesiveness, springiness, cohesion and chewiness. The texture analyzer was calibrated with a 50-kg load cell before measurement; a computer program Exponent V.6 was also provided with the apparatus. After drying, due to the shrinkage phenomena, samples had wrinkled non-uniform surfaces. Both the ball probe (BP) and compression plate (CP) were applied for texture measurement of semi dried and dried apple slices. The ball probe measures only one local point on the surface of the sample whereas the compression plate measures the whole surfaces of samples. A moderate compression strain of 20% was used in this study. Two-cycle compressions were performed for every sample, with constant 2 mm/s falling rate and 5 seconds delay from the end of the first cycle to the beginning of the second cycle, which gave enough time for samples to recover. To obtain a uniform force of compression across the whole sample surface, a 5.08cm compression plate probe TA-25A was used (Texture Technologies, Hamilton, MA, USA). A 1.27cm stainless steel ball probe (BP, T-18), which covered less area and gave local pressure, was also used for texture measurement on the geometrical center of the sample (Texture Technologies, Hamilton, MA, USA). The height was calibrated before compression by lowering the plate probe which was attached to the TA-XT Plus texture analyzer to contact with the test table, so the instrument could determine the base position. The thickness of samples was measured automatically when the probe touched them and the computer then determined the difference between the first time it touched the samples and the base position. Then the probe went continuously with 2 mm/s speed and the force was recorded by the computer once it reached 20 % deformation. The force-time curve (Figure 2-4), which also represented hardness-time, was automatically

plotted in real-time by the computer program as soon as the probe touched the sample. The other texture parameters (cohesion, adhesiveness, springiness and chewiness) were also shown or calculated from the force-time curve (Table 2-2). For each sample, texture measurements were carried out first with BP and followed by CP, due to the potential risk of breaking the crispy samples. All measurements were performed in triplicate at room temperature (20 °C).

6.2.3 Experimental Procedure

Before each experiment, the dryer was preheated to a target temperature of 40 °C, 60 °C and 80 °C to investigate the effects of glass transition at the end of the drying period on material texture. Throughout the entire process, three samples were randomly taken out of the dryer every 30 minutes at 80 °C, every 45 minutes at 60 °C and every 60 minutes at 40 °C and cooled to room temperature for mass and texture measurements.

6.3 Results and Discussion

6.3.1 Effects of Drying Temperature and Moisture Content on Porosity

As moisture was removed, the porosity of materials under convective drying at different temperatures showed the same trend, which increased and reached maximum when moisture content decreased to around 0.5 g/g (Figure 6-5). All porosities dropped rapidly when moisture content was lower than 0.5 g/g. In terms of the drying temperature, at same moisture content ranging from 9.1 g/g to 0.25 g/g, higher temperature maintained more porous structure. Porosity of material at 0.4 g/g were found to be 0.8, 0.7 and 0.6 when samples were dried at 80 °C, 60 °C and 40 °C. Hence, moisture removal determined the development of porosity, however, the extent of porous structure was dependent on drying temperature. Porosity increased more rapidly and intensely at higher drying

temperatures. Under high temperatures (e.g. 80 °C), moisture was removed quickly and shrinkage was unable to compensate for the increased air space, which created porosity. Under low temperatures, the slower removal of moisture provided time for the material to shrink and compensate for the volume, which was firstly occupied by water and then by air.

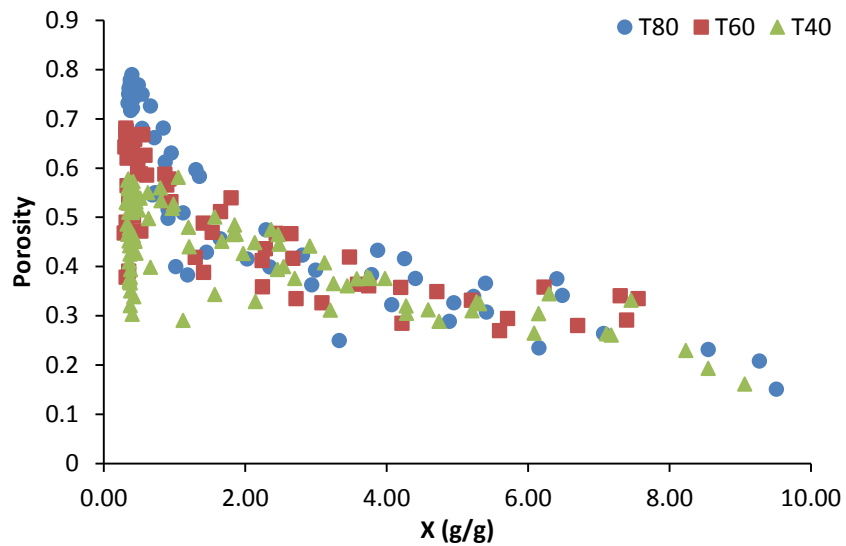


Figure 6-5 Porosity development respect to moisture content under different drying temperatures

6.3.2 Effects of Moisture Content on Texture

The general texture tendency of apple slices under convective drying with different temperatures was interpreted by Martynenko and Janaszek (2014). As reported, the drying process was assigned into three periods, softening, uniform hardness and hardening, with respect to moisture content. However, texture changes at the last period-hardening of apple drying process have not been studied.

At the beginning of drying, hardness per unit area, as measured with CP and BP, had no significant difference (Figure 6-6), which could be explained by the evenly distributed moisture and turgor pressure within the material. Both CP and BP showed a decreasing

trend of hardness, which indicated softening of the material. Moisture is removed rapidly at high temperatures, leading to a drop in shrinkage (Figure 5-3). Pores were developed when shrinkage was unable to compensate for evaporated volume of moisture. Due to the removal of moisture at the beginning of drying, the development of pores within the rubbery materials gave low and uniform hardness in the moisture range from 6 g/g to 0.5 g/g. In the period of hardening when moisture content reached around 0.5 g/g, BP showed more rapid increasing of hardness than that measured with CP.

As drying continued to the end at extremely low moisture contents, unbalanced shrinkage and moisture removal rate converted most of the open pores into closed pores. The cell wall became rigid and strong, especially on the outer layer of materials, which increased hardness at the glass transition point (Lewicki, 1998). As indicated in Figure 6-6, dried apple slices had around twice hardness than fresh apple flesh. The hardened texture of apple slices measured with CP mostly reflects hardness of the edge cells, which was due to the non-uniform surface caused by shrinkage as moisture was removed (Martyntenko and Janaszek, 2014). In addition, a bending elasticity was measured by CP when materials were bent.

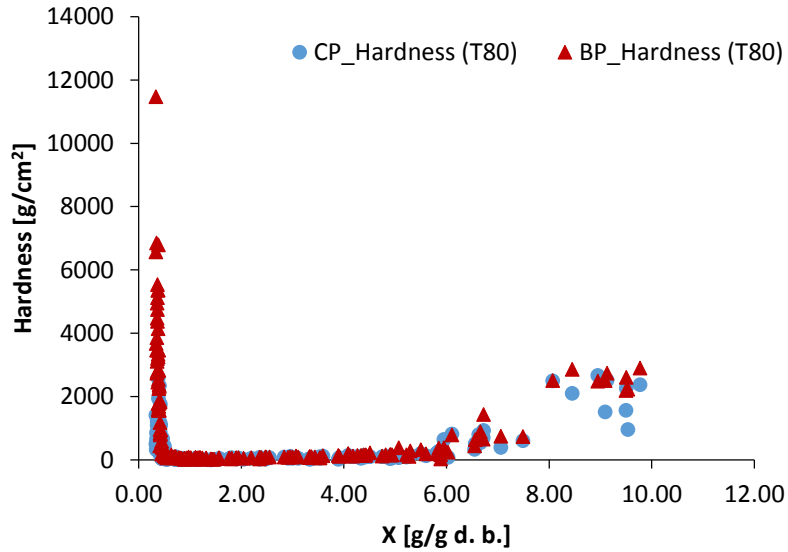


Figure 6-6 Hardness changes during drying of apple slices in moisture content domain

Hence, BP measurement was more representative of the hardness of dried apple slices.

The increasing hardness in this period could be explained as glass transition phenomena. Under air temperature as high as 80 °C, once moisture content of high sugar product (e.g. apple slices) reached critical glass transition point, samples became harder (glass transition) as product material dropped below critical temperature (Bhandari and Howes, 1999). Under low moisture content, hemicellulose, pectin substances and carbohydrates, provided resistance to the cell wall and affect the textural attribute of dried apple slices.

It was observed that, adhesiveness measured using BP did not show significant changes during drying moisture content domain (Figure 6-7). According to the definition of adhesiveness, which is based on surface measurement, CP measurement was considered as more accurate than BP measurement.

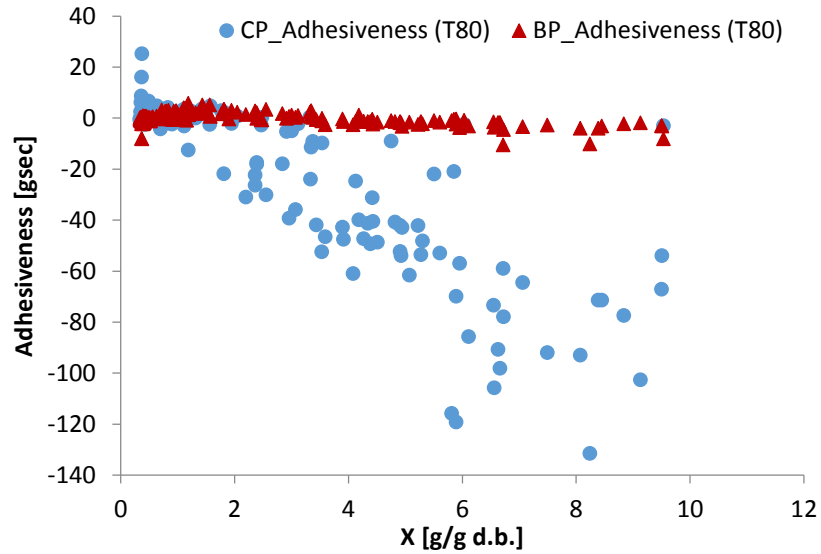


Figure 6-7 Adhesiveness changes during drying of apple slices in moisture content domain

Adhesiveness was greatly related to the moisture, porosity and sugar content on the material surface. At the beginning of dehydration, high adhesiveness was a reflection of high moisture and sugar content and low porosity, and it decreased as moisture was removed. The viscous component in the samples could be the reason for the decreasing adhesiveness (Martynenko and Janaszek, 2014). When moisture content reached around 0.5 g/g, adhesiveness remained constant at zero, as there was no free water available on the surface of the material.

Springiness and cohesion also showed three distinct periods, corresponding to softening, uniform hardness and hardening period. At the end of drying, when samples with moisture content less than 0.5 g/g, springiness and cohesion noticeably dropped.

Springiness reflects the ability of a deformed material to return to its original shape. Both BP and CP measurements gave similar changes during drying (Figure 6-8).

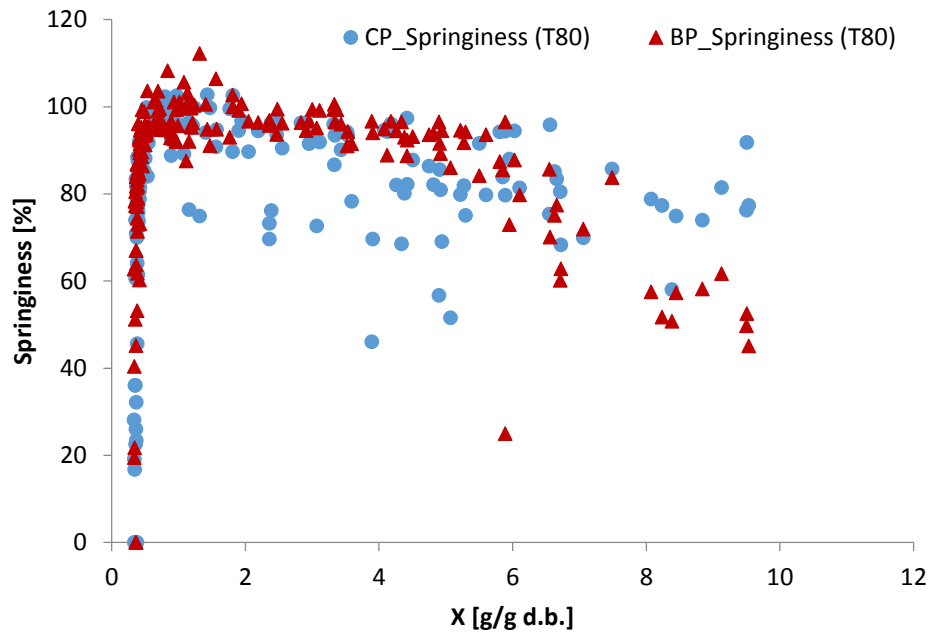


Figure 6-8 Springiness changes during drying of apple slices in moisture content domain

Dehydration softened the material as moisture was removed, which gave elastic properties to the material. As drying continued, springiness reached maximum of 100 % at a moisture content of approximately 0.5 g/g, then it decreased sharply. These changes in springiness agreed with results obtained by Bourne (1986). After glass transition, material became plastic and was not able to recover. An increase of hardness caused a decline in springiness which further led to a dropping of cohesion.

In terms of cohesion (Figure 6-9), CP measurements showed a constant cohesion, then it dropped rapidly until moisture content reached around 0.5 g/g. Ball probe revealed an increasing cohesion from 0.4 to 0.8 at the beginning of drying while the material matrix was in a rubbery state. Guiné (2013) and Guine and Barroca (2011) stated that shrinkage could be the reason for the increasing of cohesion. Samples became brittle with low moisture contents (less than 0.5 g/g) leading to difficulties maintaining the integrity and decreased cohesion.

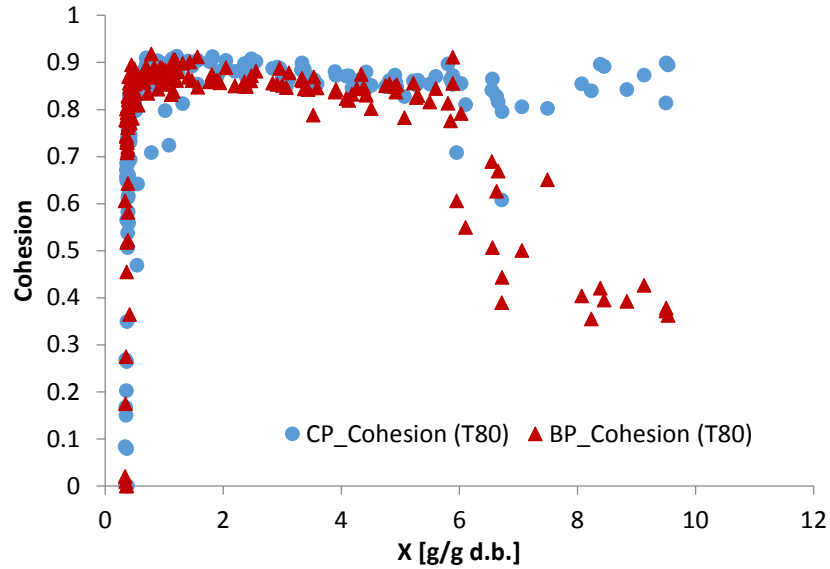


Figure 6-9 Cohesion changes during drying of apple slices in moisture content domain

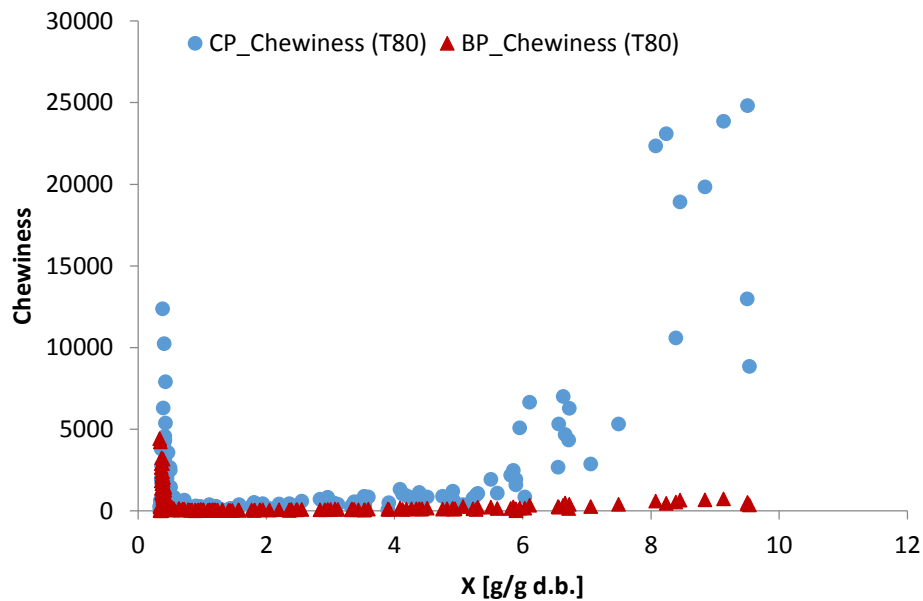


Figure 6-10 Chewiness changes during drying of apple slices in moisture content domain

There are three periods of chewiness measured with CP during drying in Figure 6-10: decreasing, constant and increasing of chewiness. Materials with high moisture content in a rubbery state have a chewy texture. As moisture was removed and reached 0.5 g/g, materials became rigid and tough, which decreased chewiness. Chewiness of dried material measured with CP was around two times higher than that measured with BP. This was

similar to hardness changes and could be explained by the non-uniform shrinkage of material at the final stage, where CP caused the chewiness of the edge cells. Since texture changes of dried material was the topic of interest, BP was recommended for analysis of dried or semi-dried samples because it measured chewiness at the center of the material.

Ball and cylinder compression probes were applied on the same samples for texture measurement to investigate the effect of probes on texture measurement. This research indicated that BP and CP gave different textural results. Different probes should be applied depending on the textural parameters and the physical properties of the materials. For instance, CP is more suitable for adhesiveness measurements because it accounts for the overall area of the material and BP is more suitable for other texture parameter measurements including hardness, springiness, cohesion etc., because of the ability to be used on a specific region, even with non-uniform materials.

6.3.3 Effects of Drying Temperature, Porosity and Glass Transition on Texture

As discussed in section 6.3.2, CP gives texture measurement on the edge cells, BP was applied for most of texture parameter measurement, while adhesiveness was measured using CP. This section revealed the relationship how texture characteristics were affected by drying temperature, porosity and occurrence of glass transition phenomena. Total porosity was evaluated using methodology from theoretical model (Equation 2-9).

The higher the drying temperature, the more rapid the temperature drop that the material suffered after cooling. As mentioned above in section 6.3.1, the rapid drop of material temperature resulted in an increase of hardness (Figure 6-11).

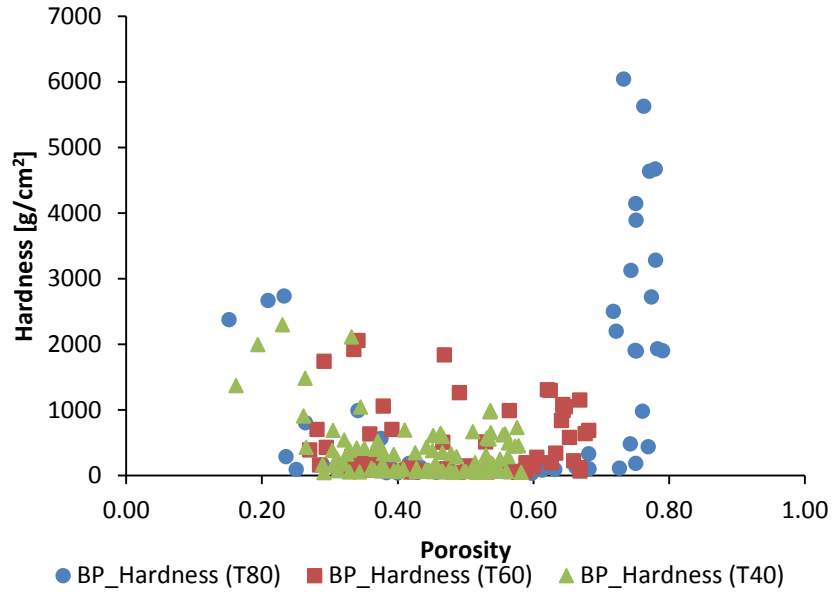


Figure 6-11 Hardness changes in porosity domain at different drying temperatures

At the early stage of drying, temperatures ranging from 40 °C to 80 °C did not influence hardness significantly, instead, hardness decreased and reached a minimum as porosity increased to around 0.4. For 40 °C drying, hardness decreased and reached a minimum at around 1000 g/cm². While for 60 °C, hardness showed a similar trend and constant at 1500 g/cm² when porosity reached 0.6. In general, temperature had a great impact on hardness and porosity of dried apple slices. The higher temperature led to more porous materials with higher hardness.

Adhesiveness decreased and reached zero as porosity increased to 0.4 for all temperatures (Figure 6-12). This could be explained by the decreasing surface moisture which created a porous material structure. Hence, adhesiveness was considered to be temperature independent but porosity and moisture content dependent.

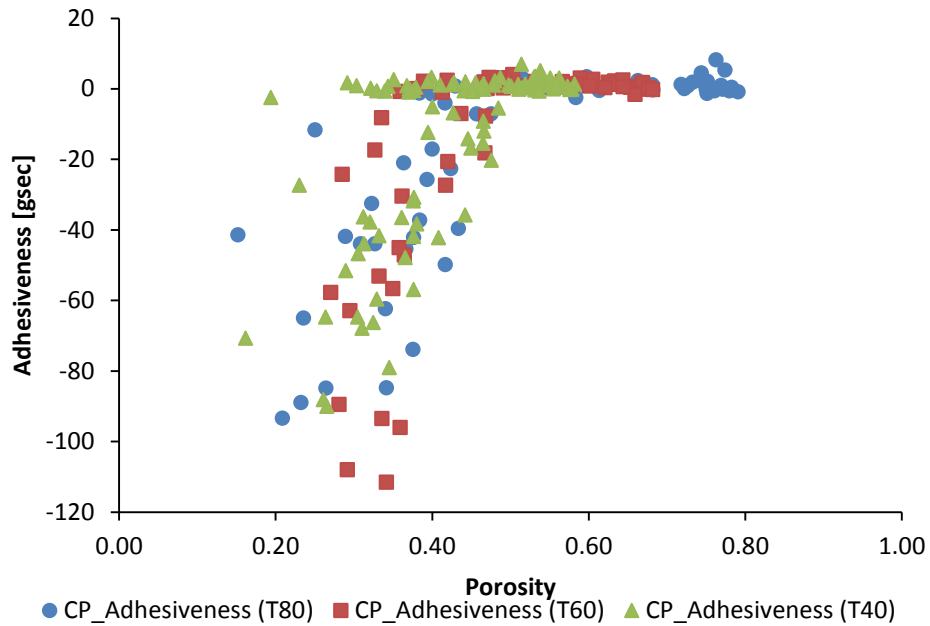


Figure 6-12 Adhesiveness changes in porosity domain at different drying temperatures

Cohesion and springiness did not show three different periods at 40 °C and 60 °C of drying. The cohesion of fresh material is approximately 0.35, then it increased and remained at 0.9 (Figure 6-13) as porosity increased. Springiness of fresh materials is about 50% and it increased as porosity increased to approximately 0.4 and kept constant at 100% when porosity was further increased to 0.65 (Figure 6-14). Significant drops of both cohesion and springiness were observed when increased porosity from 0.65 to 0.75, which could be caused by the glass transition phenomena.

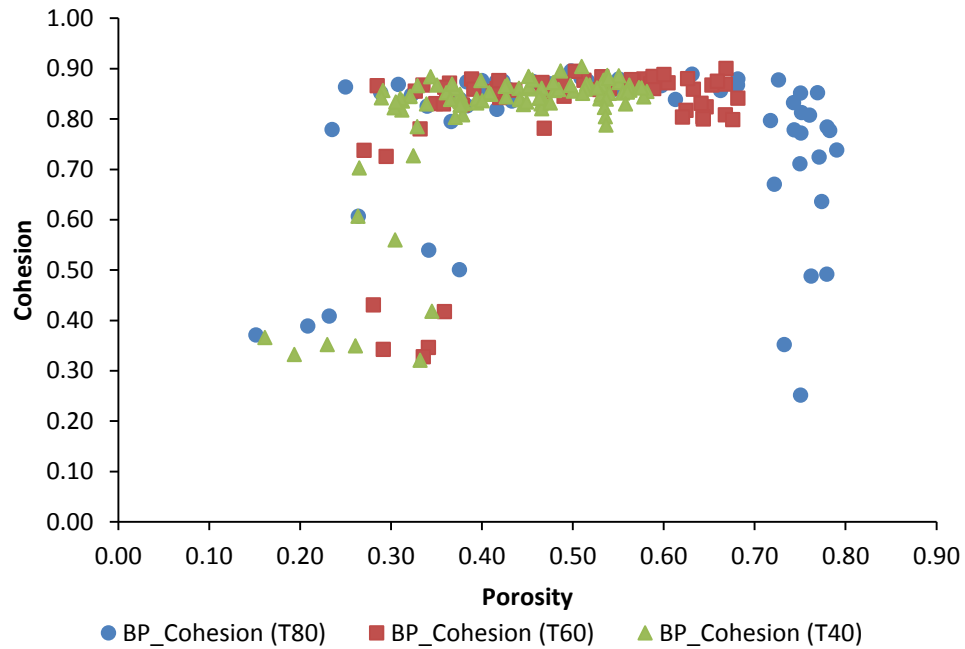


Figure 6-13 Cohesion changes in porosity domain at different drying temperatures

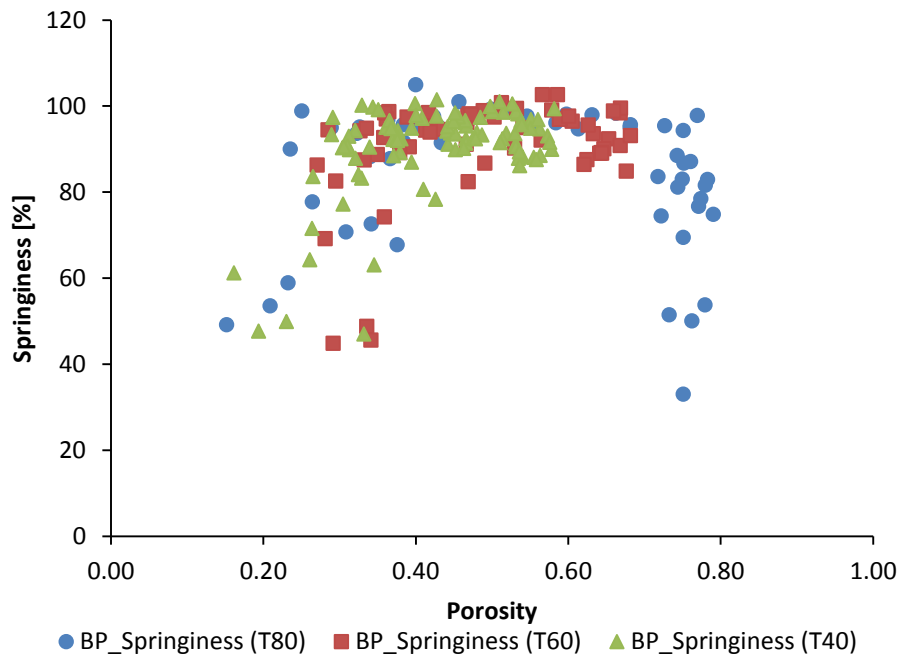


Figure 6-14 Springiness changes in porosity domain at different drying temperatures

Similar to hardness changes, drying temperature had a great impact on chewiness.

Chewiness increased as materials dried at higher temperatures. Figure 6-15 demonstrated

that an increased temperature among 40 °C, 60 °C and 80 °C resulted in a growing of chewiness from 700 g, 1000 g to 2500 g. Besides that, porous structure and the occurrence of glass transition phenomena also contributed to chewy dried materials. Before the occurrence of the glass transition, as moisture decreased, open pore porosity increased in rubbery materials, which gave a chewy texture. After the glass transition, due to the low moisture content and structural changes of the porosity, from open pores to closed pores, samples became rigid and tough. This change increased their chewiness and higher than the initial chewiness of fresh apple slices.

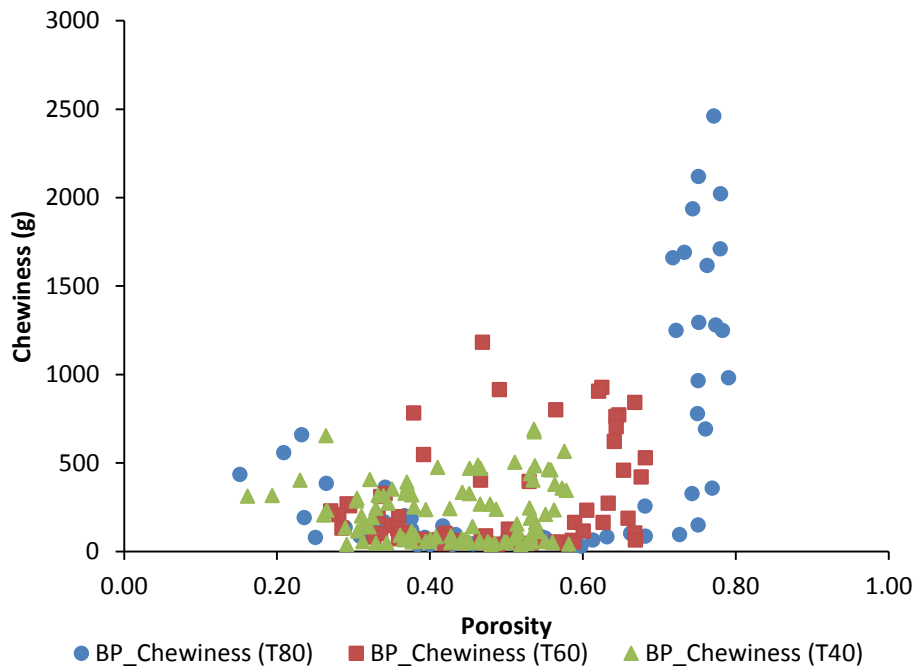


Figure 6-15 Chewiness changes in porosity domain at different drying temperatures

Texture changes of apple slices that underwent convective drying were substantially dependent on moisture removal and porosity development. Textural parameters suffered sharp changes when moisture content reached the critical point of about 0.5 g/g with a porosity of 0.7. Lewicki and Lukaszuk (2000) found that work of deformation decreased and reached a minimum when moisture content was 1.8 g/g, and then it slightly increased,

when a deformation of 4 % was applied. The same critical moisture content was also found by Krokida et al. (2000a), they stated that considerable changes of structure occurred when moisture content was lower than 1.8 g/g. However, Bourne (1986) reported that hardness of dried apple slices significantly increased at a moisture content around 0.04 g/g with water activity between 0.12 and 0.23. Additionally, this critical moisture content agrees with Bai et al. (2001). A glass transition (critical) moisture content equation was derived (Equation 6-1) based on the Gordon-Taylor equation. When storing dried apple slices at room temperature using $T_g = 20$ °C, $T_{gs} = 41.3$ °C, $T_{gw} = -135$ °C and $k = 3.59$, the estimated critical moisture content was 3.69 % (w.b.) and 0.04 g/g (d.b.). The difference of critical moisture content between 1.8 g/g and 0.04 g/g could be explained by the different methods and materials used. Lewicki and Lukaszuk (2000) and Krokida et al. (2000a) dried apple under 70 °C convective drying with 10mm cubes, and 20 by 20 mm cylinders, respectively. In their cases, they measured the average moisture content of apple slices during drying. Under convective drying, the surface moisture was removed faster than inner moisture due to low water diffusivity. Especially at the end of drying, as it is mentioned in Chapter 4, due to the shrinkage phenomena, most of the open pores closed, which blocked moisture diffusion to the surface from the inside of the material. This explained the different critical moisture contents and increased hardness as reported in different literatures. Due to the uneven distribution of moisture, at the final period of drying, the center of material still had a higher moisture content than that on the surface (Figure 6-16).

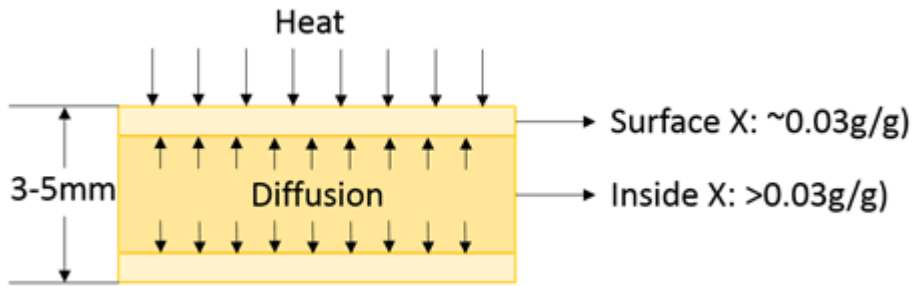


Figure 6-16 Moisture distribution of apple slices under convective drying

In other words, the surface became hard when it reached critical moisture content, whereas the inner part of materials still had a relatively high moisture content, which led to a varied critical moisture content from 0.5 g/g to 1.8 g/g. Bourne (1986) reported that it is possible for the inner moisture to escape if apple slices were kept in a desiccator with a constant relative humidity and the samples reached the specific water activity. In this case, moisture was evenly distributed within the material and maintained a constant moisture content. Under low moisture contents (<0.04 g/g), materials under the glass transition not only demonstrated case hardening, but also revealed fragile behavior (Bourne, 1986).

Textural parameters and physical properties are largely dependent on initial materials and drying technologies. For example, water is removed by sublimation under freeze drying with negligible volume changes. Freeze dried materials are characterized by a porous and fragile texture (Prothon et al., 2003). Materials under microwave vacuum drying demonstrated that with a 100 % expansion rate, hardness remained constant at 169.85 g and increased rapidly around 30 times to 5000 g when volume was constant at an expansion rate of 180 % (Zheng et al., 2013). Zheng et al. (2013) explained that at the early stage, materials expanded to maintain hardness meanwhile the spaces, filled with moisture and then air, were able to support the sample's structure. At the second stage, material became

rigid and hard to keep the volume from further expanding. The puffing phenomena resulted in a crispy and delicate texture (Sham et al., 2001, Zheng et al., 2013).

Since texture was not directly measurable, an estimation of texture parameters from physical parameters (moisture content and porosity) was advised. From this study, in order to get crispy apple slices with hardness around 6000 g/cm² under convective drying, materials should be dried to a moisture content less than 0.5 g/g (d.b) with an approximate porosity between 0.7 and 0.8 at 80 °C. Hence, the knowledge from this chapter gives a possibility for the food processing industry to predict and control food porosity or moisture content to achieve desirable texture under convective drying.

6.4 Conclusions

The glass transition phenomena played an important role in texture changes of apple slices at 80 °C under convective drying. Samples experienced a rapidly cooling temperature from 80 °C to 20 °C when they were taken out of the dryer, at this point, samples changed from rubbery to vitreous or glassy solids, due to an extreme heat capacity change (Parks and Huffman, 1926, Kasapis, 2009). Under high temperature drying, materials became soft and uniform, and pores were open as moisture was removed. As drying continued, plant tissue became hard and rigid due to a sharp drop of water, which acted as a plasticizer. The conversion of open pores to closed pores took place when it reached the critical moisture content and consequently caused the occurrence of glass transition (Kurozawa et al., 2012). After the glass transition point, hardness and chewiness increased rapidly with a dramatic decrease of springiness and cohesion.

Water, as a plasticizer, maintains the structure and elasticity of the cell wall so textural parameters are largely dependent on moisture content. At the end of drying, when the

moisture was almost removed and reached a critical moisture content, solid content played an important role in maintaining structure by creating closed pores. Samples became plastic and rigid, the conversion of open pores to closed pores at the glass transition point increased hardness and chewiness, and reduced springiness and cohesion. It was further explained that materials that underwent a glass transition were characterized as brittle, high in strength, low in molecular mobility and high in porosity (Rahman, 1995).

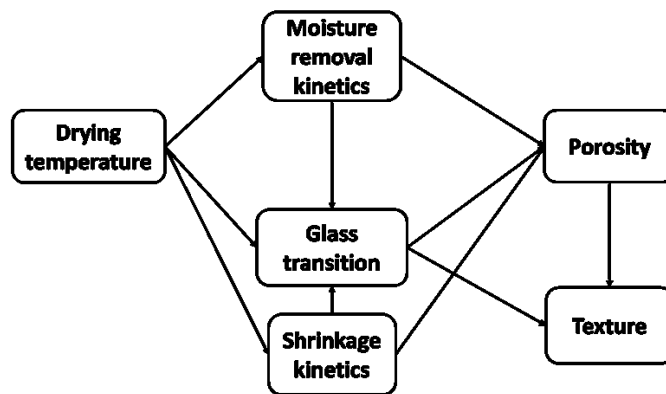


Figure 6-17 Effects of drying regimes on texture development

Drying temperature was considered as a dominant factor that influence texture of the dried apple slices. The occurrence of glass transition, moisture removal rate and shrinkage kinetics were greatly and directly related to the drying temperature. Glass transition occurred while drying materials at high temperatures (for example 80 °C in this research), and cooled rapidly to room temperature. The difference of moisture removal and shrinkage rates, as well as the occurrence of glass transition, created porous structure of the dried material. The evolution of porosity and glass transition phenomena brought different texture to the dried materials. In general, drying temperature is a vital factor that conditions the final properties of the dried materials as indicated in Figure 6-17.

To summarize, texture of samples under convective drying were suffering three-period changes, softening, uniform hardness and hardening, and the behavior was strongly

influenced by drying temperature, moisture content and evolution of porosity. Knowledge of the relationship between microstructure (porosity and moisture content) and macrostructure (texture attributes) under different drying technologies are also essential, and should be further investigated.

Chapter 7 General Conclusions and Recommendations

7.1 Achievements and General Discussion of the Results

To date, most researchers focused on the effect of drying regimes on either microstructure or texture of fruits and vegetables, as food texture is closely related to the food microstructure. However, the knowledge of how they are related under different drying technologies is scarce. This research revealed the relationship between microstructure (moisture content and porosity) on textural parameters of apple slices under convective drying in order to improve the quality of dried materials.

Total, open- and closed- pore porosity are additive and they could be estimated separately from moisture content and volume shrinkage monitored by CV. Total porosity can be calculated from the theoretical model $\varepsilon = 1 - \alpha \frac{1+\beta*X}{1+X_0} * \frac{1}{\xi}$. Open-pore porosity is able to be measured using helium pycnometer, which is applicable in measurements of multiphase particle volume. Closed-pore porosity can be calculated from the difference of estimated total pore porosity and measured open-pore porosity. As moisture content decreased, total and open-pore porosity increased with negligible closed-pore porosity until moisture content reached 1.0 g/g. Open-pore porosity dropped rapidly with a dramatic increase of closed-pore porosity when moisture content was below 0.26 g/g. Glass transition for apple tissues occurred at moisture content between 1.0 g/g and 0.26 g/g.

Bulk volume from dimensional measurement and diameter measured from CV in real-time was successfully related, which means CV is applicable in real-time estimation of bulk volume shrinkage. Due to the non-uniform thickness shrinkage and bending phenomena, it was not possible to directly estimate thickness shrinkage from CV. The correlation of diameter shrinkage measured from physical caliper and imaging was verified under

convective drying of air temperature at 40 °C and 60 °C. Hence, CV is applicable for bulk shrinkage estimation under convective drying in real-time.

Texture parameters showed three regions during convective drying, softening, uniform hardness and hardening. Moisture removal and porosity evolution significantly affected texture development of apple slices under convective drying especially at the end of drying after glass transition phenomena. When moisture content reached 0.5 g/g with a porosity more than 0.7, hardness increased sharply which was around two times higher than that of the fresh apple disks. Adhesiveness decreased to zero when there was little surface water left. Springiness and cohesion dropped while chewiness increased as moisture content decreased to the glass transition point. The reason for these changes was possibly due to the conversion of porosity from open to closed pores under convective drying at the end of drying.

7.2 Recommendations for Future Research

Due to the non-uniform shrinkage and bending phenomena, direct measurement of volume shrinkage in real-time was not achieved in this research. Attention should be drawn in future study to overcome this challenge with more advanced computer vision and imaging technology.

Texture of apple slices under convective drying was largely dependent on moisture content and porosity development. In this research, moisture content of 0.5 g/g (d.b.) and porosity of 0.7 were considered as critical point where glass transition takes place. The apple slices dried at 80 °C with low moisture content (less than 0.5 g/g) and high porosity (more than 0.7) are considered with crispy texture. A rubbery dried product could be obtained by drying material with moisture content above 0.5 g/g and porosity lower than

0.7. Bourne (1986) reported a critical moisture content of 0.04, which is closed to 0.0383 reported by Bai et al. (2001). Lewicki and Lukaszuk (2000) and Krokida et al. (2000b) found a critical point with moisture content of 1.8 g/g. The difference between these moisture content could be explained by different drying regimes, methods of measurements, material properties and some other unknown and uncontrolled parameters, which need further investigation.

This research proved that moisture content and porosity have significant impacts on texture parameters when materials undergo convective drying. Zheng et al. (2013) found that one of texture parameter, hardness, was related to puffing phenomena under microwave vacuum drying. However, there is little research investigating the relationship between texture and microstructures in other drying technologies, such as freeze drying and microwave drying, future research on this topic is recommended.

In conclusion, the results obtained from this thesis significantly contribute in building a database on physical and textural properties of food materials. This knowledge is important in designing a CV to monitor and control food quality in real-time at an industrial scale during the drying process.

References

- ABBAS, K., LASEKAN, O. & KHALIL, S. K. 2010. The significance of glass transition temperature in processing of selected fried food products: A review. *Modern Applied Science*, 4, p3.
- ACEVEDO, N. C., BRIONES, V., BUERA, P. & AGUILERA, J. M. 2008. Microstructure affects the rate of chemical, physical and color changes during storage of dried apple discs. *Journal of Food Engineering*, 85, 222-231.
- AGUILERA, J. & STANLEY, D. 1999. Simultaneous heat and mass transfer: dehydration. *Microstructural Principles of Food Processing and Engineering*, 373-407.
- AGUILERA, J. M. 2005. Why food microstructure? *Journal of Food Engineering*, 67, 3-11.
- AGUILERA, J. M., CHIRALT, A. & FITO, P. 2003. Food dehydration and product structure. *Trends in Food Science & Technology*, 14, 432-437.
- ALVAREZ, M. D., SAUNDERS, D. E. J. & VINCENT, J. F. V. 2000. Fracture properties of stored fresh and osmotically manipulated apple tissue. *European Food Research and Technology*, 211, 284-290.
- ANANTHESWARAN, R., MCLELLAN, M. & BOURNE, M. 1985. Thermal degradation of texture in apples. *Journal of Food Science*, 50, 1136-1138.
- ANDRES, A., BILBAO, C. & FITO, P. 2004. Drying kinetics of apple cylinders under combined hot air–microwave dehydration. *Journal of Food Engineering*, 63, 71-78.
- ANGLEA, S. A. 1994. *Structural collapse during dehydration of plant tissues and a model system*. Michigan.

- ASKARI, G., EMAM-DJOMEH, Z. & MOUSAVI, S. 2006. Effects of combined coating and microwave assisted hot-air drying on the texture, microstructure and rehydration characteristics of apple slices. *Food Science and Technology International*, 12, 39-46.
- ASKARI, G. R., EMAM-DJOMEH, Z. & TAHMASBI, M. 2009. Effect of various drying methods on texture and color of tomato halves. *Journal of Texture Studies*, 40, 371-389.
- AZZOUZ, S., GUIZANI, A., JOMAA, W. & BELGHITH, A. 2002. Moisture diffusivity and drying kinetic equation of convective drying of grapes. *Journal of Food Engineering*, 55, 323-330.
- BAI, Y., RAHMAN, M. S., PERERA, C. O., SMITH, B. & MELTON, L. D. 2001. State diagram of apple slices: glass transition and freezing curves. *Food Research International*, 34, 89-95.
- BAIANO, A., TERRACONE, C., PERI, G. & ROMANIELLO, R. 2012. Application of hyperspectral imaging for prediction of physico-chemical and sensory characteristics of table grapes. *Computers and Electronics in Agriculture*, 87, 142-151.
- BARBOSA-CÁNOVAS, G. V., FERNÁNDEZ-MOLINA, J. J., ALZAMORA, S. M., TAPIA, M. S., LÓPEZ-MALO, A., & CHANES, J. W. 2003. General considerations for preservation of fruits and vegetables. *Handling and Preservation of Fruits and Vegetables by Combined Methods for Rural Areas*. Rome: Food and Agriculture Organization of the United Nations. Online available: <http://www.fao.org/docrep/005/y4358e/y4358e06.htm#bm06.1.3>

- BHANDARI, B. & HOWES, T. 1999. Implication of glass transition for the drying and stability of dried foods. *Journal of Food Engineering*, 40, 71-79.
- BILIADERIS, C. G., PAGE, C. M., MAURICE, T. J. & JULIANO, B. O. 1986. Thermal characterization of rice starches: A polymeric approach to phase transitions of granular starch. *Journal of Agricultural and Food Chemistry*, 34, 6-14.
- BLAIR, G. S. 1958. Rheology in food research. *Advances in food research*, 8, 1-61.
- BOLIN, H. & HUXSOLL, C. 1993. Partial drying of cut pears to improve freeze/thaw texture. *Journal of Food Science*, 58, 357-360.
- BOURNE, M. 2002. *Food texture and viscosity: concept and measurement*, Academic press.
- BOURNE, M. C. 1986. Effect of water activity on texture profile parameters of apple flesh. *Journal of Texture Studies*, 17, 331-340.
- BREENE, W. M. 1975. Application of texture profile analysis to instrumental food texture evaluation*. *Journal of Texture Studies*, 6, 53-82.
- BROSNAN, T. & SUN, D. W. 2004. Improving quality inspection of food products by computer vision—a review. *Journal of Food Engineering*, 61, 3-16.
- BRUNI, F. & LEOPOLD, A. C. 1991. Glass transitions in soybean seed Relevance to anhydrous biology. *Plant Physiology*, 96, 660-663.
- CAMPANELLA, O. & PELEG, M. 1988. ON FOOD COMPRESSION BY SOFT MACHINES¹. *Journal of Texture Studies*, 19, 39-50.
- CARPITA, N. C. & GIBEAUT, D. M. 1993. Structural models of primary cell walls in flowering plants: consistency of molecular structure with the physical properties of the walls during growth. *The Plant Journal*, 3, 1-30.

- CHAN, R., PATHMANATHAN, K. & JOHARI, G. 1986. Dielectric relaxations in the liquid and glassy states of glucose and its water mixtures. *The Journal of Physical Chemistry*, 90, 6358-6362.
- CHANG, C. S. 1988. Measuring density and porosity of grain kernels using a gas pycnometer. *Cereal Chem*, 65, 13-15.
- CHAUVIN, M. A., ROSS, C. F., PITTS, M., KUPFERMAN, E. & SWANSON, B. 2010. Relationship between instrumental and sensory determination of apple and pear texture. *Journal of Food Quality*, 33, 181-198.
- CHEN, L. & OPARA, U. L. 2013. Texture measurement approaches in fresh and processed foods—A review. *Food Research International*, 51, 823-835.
- CHEN, Y. & MARTYNENKO, A. 2013. Computer vision for real-time measurements of shrinkage and color changes in blueberry convective drying. *Drying Technology*, 31, 1114-1123.
- CHIRIFE, J. & BUERA, M. P. 1995. A critical review of some non-equilibrium situations and glass transitions on water activity values of foods in the microbiological growth range. *Journal of Food Engineering*, 25, 531-552.
- CRAPISTE, G., WHITAKER, S. & ROTSTEIN, E. 1988. Drying of cellular material—I. A mass transfer theory. *Chemical Engineering Science*, 43, 2919-2928.
- CUI, Z., LI, C., SONG, C. & SONG, Y. 2008. Combined microwave-vacuum and freeze drying of carrot and apple chips. *Drying Technology*, 26, 1517-1523.
- DELTEL, G., GAGNÉ, C., LEMIEUX, A., LEVERT, M., LIU, X., NAJJAR, L. & MALDAGUE, X. 2001. Automated measurement of cylinder volume by vision. *Elsevier, Fringe 2001*, 692-697.

- DO TRONG, N. N., RIZZOLO, A., HERREMANS, E., VANOLI, M., CORTELLINO, G., ERKINBAEV, C., TSUTA, M., SPINELLI, L., CONTINI, D. & TORRICELLI, A. 2014. Optical properties–microstructure–texture relationships of dried apple slices: Spatially resolved diffuse reflectance spectroscopy as a novel technique for analysis and process control. *Innovative Food Science & Emerging Technologies*, 21, 160-168.
- DOLAN, J. P. 1994. Microwave freeze-drying of aqueous solutions. *Advances in Heat and Mass Transfer in Biological Systems*, 288, 97-98.
- DONSI, G., FERRARI, G., NIGRO, R. & MATTEO, P. D. 1998. Combination of mild dehydration and freeze-drying processes to obtain high quality dried vegetables and fruits. *Food and Bioproducts Processing*, 76, 181-187.
- DROUZAS, A. E. & SCHUBERT, H. 1996. Microwave application in vacuum drying of fruits. *Journal of Food Engineering*, 28, 203-209.
- DUAN, X., ZHANG, M. & MUJUMDAR, A. S. 2007. Study on a combination drying technique of sea cucumber. *Drying Technology*, 25, 2011-2019.
- FARKAS, D. F. & LAZAR, M. E. 1969. Osmotic dehydration of apple pieces: effect of temperature and syrup concentration on rates. *Food Technology*.
- FEINBERG, B., SCHWIMMER, S., REEVE, R. & JUILLY, M. 1973. Vegetables. *Food Dehydration*, 2, 1-82.
- FIGIEL, A. 2007. Dehydration of apples by a combination of convective and vacuum-microwave drying. *Polish Journal of Food and Nutrition Sciences*, 57, 131-135.

- FINEGOLD, L., FRANKS, F. & HALTEY, R. H. 1989. Glass/rubber transitions and heat capacities of binary sugar blends. *Journal of the Chemical Society, Faraday Transactions 1: Physical Chemistry in Condensed Phases*, 85, 2945-2951.
- FLINK, J. M. 1983. Structure and structure transitions in dried carbohydrate materials. In: IN M. PELEG, E. B. B. E. (ed.) *Physical Properties of Foods*.
- FUNEBO, T. & OHLSSON, T. 1998. Microwave-assisted air dehydration of apple and mushroom. *Journal of Food Engineering*, 38, 353-367.
- GEKAS, V. & MAVROUDIS, N. 1998. Mass transfer properties of osmotic solutions. II. Diffusivities. *International Journal of Food Properties*, 1, 181-195.
- GORDON, M. & TAYLOR, J. S. 1952. Ideal copolymers and the second - order transitions of synthetic rubbers. i. non - crystalline copolymers. *Journal of Applied Chemistry*, 2, 493-500.
- GUINE, R. P. 2013. Variation of textural attributes of S. Bartolomeu pears at maturation, storage, and drying. *International Journal of Food Properties*, 16, 180-192.
- GUINE, R., M 2006. Influence of drying method on density and porosity of pears. *Food and Bioproducts Processing*, 84, 179-185.
- GUINE, R., RAMOS, M. & FIGUEIREDO, M. 2006. Shrinkage characteristics and porosity of pears during drying. *Drying Technology*, 24, 1525-1530.
- GUINE, R. P. & BARROCA, M. J. 2011. Effect of drying on the textural attributes of bell pepper and pumpkin. *Drying Technology*, 29, 1911-1919.
- HAHN, F. & SANCHEZ, S. 2000. Carrot volume evaluation using imaging algorithms. *Journal of Agricultural Engineering Research*, 75, 243-249.

- HAN, Q. H., YIN, L. J., LI, S. J., YANG, B. N. & MA, J. W. 2010. Optimization of process parameters for microwave vacuum drying of apple slices using response surface method. *Drying Technology*, 28, 523-532.
- HATAKEYAMA, T., NAKAMURA, K., YOSHIDA, H. & HATAKEYAMA, H. 1989. Mesomorphic properties of highly concentrated aqueous solutions of polyelectrolytes from saccharides. *Food Hydrocolloids*, 3, 301-311.
- HILLS, B. P. & REMIGEREAU, B. 1997. NMR studies of changes in subcellular water compartmentation in parenchyma apple tissue during drying and freezing. *International Journal of Food Science and Technology*, 32, 51-61.
- HO, Q. T., VERBOVEN, P., MEBATSION, H. K., VERLINDEN, B., VANDEWALLE, S. & NICOLA, B. 2009. Microscale mechanisms of gas exchange in fruit tissue. *New Phytologist*, 182, 163-174.
- HU, Q. G., ZHANG, M., MUJUMDAR, A. S., XIAO, G. N. & JIN-CAI, S. 2006. Drying of edamames by hot air and vacuum microwave combination. *Journal of Food Engineering*, 77, 977-982.
- ILKER, R. & SZCZESNIAK, A. S. 1990. Structural and chemical bases for texture of plant foodstuffs. *Journal of Texture Studies*, 21, 1-36.
- INSTRUMENTS, Q. 2012. Multipycnometer manual. *Quantachrome Instruments*. MVP-6DC.
- ISMAIL, B., HAFFAR, I., BAALBAKI, R. & HENRY, J. 2001. Development of a total quality scoring system based on consumer preference weightings and sensory profiles: application to fruit dates (Tamr). *Food Quality and Preference*, 12, 499-506.

- JOARDDER, M. U. H., BROWN, R. J., KUMAR, C. & KARIM, A. 2015. A micro-level investigation of the solid displacement method for porosity determination of dried food. *Journal of Food Engineering*, 166, 156-164.
- JOHARI, G., HALLBRUCKER, A. & MAYER, E. 1987. The glass-liquid transition of hyperquenched water. *Nature*, 330, 552-553.
- JOWITT, R. 1974. The terminology of food texture. *Journal of Texture Studies*, 5, 351-358.
- KALETUNC, G., NORMAND, M., NUSSINOVITCH, A. & PELEG, M. 1991. Determination of elasticity of gels by successive compression-decompression cycles. *Food Hydrocolloids*, 5, 237-247.
- KARATHANOS, V. 1993. Collapse of structure during drying of celery. *Drying Technology*, 11, 1005-1023.
- KARATHANOS, V., KANELLOPOULOS, N. & BELESSIOTIS, V. 1996. Development of porous structure during air drying of agricultural plant products. *Journal of Food Engineering*, 29, 167-183.
- KAREL, M. Physical structure and quality of dehydrated foods. 7 th International Drying Symposium in conjunction with the CSISA'90 Congress, Prague, Czech, 08/90, 1991. 26-35.
- KARMAS, R., PILAR BUERA, M. & KAREL, M. 1992. Effect of glass transition on rates of nonenzymic browning in food systems. *Journal of Agricultural and Food Chemistry*, 40, 873-879.

- KASAPIS, S. 2009. Glass transitions in foodstuffs and biomaterials: Theory and measurements. In: RAHMAN, M. S. (ed.) *Food Properties Handbook*. New York: CRC Press.
- KATEKAWA, M. & SILVA, M. Study of porosity behavior in convective drying of bananas. Proceedings of the 14 th International Drying Symposium, vol. B, 2004.
- KATEKAWA, M. E. & SILVA, M. A. 2007. On the influence of glass transition on shrinkage in convective drying of fruits: a case study of banana drying. *Drying Technology*, 25, 1659-1666.
- KAWAS, M. & MOREIRA, R. 2001. Effect of degree of starch gelatinization on quality attributes of fried tortilla chips. *Journal of Food Science*, 66, 300-306.
- KHAN, A. & VINCENT, J. 1993. Anisotropy in the fracture properties of apple flesh as investigated by crack-opening tests. *Journal of Materials Science*, 28, 45-51.
- KHRAISHEH, M., COOPER, T. & MAGEE, T. 1997. Shrinkage characteristics of potatoes dehydrated under combined microwave and convective air conditions. *Drying Technology*, 15, 1003-1022.
- KHRAISHEH, M., MCMINN, W. & MAGEE, T. 2004. Quality and structural changes in starchy foods during microwave and convective drying. *Food Research International*, 37, 497-503.
- KROKIDA, M., KARATHANOS, V. & MAROULIS, Z. 1998. Effect of freeze-drying conditions on shrinkage and porosity of dehydrated agricultural products. *Journal of Food Engineering*, 35, 369-380.
- KROKIDA, M., KARATHANOS, V. & MAROULIS, Z. 2000a. Compression analysis of dehydrated agricultural products. *Drying technology*, 18, 395-408.

- KROKIDA, M., KIRANOUDIS, C., MAROULIS, Z. & MARINOS-KOURIS, D. 2000b. Drying related properties of apple. *Drying Technology*, 18, 1251-1267.
- KROKIDA, M. & MAROULIS, Z. 1997. Effect of drying method on shrinkage and porosity. *Drying Technology*, 15, 2441-2458.
- KUDRA, T. & MUJUMDAR, A. S. 2009. *Advanced Drying Technologies*, CRC Press.
- KUROZAWA, L. E., HUBINGER, M. D. & PARK, K. J. 2012. Glass transition phenomenon on shrinkage of papaya during convective drying. *Journal of Food Engineering*, 108, 43-50.
- LEONARD, A., BLACHER, S., PIRARD, R., MARCHOT, P., PIRARD, J.-P. & CRINE, M. 2003. Multiscale texture characterization of wastewater sludges dried in a convective rig. *Drying Technology*, 21, 1507-1526.
- LABUZA, T., NELSON, K. & COPPERMITH, C. 1992. Glass transition temperatures of food systems.
- LEVI, G. & KAREL, M. 1995. Volumetric shrinkage (collapse) in freeze-dried carbohydrates above their glass transition temperature. *Food Research International*, 28, 145-151.
- LEVINE, H. & SLADE, L. 1986. A polymer physico-chemical approach to the study of commercial starch hydrolysis products (SHPs). *Carbohydrate Polymers*, 6, 213-244.
- LEVINE, L., HUANG, V. T. & SAGUY, I. 1990. Use of computer vision for real time estimation of volume increase during microwave baking. *Cereal Chem*, 67, 104.

- LEWICKI, P. & DRZEWUCKA-BUJAK, J. Effect of drying on tissue structure of selected fruits and vegetables. Proceedings of the 11th International Drying Symposium Drying, 1998. 1093-1099.
- LEWICKI, P. P. 1998. Effect of pre-drying treatment, drying and rehydration on plant tissue properties: A review. *International Journal of Food Properties*, 1, 1-22.
- LEWICKI, P. P. & JAKUBCZYK, E. 2004. Effect of hot air temperature on mechanical properties of dried apples. *Journal of Food Engineering*, 64, 307-314.
- LEWICKI, P. P. & LUKASZUK, A. 2000. Changes of rheological properties of apple tissue undergoing convective drying. *Drying technology*, 18, 707-722.
- LEWICKI, P. P. & PAWLAK, G. 2003. Effect of drying on microstructure of plant tissue. *Drying Technology*, 21, 657-683.
- LEWICKI, P. P. & PORZECKA-PAWLAK, R. 2005. Effect of osmotic dewatering on apple tissue structure. *Journal of Food Engineering*, 66, 43-50.
- LIEVONEN, S. & ROOS, Y. 2002. Water sorption of food models for studies of glass transition and reaction kinetics. *Journal of Food Science*, 67, 1758-1766.
- LIN, T. M., DURANCE, T. D. & SCAMAN, C. H. 1998. Characterization of vacuum microwave, air and freeze dried carrot slices. *Food Research International*, 31, 111-117.
- LIU, P., ZHANG, M. & MUJUMDAR, A. S. 2012. Comparison of three microwave-assisted drying methods on the physiochemical, nutritional and sensory qualities of re-structured purple-fleshed sweet potato granules. *International Journal of Food Science & Technology*, 47, 141-147.

- LOZANO, J., ROTSTEIN, E. & URBICAIN, M. 1980. Total porosity and open-pore porosity in the drying of fruits. *Journal of Food Science*, 45, 1403-1407.
- LOZANO, J., ROTSTEIN, E. & URBICAIN, M. 1983. Shrinkage, porosity and bulk density of foodstuffs at changing moisture contents. *Journal of Food Science*, 48, 1497-1502.
- MADAMBA, P. S. 2003. Physical changes in bamboo (*Bambusa phyllostachys*) shoot during hot air drying: Shrinkage, density, and porosity. *Drying Technology*, 21, 555-568.
- MADIOULI, J., LECOMTE, D., NGANYA, T., CHAVEZ, S., SGHAIER, J. & SAMMOUDA, H. 2007. A method for determination of porosity change from shrinkage curves of deformable materials. *Drying Technology*, 25, 621-628.
- MADIOULI, J., SGHAIER, J., ORTEU, J.-J., ROBERT, L., LECOMTE, D. & SAMMOUDA, H. 2011. Non-contact measurement of the shrinkage and calculation of porosity during the drying of banana. *Drying Technology*, 29, 1358-1364.
- MAGUER, M. L. 1997. Mass transfer modeling in structured foods. *Food Engineering* 2000, 253-269.
- MAROUSIS, S. & SARAVACOS, G. 1990. Density and porosity in drying starch materials. *Journal of Food Science*, 55, 1367-1372.
- MARTYNENKO, A. 2006. Computer-vision system for control of drying processes. *Drying Technology*, 24, 879-888.
- MARTYNENKO, A. 2008. The system of correlations between moisture, shrinkage, density, and porosity. *Drying Technology*, 26, 1497-1500.

- MARTYNENKO, A. & JANASZEK, M. A. 2014. Texture changes during drying of apple slices. *Drying Technology*, 32, 567-577.
- MARTYNENKO, A. I. 2011. Porosity evaluation of ginseng roots from real-time imaging and mass measurements. *Food and Bioprocess Technology*, 4, 417-428.
- MAVROUDIS, N. E., GEKAS, V. & SJ HOLM, I. 1998. Osmotic dehydration of apples. Shrinkage phenomena and the significance of initial structure on mass transfer rates. *Journal of Food Engineering*, 38, 101-123.
- MAY, B. & PERR, P. 2002. The importance of considering exchange surface area reduction to exhibit a constant drying flux period in foodstuffs. *Journal of Food Engineering*, 54, 271-282.
- MAYOR, L. & SERENO, A. 2004. Modelling shrinkage during convective drying of food materials: a review. *Journal of Food Engineering*, 61, 373-386.
- MOHSENIN, N., COOPER, H. & TUKEY, L. 1963. Engineering approach to evaluating textural factors in fruits and vegetables. *Transactions of the ASAE*, 6, 85-88.
- MOHSENIN, N. N. 1970. Physical properties of plant and animal materials. Vol. 1. Structure, physical characteristics and mechanical properties. *Physical properties of plant and animal materials. Vol. 1. Structure, physical characteristics and mechanical properties.*, 1.
- MONSALVE-GONALEZ, A., BARBOSA-CANOVAS, G. V. & CAVALIERI, R. P. 1993. Mass transfer and textural changes during processing of apples by combined methods. *Journal of Food Science*, 58, 1118-1124.
- MONTGOMERY, D. C. 2013. *Design and analysis of experiments*, MA, John Wiley & Sons: Danvers.

- MOREIRA, R., FIGUEIREDO, A. & SERENO, A. 2000. Shrinkage of apple disks during drying by warm air convection and freeze drying. *Drying Technology*, 18, 279-294.
- MUJUMDAR, A. S. 1995. *Handbook of industrial drying*, CRC Press.
- MUSIELAK, G. 2000. Influence of the drying medium parameters on drying induced stresses. *Drying Technology*, 18, 561-581.
- NAHIMANA, H. & ZHANG, M. 2011. Shrinkage and color change during microwave vacuum drying of carrot. *Drying Technology*, 29, 836-847.
- NEUMANN, H. 1972. Dehydrated celery: Effects of predrying treatments and rehydration procedures on reconstitution. *Journal of Food Science*, 37, 437-441.
- NIJHUIS, H., TORRINGA, H., MURESAN, S., YUKSEL, D., LEGUIJT, C. & KLOEK, W. 1998. Approaches to improving the quality of dried fruit and vegetables. *Trends in Food Science & Technology*, 9, 13-20.
- OCHOA, M., KESSELER, A., PIRONE, B., MARQUEZ, C. & DE MICHELIS, A. 2002. Volume and area shrinkage of whole sour cherry fruits (*Prunus cerasus*) during dehydration. *Drying Technology*, 20, 147-156.
- OPPENHEIMER, J. R., MARTIN, A. G. & WALKER, L. P. 1997. Measurements of air-filled porosity in unsaturated organic matrices using a pycnometer. *Bioresource Technology*, 59, 241-247.
- PAAKKONEN, K. & ROOS, Y. H. 1990. Effects of drying conditions on water sorption and phase transitions of freeze - dried horseradish roots. *Journal of Food Science*, 55, 206-209.
- PAKOWSKI, Z. & ADAMSKI, R. 2012. Formation of underpressure in an apple cylinder during convective drying. *Drying Technology*, 30, 1238-1246.

- PARKS, G. S. & HUFFMAN, H. M. 1926. Glass as a fourth state of matter. *Science*, 64, 363-364.
- PELEG, M. 1994. A model of mechanical changes in biomaterials at and around their glass transition. *Biotechnology Progress*, 10, 385-388.
- PROTHON, F., AHRN, L. & SJ HOLM, I. 2003. Mechanisms and prevention of plant tissue collapse during dehydration: a critical review. *Critical Reviews in Food Science and Nutrition*, 43, 447-479.
- PTASZNIK, W., ZYGMUNT, S. & KUDRA, T. 1990. Simulation of RF-assisted convective drying for seed quality broad bean. *Drying Technology*, 8, 977-992.
- QUEVEDO, R. & AGUILERA, J. 2010. Computer vision and stereoscopy for estimating firmness in the salmon (Salmon salar) fillets. *Food and Bioprocess Technology*, 3, 561-567.
- RAHMAN, M. 1999. Glass transition and other structural changes in foods. *Handbook of Food Preservation*. New York: Marcel Dekker.
- RAHMAN, M. S. 1995. Phase transitions in foods. In: RAHMAN, M. S. (ed.) *Food Properties Handbook*. New York: CRC Press.
- RAHMAN, M. S. 2003. A theoretical model to predict the formation of pores in foods during drying. *International Journal of Food Properties*, 6, 61-72.
- RAHMAN, M. S., AL-ZAKWANI, I. & GUIZANI, N. 2005. Pore formation in apple during air-drying as a function of temperature: porosity and pore-size distribution. *Journal of the Science of Food and Agriculture*, 85, 979-989.
- RAMASWAMY, H. S. & MARCOTTE, M. 2005. *Food processing: principles and applications*, CRC Press.

- RAWSON, A., PATRAS, A., TIWARI, B., NOCI, F., KOUTCHMA, T. & BRUNTON, N. 2011. Effect of thermal and non thermal processing technologies on the bioactive content of exotic fruits and their products: Review of recent advances. *Food Research International*, 44, 1875-1887.
- RIBEIRO, C., ZIMERI, J., YILDIZ, E. & KOKINI, J. 2003. Estimation of effective diffusivities and glass transition temperature of polydextrose as a function of moisture content. *Carbohydrate Polymers*, 51, 273-280.
- RODR GUEZ-RAM REZ, J., M NDEZ-LAGUNAS, L., L PEZ-ORTIZ, A. & TORRES, S. S. 2012. True density and apparent density during the drying process for vegetables and fruits: A review. *Journal of Food Science*, 77, R146-R154.
- ROOS, Y. 1995. Water activity and glass transition temperature: How do they complement and how do they differ. Technomic Publishing Co., Lancaster.
- ROOS, Y. & KAREL, M. 1991. Phase transitions of mixtures of amorphous polysaccharides and sugars. *Biotechnology Progress*, 7, 49-53.
- SABLIOV, C., BOLDOR, D., KEENER, K. & FARKAS, B. 2002. Image processing method to determine surface area and volume of axi-symmetric agricultural products. *International Journal of Food Properties*, 5, 641-653.
- SADIQ NARGAL, M. & OORAIKUL, B. 1996. Effect of some physical and chemical pretreatments on improvement of drying characteristics of hash-brown potatoes. *Journal of Food Science and Technology*, 33, 436-439.
- SARAVACOS, G. 1967. Effect of the drying method on the water sorption of dehydrated apple and potato. *Journal of Food Science*, 32, 81-84.

- SARAVACOS, G. 1993. Technological developments in fruit and vegetable dehydration. *Developments in Food Science*.
- SCHOTSMANS, W., VERLINDEN, B. E., LAMMERTYN, J., PEIRS, A., JANCS K, P. T., SCHEERLINCK, N. & NICOLAÏ, B. M. 2002. Factors affecting skin resistance measurements in pipfruit. *Postharvest Biology and Technology*, 25, 169-179.
- SERENO, A. M., SILVA, M. A. & MAYOR, L. 2007. Determination of particle density and porosity in foods and porous materials with high moisture content. *International Journal of Food Properties*, 10, 455-469.
- SHAM, P., SCAMAN, C. & DURANCE, T. 2001. Texture of vacuum microwave dehydrated apple chips as affected by calcium pretreatment, vacuum level, and apple variety. *Journal of Food Science*, 66, 1341-1347.
- SOESANTO, T. & WILLIAMS, M. C. 1981. Volumetric interpretation of viscosity for concentrated and dilute sugar solutions. *The Journal of Physical Chemistry*, 85, 3338-3341.
- SOYSAL, Y. 2004. Microwave drying characteristics of parsley. *Biosystems Engineering*, 89, 167-173.
- SPERLING, L. H. 2015. *Introduction to physical polymer science*, John Wiley & Sons.
- STERLING, C. 1963. Texture and cell wall polysaccharides in foods. *Recent Advances in Food Science*, 3.
- SUN, D. W. 2004. Computer vision—an objective, rapid and non-contact quality evaluation tool for the food industry. *Journal of Food Engineering*, 61, 1-2.
- SZCZESNIAK, A. S. 1963a. Classification of textural characteristics. *Journal of Food Science*, 28, 385-389.

- SZCZESNIAK, A. S. 1963b. Objective measurements of food texture. *Journal of Food Science*, 28, 410-420.
- SZCZESNIAK, A. S. 2002. Texture is a sensory property. *Food Quality and Preference*, 13, 215-225.
- THERDTHAI, N. & ZHOU, W. 2009. Characterization of microwave vacuum drying and hot air drying of mint leaves (*Mentha cordifolia* Opiz ex Fresen). *Journal of Food Engineering*, 91, 482-489.
- TREITEL, O. 1944. Elasticity of plant tissues. *Transactions of the Kansas Academy of Science (1903)*, 219-239.
- TSAMI, E. & KATSIOTI, M. 2000. Drying kinetics for some fruits: Predicting of porosity and color during dehydration. *Drying Technology*, 18, 1559-1581.
- TSOUROUFLIS, S., FLINK, J. M. & KAREL, M. 1976. Loss of structure in freeze - dried carbohydrates solutions: effect of temperature, moisture content and composition. *Journal of the Science of Food and Agriculture*, 27, 509-519.
- USDA 2014. National nutrient database for standard reference. *The National Agricultural Library*.
- VENIR, E., MUNARI, M., TONIZZO, A. & MALTINI, E. 2007. Structure related changes during moistening of freeze dried apple tissue. *Journal of Food Engineering*, 81, 27-32.
- VENKATACHALAPATHY, K. & RAGHAVAN, G. 2000. Microwave drying of whole, sliced and pureed strawberries. *Agricultural Engineering Journal*, 9, 29-39.

- VENNAT, E., BOGICEVIC, C., FLEUREAU, J.-M. & DEGRANGE, M. 2009. Demineralized dentin 3D porosity and pore size distribution using mercury porosimetry. *Dental Materials*, 25, 729-735.
- VILLOTA, R., SAGUY, I. & KAREL, M. 1980. Storage stability of dehydrated food evaluation of literature data. *Journal of Food Quality*, 3, 123-212.
- WANG, T. Y. & NGUANG, S. K. 2007. Low cost sensor for volume and surface area computation of axi-symmetric agricultural products. *Journal of Food Engineering*, 79, 870-877.
- WEBB, P. A. 2001. Volume and density determinations for particle technologists. *Micromeritics Instrument Corp*, 2, 01.
- WHITE, G. & CAKEBREAD, S. 1966. The glassy state in certain sugar - containing food products*. *International Journal of Food Science & Technology*, 1, 73-82.
- WILKINSON, C., DIJKSTERHUIS, G. & MINEKUS, M. 2000. From food structure to texture. *Trends in Food Science & Technology*, 11, 442-450.
- WITROWA-RAJCHERT, D., LEWICKI, P. & LENART, A. 1995. Influence of osmotic dewatering on the kinetics of convection drying of apples. *Osmotic Dehydration of Fruits and Vegetables*, 121-130.
- WU, L., ORIKASA, T., OGAWA, Y. & TAGAWA, A. 2007. Vacuum drying characteristics of eggplants. *Journal of Food Engineering*, 83, 422-429.
- XU, Y., ZHANG, M., MUJUMDAR, A. S., ZHOU, L. Q. & SUN, J.-C. 2004. Studies on hot air and microwave vacuum drying of wild cabbage. *Drying Technology*, 22, 2201-2209.

- YAN, W. Q., ZHANG, M., HUANG, L. L., TANG, J., MUJUMDAR, A. S. & SUN, J. C. 2010. Studies on different combined microwave drying of carrot pieces. *International Journal of Food Science & Technology*, 45, 2141-2148.
- YAN, Z., SOUSA-GALLAGHER, M. J. & OLIVEIRA, F. A. 2008. Shrinkage and porosity of banana, pineapple and mango slices during air-drying. *Journal of Food Engineering*, 84, 430-440.
- ZELEZNAK, K. & HOSENEY, R. 1987. The Glass Transition in Starch1. *Cereal Chem*, 64, 121-124.
- ZHANG, M., JIANG, H. & LIM, R. X. 2010. Recent developments in microwave-assisted drying of vegetables, fruits, and aquatic products—Drying kinetics and quality considerations. *Drying Technology*, 28, 1307-1316.
- ZHANG, M., TANG, J., MUJUMDAR, A. & WANG, S. 2006. Trends in microwave-related drying of fruits and vegetables. *Trends in Food Science & Technology*, 17, 524-534.
- ZHENG, X., LIU, C., SHI, J., XUE, S., MU, Y., LIN, Z. & LIU, H. 2013. Analysis of volume expansion and dehydration rate of berry slab under microwave-vacuum puffing conditions. *LWT-Food Science and Technology*, 52, 39-48.
- ZOERB, G. & HALL, C. 1960. Some mechanical and rheological properties of grains. *Journal of Agricultural Engineering Research*, 5, 83-93.
- ZOGZAS, N., MAROULIS, Z. & MARINOS-KOURIS, D. 1994. Densities, shrinkage and porosity of some vegetables during air drying. *Drying Technology*, 12, 1653-1666.

Appendices

Copyright Permission (A)

8/1/2016

Rightslink® by Copyright Clearance Center



RightsLink®

Home

Account Info

Help



Title: ON FOOD COMPRESSION BY SOFT MACHINES1
Author: O. H. CAMPANELLA,M. PELEG
Publication: Journal of Texture Studies
Publisher: John Wiley and Sons
Date: Jan 30, 2007
Copyright © 2007, John Wiley and Sons

Logged in as:
Dandan Wang
Account #:
3001039479

LOGOUT

Order Completed

Thank you for your order.

This Agreement between Dandan Wang ("You") and John Wiley and Sons ("John Wiley and Sons") consists of your license details and the terms and conditions provided by John Wiley and Sons and Copyright Clearance Center.

Your confirmation email will contain your order number for future reference.

[Get the printable license.](#)

License Number	3920320968201
License date	Aug 01, 2016
Licensed Content Publisher	John Wiley and Sons
Licensed Content Publication	Journal of Texture Studies
Licensed Content Title	ON FOOD COMPRESSION BY SOFT MACHINES1
Licensed Content Author	O. H. CAMPANELLA,M. PELEG
Licensed Content Date	Jan 30, 2007
Licensed Content Pages	12
Type of use	Dissertation/Thesis
Requestor type	University/Academic
Format	Print and electronic
Portion	Figure/table
Number of figures/tables	1
Original Wiley figure/table number(s)	Figure 1
Will you be translating?	No
Title of your thesis / dissertation	PREDICTION OF TEXTURE CHARACTERISTICS IN APPLE DRYING USING COMPUTER VISION
Expected completion date	Aug 2016
Expected size (number of pages)	140
Requestor Location	Dandan Wang Apt 11, 317 College Road Truro, NS B2N2P6 Canada Attn: Dandan Wang
Publisher Tax ID	EU826007151
Billing Type	Invoice
Billing address	Dandan Wang Apt 11, 317 College Road Truro, NS B2N2P6

https://s100.copyright.com/AppDispatchServlet

1/2

8/1/2016

Rightslink® by Copyright Clearance Center

Total Canada
 Attn: Dandan Wang
 0.00 CAD

Would you like to purchase the full text of this article? If so, please continue on to the content ordering system located here: [Purchase PDF](#)

If you click on the buttons below or close this window, you will not be able to return to the content ordering system.

[ORDER MORE](#)

[CLOSE WINDOW](#)

Copyright © 2016 [Copyright Clearance Center, Inc.](#) All Rights Reserved. [Privacy statement](#). [Terms and Conditions](#).
Comments? We would like to hear from you. E-mail us at customercare@copyright.com

Copyright Permission (B)



RightsLink®

Home

Account Info

Help



Title: Mechanisms and Prevention of Plant Tissue Collapse during Dehydration: A Critical Review
Author: Frédéric Prothon, Lilia Ahmé, Ingegerd Sjöholm

Publication: Critical Reviews in Food Science and Nutrition

Publisher: Taylor & Francis

Date: Jul 1, 2003

Copyright © 2003 Taylor & Francis

Logged in as:

Dandan Wang

Account #:

3001039479

LOGOUT

Thesis/Dissertation Reuse Request

Taylor & Francis is pleased to offer reuses of its content for a thesis or dissertation free of charge contingent on resubmission of permission request if work is published.

BACK

CLOSE WINDOW

Copyright © 2016 [Copyright Clearance Center, Inc.](#) All Rights Reserved. [Privacy statement](#). [Terms and Conditions](#).
Comments? We would like to hear from you. E-mail us at customercare@copyright.com

Copyright Permission (C)



6/22/2016

RE: Co-authors' permission for paper "Estimation of Total, Open-and Close-Pore Porosity of Apple Slices during Drying"

 Reply all |   Delete Junk |  ... 

RE: Co-authors' permission for paper "Estimation of Total, Open-and Close-Pore Porosity of Apple Slices during Drying"

Alex Martynenko

 Today 2:57 PM
Dandan Wang 

  Reply all | 

Inbox

Dear Dandan,

You have my permission for the material described above to be included in the copy of your thesis that is sent to the Library and Archives of Canada (formerly National Library of Canada) for the reproduction and distribution.

Thank you,
Alex

From: Dandan Wang

Sent: Wednesday, June 22, 2016 2:55 PM

To: Alex Martynenko <Alex.Martynenko@Dal.Ca>

Subject: Re: Co-authors' permission for paper "Estimation of Total, Open-and Close-Pore Porosity of Apple Slices during Drying"

Dear Dr. Martynenko,

I am currently preparing my MSc. Thesis for submission to the Faculty of Graduate Studies at Dalhousie University, Halifax, Nova Scotia, Canada. I am seeking your permission to include a manuscript version of the following paper(s) as a chapter in the thesis:

Title of paper: Estimation of Total, Open-and Close-Pore Porosity of Apple Slices during Drying;

Authors: Dandan Wang & Alex Martynenko

Paper's status: published in the journal : Drying Technology: An International Journal, 34 (2016) 892-899.

Canadian graduate theses are reproduced by the Library and Archives of Canada (formerly National Library of Canada) through a non-exclusive, world-wide license to reproduce, loan, distribute, or sell theses. I am also seeking your permission for the material described above to be reproduced and distributed by the LAC (NLC). Further details about the LAC (NLC) thesis program are available on the LAC (NLC) website (www.nlc-bnc.ca).

Full publication/processing details and a copy of this permission letter will be included in this thesis. Please respond this email with your agreement/exception, also select/write down the granted choice (a or b) shown as below (please select b):

<https://outlook.office365.com/owa/projection.aspx>

1/2

6/22/2016

RE: Co-authors' permission for paper "Estimation of Total, Open and Close-Pore Porosity of Apple Slices during Drying"

Permission is granted for:

- a) The inclusion of the material described above in your thesis.
- b) For the material described above to be included in the copy of your thesis that is sent to the Library and Archives of Canada (formerly National Library of Canada) for the reproduction and distribution.

Your sincerely,
Dandan Wang

M.Sc Student
Department of Engineering
Faculty of Agriculture
Dalhousie University
PO Box 550
Truro NS B2N 5E3
Email: Dandan.Wang@Dal.Ca
TEL: 902-843-3166



Title: Estimation of total, open-, and closed-pore porosity of apple slices during drying
Author: Dandan Wang, Alex Martynenko
Publication: Drying Technology
Publisher: Taylor & Francis
Date: Jun 10, 2016
Copyright © 2016 Taylor & Francis

Logged in as:
Dandan Wang
Account #:
3001039479

[LOGOUT](#)

Thesis/Dissertation Reuse Request

Taylor & Francis is pleased to offer reuses of its content for a thesis or dissertation free of charge contingent on resubmission of permission request if work is published.


[BACK](#)[CLOSE WINDOW](#)

Copyright Permission (D)

8/22/2016

RE: Re: Co-authors' permission for the paper "Computer vision for bulk volume estimation of apple slices during drying"

 Reply all | v

 Delete Junk | v

...





RE: Re: Co-authors' permission for the paper "Computer vision for bulk volume estimation of apple slices during drying"

KC Kenneth Corscadden

Today 2:47 PM

Dandan Wang; Sophia He; Alex Martynenko v

  Reply all | v

Inbox

You have my permission

Kenny

From: Dandan Wang

Sent: Wednesday, June 22, 2016 2:25 PM

To: Kenneth Corscadden; Sophia He; Alex Martynenko

Subject: Re: Co-authors' permission for the paper "Computer vision for bulk volume estimation of apple slices during drying"

Dear Professors,

I am currently preparing my MSc. Thesis for submission to the Faculty of Graduate Studies at Dalhousie University, Halifax, Nova Scotia, Canada. I am seeking your permission to include a manuscript version of the following paper(s) as a chapter in the thesis:

Title of paper: Computer vision for bulk volume estimation of apple slices during drying;

Authors: Dandan Wang, Alex Martynenko, Kenneth Corscadden, Quan (Sophia) He

Paper's status: submitted to the journal : Drying Technology: An International Journal.

Canadian graduate theses are reproduced by the Library and Archives of Canada (formerly National Library of Canada) through a non-exclusive, world-wide license to reproduce, loan, distribute, or sell theses. I am also seeking your permission for the material described above to be reproduced and distributed by the LAC (NLC). Further details about the LAC (NLC) thesis program are available on the LAC (NLC) website (www.nlc-bnc.ca).

Full publication/processing details and a copy of this permission letter will be included in this thesis. Please respond this email with your agreement/exception, also select/write down the granted choice (a or b) shown as below (please select b):

Permission is granted for:

- a) The inclusion of the material described above in your thesis.
- b) For the material described above to be included in the copy of your thesis that is sent to the Library and Archives of Canada (formerly National Library of Canada) for the reproduction and distribution.

Your sincerely,
Dandan Wang

<https://outlook.office365.com/owa/projection.aspx>

1/2




6/22/2016

RE: Re: Co-authors' permission for the paper "Computer vision for bulk volume estimation of apple slices during drying"

M.Sc Student
Department of Engineering
Faculty of Agriculture
Dalhousie University
[PO Box 550](#)
[Truro NS B2N 5E3](#)
Email: Dandan.Wang@Dal.Ca
TEL: 902-843-3166

6/22/2016

RE: Re: Co-authors' permission for the paper "Computer vision for bulk volume estimation of apple slices during drying"

 Reply all |  Delete | Junk | 



RE: Re: Co-authors' permission for the paper "Computer vision for bulk volume estimation of apple slices during drying"





Sophia He

Today 2:39 PM

Alex Martynenko; Dandan Wang; Kenneth Corscadden



 Reply all | 

Inbox

You have my permission , Dandan.

From: Alex Martynenko
Sent: Wednesday, June 22, 2016 2:30 PM
To: Dandan Wang; Kenneth Corscadden; Sophia He
Subject: RE: Re: Co-authors' permission for the paper "Computer vision for bulk volume estimation of apple slices during drying"

Thank you Dandan,

You have my permission for the material described in this paper to be included in the copy of your thesis that is sent to the Library and Archives of Canada (formerly National Library of Canada) for the reproduction and distribution.

Alex Martynenko

From: Dandan Wang
Sent: Wednesday, June 22, 2016 2:25 PM
To: Kenneth Corscadden <Kenneth.Corscadden@Dal.Ca>; Sophia He <Quan.He@Dal.Ca>; Alex Martynenko <Alex.Martynenko@Dal.Ca>
Subject: Re: Co-authors' permission for the paper "Computer vision for bulk volume estimation of apple slices during drying"

Dear Professors,

I am currently preparing my MSc. Thesis for submission to the Faculty of Graduate Studies at Dalhousie University, Halifax, Nova Scotia, Canada. I am seeking your permission to include a manuscript version of the following paper(s) as a chapter in the thesis:

Title of paper: Computer vision for bulk volume estimation of apple slices during drying;
Authors: Dandan Wang, Alex Martynenko, Kenneth Corscadden, Quan (Sophia) He
Paper's status: submitted to the journal : Drying Technology: An International Journal.

Canadian graduate theses are reproduced by the Library and Archives of Canada (formerly National Library of Canada) through a non-exclusive, world-wide license to reproduce, loan, distribute, or sell theses. I am

<https://outlook.office365.com/owa/projection.aspx>

1/2

8/22/2016

RE: Re: Co-authors' permission for the paper "Computer vision for bulk volume estimation of apple slices during drying"

also seeking your permission for the material described above to be reproduced and distributed by the LAC (NLC). Further details about the LAC (NLC) thesis program are available on the LAC (NLC) website (www.nlc-bnc.ca).

Full publication/processing details and a copy of this permission letter will be included in this thesis. Please respond this email with your agreement/exception, also select/write down the granted choice (a or b) shown as below (please select b):

Permission is granted for:

- a) The inclusion of the material described above in your thesis.
- b) For the material described above to be included in the copy of your thesis that is sent to the Library and Archives of Canada (formerly National Library of Canada) for the reproduction and distribution.

Your sincerely,
Dandan Wang

M.Sc Student
Department of Engineering
Faculty of Agriculture
Dalhousie University
PO Box 550
Truro NS B2N 5E3
Email: Dandan.Wang@Dal.Ca
TEL: 902-843-3166

Copyright Permission (E)

7/5/2016

RightsLink Printable License

JOHN WILEY AND SONS LICENSE TERMS AND CONDITIONS

Jul 05, 2016

This Agreement between Dandan Wang ("You") and John Wiley and Sons ("John Wiley and Sons") consists of your license details and the terms and conditions provided by John Wiley and Sons and Copyright Clearance Center.

License Number	3902730180892
License date	Jul 05, 2016
Licensed Content Publisher	John Wiley and Sons
Licensed Content Publication	International Journal of Food Science & Technology
Licensed Content Title	The glassy state in certain sugar-containing food products *
Licensed Content Author	G. W. WHITE,S. H. CAKEBREAD
Licensed Content Date	Jun 28, 2007
Licensed Content Pages	10
Type of use	Dissertation/Thesis
Requestor type	University/Academic
Format	Print and electronic
Portion	Figure/table
Number of figures/tables	1
Original Wiley figure/table number(s)	Figure 1
Will you be translating?	No
Title of your thesis / dissertation	PREDICTION OF TEXTURE CHARACTERISTICS IN APPLE DRYING USING COMPUTER VISION
Expected completion date	Aug 2016
Expected size (number of pages)	140
Requestor Location	Dandan Wang Apt 11, 317 College Road Truro, NS B2N2P6 Canada Attn: Dandan Wang
Publisher Tax ID	EU826007151
Billing Type	Invoice
Billing Address	Dandan Wang Apt 11, 317 College Road Truro, NS B2N2P6 Canada Attn: Dandan Wang
Total	0.00 CAD
Terms and Conditions	

<https://s100.copyright.com/AppDispatchServlet>

1/5

Copyright Permission (F)



FAO CORPORATE DOCUMENT REPOSITORY

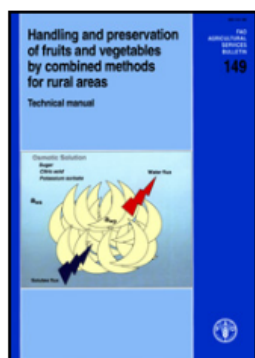
Title: Handling and preservation of fruits and vegetables by combined methods for ...

Produced by: Agriculture and Consumer Protection

PDF version

[More details](#)

Handling and Preservation of Fruits and Vegetables by Combined Methods for Rural Areas



TECHNICAL MANUAL
FAO Agricultural Services Bulletin 149

by
Gustavo V. Barbosa-Cánovas
Juan J. Fernández-Molina
Stella M. Alzamora
Maria S. Tapia
Aurelio López-Malo
Jorge Welti Chanes

FOOD AND AGRICULTURE ORGANIZATION OF THE UNITED NATIONS
Rome, 2003

ISBN 92-5-104861-4

[Table of Contents](#)

The designations employed and the presentation of material in this information product do not imply the expression of any opinion whatsoever on the part of the Food and Agriculture Organization of the United Nations concerning the legal status of any country, territory, city or area of its authorities, or concerning the delimitation of its frontiers or boundaries.

All rights reserved. Reproduction and dissemination of material in this information product for educational or other non-commercial purposes are authorized without any prior written permission from the copyright holders provided the source is fully acknowledged. Reproduction of material in this information product for resale or other commercial purposes is prohibited without written permission of the copyright holders. Applications for such permission should be addressed to the Chief, Publishing Management Service, Information Division, FAO, Viale delle Terme di Caracalla, 00100 Rome, Italy or by e-mail to copyright@fao.org <mailto:copyright@fao.org>.

FAO 2003

Copyright Permission (G)

7/5/2016

Rightslink® by Copyright Clearance Center



RightsLink®

Home

Account Info

Help



Title: EFFECT OF WATER ACTIVITY ON TEXTURE PROFILE PARAMETERS OF APPLE FLESH

Author: MALCOLM C. BOURNE

Publication: Journal of Texture Studies

Publisher: John Wiley and Sons

Date: Jan 30, 2007

Copyright © 2007, John Wiley and Sons

Logged in as:

Dandan Wang

Account #:

3001039479

LOGOUT

Order Completed

Thank you for your order.

This Agreement between Dandan Wang ("You") and John Wiley and Sons ("John Wiley and Sons") consists of your license details and the terms and conditions provided by John Wiley and Sons and Copyright Clearance Center.

Your confirmation email will contain your order number for future reference.

[Get the printable license.](#)

License Number	3902740310667
License date	Jul 05, 2016
Licensed Content Publisher	John Wiley and Sons
Licensed Content Publication	Journal of Texture Studies
Licensed Content Title	EFFECT OF WATER ACTIVITY ON TEXTURE PROFILE PARAMETERS OF APPLE FLESH
Licensed Content Author	MALCOLM C. BOURNE
Licensed Content Date	Jan 30, 2007
Licensed Content Pages	10
Type of use	Dissertation/Thesis
Requestor type	University/Academic
Format	Print and electronic
Portion	Figure/table
Number of figures/tables	1
Original Wiley figure/table number(s)	Figure 1
Will you be translating?	No
Title of your thesis / dissertation	PREDICTION OF TEXTURE CHARACTERISTICS IN APPLE DRYING USING COMPUTER VISION
Expected completion date	Aug 2016
Expected size (number of pages)	140
Requestor Location	Dandan Wang Apt 11, 317 College Road Truro, NS B2N2P6 Canada Attn: Dandan Wang
Publisher Tax ID	EU826007151
Billing Type	Invoice
Billing address	Dandan Wang Apt 11, 317 College Road

<https://s100.copyright.com/AppDispatchServlet>

1/2

7/5/2016

Rightslink® by Copyright Clearance Center

Truro, NS B2N2P6
Canada
Attn: Dandan Wang
0.00 CAD

Total

Would you like to purchase the full text of this article? If so, please continue on to the content ordering system located here: [Purchase PDF](#)

If you click on the buttons below or close this window, you will not be able to return to the content ordering system.

[ORDER MORE](#)

[CLOSE WINDOW](#)

Copyright © 2016 [Copyright Clearance Center, Inc.](#) All Rights Reserved. [Privacy statement](#). [Terms and Conditions](#).
Comments? We would like to hear from you. E-mail us at customercare@copyright.com